ABSTRACT

JULSON, ALISON JEAN. Photocatalytic Decolorization of Organic Dyes in Titanium Dioxide-Air Systems. (Under the direction of Dr. David F. Ollis.)

The photocatalytic degradation of adsorbed organic dyes in air is reported with the goal of color removal for potential catalyst characterization and application in self-cleaning surfaces.

In this study, a laboratory photoreactor equipped with 8 GE Blacklight Blue 20W lamps (peak emission at 365 nm) was the source for near-UV exposure of dye-coated Degussa P25 titanium dioxide (TiO_2) particles as well as dye coated photo-inert aluminum oxide (Al_2O_3) particles used for control experiments. The average UVA intensity of exposure for all experiments was 1.3 mW cm^{-2}. Dyes were adsorbed onto catalyst particles and inert supports in aqueous solution, and the coated particles were captured by centrifugation, dried, and hand ground to powder before near-UV exposure. The dyes included in this study were Acid Blue 9, Acid Orange 7, Reactive Black 5 and Reactive Blue 19. Sub-monolayer initial dye coverage of support particles was used. Visual evidence of color removal was recorded with digital photographic images of samples before near-UV illumination and after exposure.

Two methods, Indirect and Direct Analysis, were employed to quantitatively examine the decolorization of organic dyes with near-UV exposure. During illumination with the Indirect method, dye-coated powder samples were subject to ambient humidity and were shaken in uncovered Petri dishes in attempt to achieve uniform near-UV exposure of particles. Separate samples for each exposure time were used. Reaction products were desorbed from the support particles into basic aqueous solution, support particles were removed by centrifugation, and the resulting solution was analyzed by UV-visible

transmission spectroscopy to examine the photoreaction progress. The Direct Analysis method allowed for the examination of the same sample throughout the reaction with near-UV exposure. Dye-coated sample powder was pressed into a sealable sample holder with a quartz window which allowed for both UV exposure and analysis by diffuse reflectance UV-visible spectroscopy.

UV-visible spectroscopy was used to monitor changes in unreacted dye concentration with near-UV illumination compared to unexposed controls. Absorbance spectra obtained during Indirect Analysis was proportional to dye concentration following the Beer-Lambert law. The reflectance spectra acquired by the Direct Analysis method was transformed to Kubelka-Munk units, proportional to concentration, for all of the dye-coated TiO_2 and Al_2O_3 samples studied. For both analytic methods, a decrease in dye concentration was observed with near-UV illumination of the dye-coated TiO_2 powders for the four dyes studied. The dye did not photodegrade significantly in the absence of TiO_2.

The data obtained by UV-visible spectroscopy, for both analytic methods, was used to model the kinetics of the photocatalytic degradation. Several kinetic models were developed and applied to the reaction data. The most convincing mechanism developed for the photocatalytic degradation of organic dyes adsorbed to TiO_2 assumes a series reaction. The first step is the conversion of colored dye to colored intermediate by a first order reaction with respect to dye concentration, and the second step is conversion to colorless product by another first order reaction with respect to intermediate concentration. The rate constants for the first reaction step were of similar magnitude for all dyes, and the average rate constant, k_1, for the first step of all experiments was 0.13 min^{-1} and for the second step, k_2, was 0.0014 min^{-1}.

PHOTOCATALYTIC DECOLORIZATION OF ORGANIC DYES IN TITANIUM DIOXIDE-AIR SYSTEMS

by

ALISON JEAN JULSON

A thesis submitted to the Graduate Faculty of
North Carolina State University
in partial fulfillment of the
requirements for the Degree of
Master of Science

DEPARTMENT OF CHEMICAL AND BIOMOLECULAR ENGINEERING

Raleigh, North Carolina

January 2005

APPROVED BY:

Dr. H. Henry Lamb	Dr. Michael R. Overcash

Dr. David F. Ollis
Chair of Advisory Committee

PERSONAL BIOGRAPHY

In 1978 Alison Jean Vejtruba, now Julson, was the second girl of three born to David and Marcia Vejtruba and raised in Minnesota. As a fifth grader at Lino Lakes Elementary, Alison became an Odyssey of the Mind World Champion. The experience revealed the benefits of working diligently. Instead of attending classes at her high school as a senior, Alison attended the University of St. Thomas in St. Paul, Minnesota. During her first semester she had a capable and provoking chemistry professor who motivated her to further pursue the subject. She then spent the summer after graduation working in the physical chemistry laboratory at the university.

Alison earned a Bachelor of Science degree with a major in chemistry and minors in mathematics and physics from Bemidji State University in northern Minnesota and was the recipient of a Full Tuition Academic Scholarship. The summer after her sophomore year, Alison participated in a Research Experience for Undergraduates funded by the National Science Foundation at the Material Science Institute of the University of Oregon.

Alison graduated Magna Cum Laude from Bemidji State and then worked for about a year at the Wastewater Treatment Plant in Superior, WI as an engineering technician. In 2002 she married Adam Thomas Julson, and the newlyweds promptly moved to Raleigh so that Alison could attend North Carolina State University to pursue a master's degree in chemical engineering. She was the recipient of the Dean's Fellowship in her first year. Under the direction of Dr. David F. Ollis, she investigated the photocatalytic degradation of organic dyes adsorbed to titanium dioxide in an air system. Upon graduation, Alison and Adam will to return to Minnesota.

ACKNOWLEDGMENTS

Most importantly, I would like to thank Adam Thomas Julson, my husband, for letting me have the first turn. Thank you for understanding that even though this work consumed most of my time, I would always rather be spending time with you. Thank you for making me laugh and for doing it often. Thank you for letting me cry and for learning that sometimes I just need a hug. Thank you for being on my side. Thank you for taking care of our world while I was in mine. It wouldn't have been any fun to get to the top of the mountain without someone to jump up and down with.

I would like to thank Dr. David F. Ollis, my advisor, for not only caring about the work and my progress as a researcher, but also about my growth as a person with other interests. It was nice to know and work with someone, in this competitive and all consuming world that is academia, who realizes that a universe exists. Thank you for the guidance and opportunities.

I would like to thank Dr. Orlin D. Velev and his research group for allowing me use of their UV-visible spectrophotometer. I would also like to thank Dr. H. Henry Lamb, whose suggestion led me to the diffuse reflectance method of analysis.

Although I was the only graduate student doing research in Dr. Ollis' lab, I was not alone. I would like to thank April M. Kloxin for being a delightful office mate, helpful resource, and for being behind me, both literally and figuratively. I would also like to thank Angelica M. Sanchez, Chris J. Kloxin, Julie A. Crowe and Jim J. Semler for being exceptional resources and capable listeners with whom I could talk about successes and failures.

I feel privileged to have met so many wonderful people while attending North Carolina State University. Amy E. Zweber and Victoria A. Wagoner, you were both great people to struggle through homework with and to laugh with. Dana M. McDiffett, April M. Kloxin, Julie A. Crowe and Angelica M. Sanchez; thank you for the great memories, the fabulous conversations, and for ultimately being the dearest friends a person could have. Thank you to all the people that made my graduate school experience enjoyable.

Finally, I would like to thank my family, especially my parents, for supporting me in whatever I choose to do.

TABLE OF CONTENTS

Page Number

LIST OF TABLES

Page Number

LIST OF FIGURES

Page Number

1 INTRODUCTION AND LITERATURE REVIEW

1.1 Introduction

Self-cleaning surfaces using heterogeneous photocatalysis have recently emerged as commercial products. The most visible example is window glass sold by companies including Pilkington and Pittsburgh Plate Glass. Self-cleaning surfaces have potential environmental, financial, aesthetic, and time-saving benefits. For example, diminished or eliminated need for harsh chemical cleaning agents reduces consequent water and air pollution, as well as maintenance costs. Light-mediated stain removal has both aesthetic and time-saving benefits. Although the photocatalytic degradation of organic substances by titanium dioxide (TiO_2) and other photocatalysts has been extensively investigated in liquid-catalyst [1-5] and gas-catalyst systems [6-10], relatively little work has been reported on photocatalytic oxidations of non-volatile contaminants in air. Researchers regularly use common reactants to characterize photocatalyst activity in liquid phase (e.g. 4-chlorophenol) and air phase (e.g. trichloroethylene, acetone), but no reactant has yet emerged as a standard for so-called solid phase systems. Examples of reactants reported include (dry) deposits of long chain carboxylic acids [11-14], soot films [15, 16], microbial films [17], and non-volatile dyes [18-25].

Examination of photocatalytic degradation of solid and non-volatile contaminants in air-catalyst systems could be applied to self-cleaning surfaces and used for catalyst characterization. A standard method is needed to test the effectiveness of photocatalysts and photocatalytic coated surfaces in degrading contaminants for successful application of products. With the goal of color removal, this study reports the photocatalytic degradation of adsorbed organic dyes on TiO_2 in air. A non-photocatalytic control, alumina (Al_2O_3), was

tested to demonstrate that degradation on TiO_2 was predominately a photocatalytic, rather than photolytic, mechanism. Reaction kinetics of the photocatalytic batch degradation of the dyes was examined using UV-visible spectroscopy for both Direct and Indirect Analysis methods.

1.1.1 Photocatalysis

Photocatalysis is an "acceleration of photoreaction by the presence of a catalyst" [27]. The semiconductor photocatalytic process is reported to occur via the absorption of a photon of energy equal to or greater than the semiconductor bandgap energy, which then leads to the promotion of an electron (e^-) from the valence band to the conduction band, while creating a hole (h^+) in the valence band [1, 4, 26, 27]. Most current research reported on photocatalysis is using TiO_2, which has a bandgap of approximately 3.2 eV for the anatase structure [16, 28], corresponding to 385 nm. The photo-produced holes and electrons may migrate to the surface and are available for oxidation and reduction reactions respectively or may recombine to decrease the photocatalysis efficiency, as shown in the reactions below.

$$h\nu + TiO_2 \rightarrow h^+ + e^-$$

Reaction 1.1 Photocatalysis

$$h^+ + e^- \rightarrow heat$$

Reaction 1.2 Recombination

At the catalyst surface, the holes can scavenge electrons directly from organic contaminants or the holes may steal electrons from water or a hydroxyl nucleophile to create hydroxyl radicals, which can then in turn destroy the organic. Research conveyed in the literature demonstrates, for example, using photocatalysis to treat wastewater streams contaminated

with dissolved and complexed metals and organic solute chemicals [29], remove nitrogen oxides (NO_x) from contaminated air streams [30], clean a dried coffee stain on a TiO_2 coated surface in air [11], oxidize amino acids in water [31] and inactivate bacteria and fungi in air [17].

1.1.2 Objectives of Research

Although research on the photocatalytic degradation of organic substances in the liquid phase and the gas phase has been widely reported in literature, the documentation of research on the photocatalytic degradation of non-volatile or solid organics is relatively scarce, therefore revealing a research area to be explored. The interest in this research was to examine the photocatalytic destruction of non-volatile, adsorbed dye, specifically color removal by UV illumination of dye-coated TiO_2 particles, applicable for self-cleaning surfaces. The simple system of dye-coated TiO_2 particles was used to examine the fundamental photocatalytic kinetics of dye degradation. Specifically, the objective of this research was to quantify the kinetics of color removal during TiO_2 photocatalysis, and to develop a description of the system by proposing reaction mechanisms and corresponding kinetic models. The organic dyes investigated include Acid Blue 9 (AB9), Acid Orange 7 (AO7), Reactive Black 5 (RB5) and Reactive Blue 19 (RB19). These dyes were chosen because of previous examination of the photocatalytic degradation in the liquid phase, for example; by Yang et al. [21], Augugliaro et al. [32], Arslan and Balcioglu [33] and Lizama et al. [3], for AB9, AO7, RB5 and RB19, respectively. Also, the photocatalytic degradation in air of AB9 and AO7 has been reported by Yang et al. [21] and Vinodgopal et al. [18], respectively.

1.2 Literature Review of Photocatalysis in Air-Solid Contaminant-Catalyst Systems

The main focus of the literature review was reports of photodegradation of adsorbed dyes by TiO_2 in air. The current study may lead to a kinetic model applicable to more complex systems; therefore literature on the photocatalytic removal of other solid, non-volatile contaminants, such as soot and other stains, was also included.

1.2.1 Photodegradation of Dyes in Air

Vinodgopal, Wynkoop and Kamat [18] reported the first photocatalyzed decomposition in air of the textile dye Acid Orange 7 (AO7) on TiO_2 particles, using diffuse reflectance FTIR and diffuse reflectance visible spectroscopy. Samples of dye-coated TiO_2 and Al_2O_3 particles were prepared with dye coverages of 0.10 (high-coverage) and 0.02 (low-coverage) mmol AO7 per g of TiO_2. The dye-coated particles were exposed to visible light, of wavelength (λ) greater than 380 nm, leading to photo-induced bleaching on TiO_2, but not on Al_2O_3, as shown in Figure 1.1. The visible light-induced photodegradation pathway proposed involved photon absorption by the adsorbed organic material (dye) to excite an electron, which can then transfer charge to the semiconductor (see Figure 1.2 below).

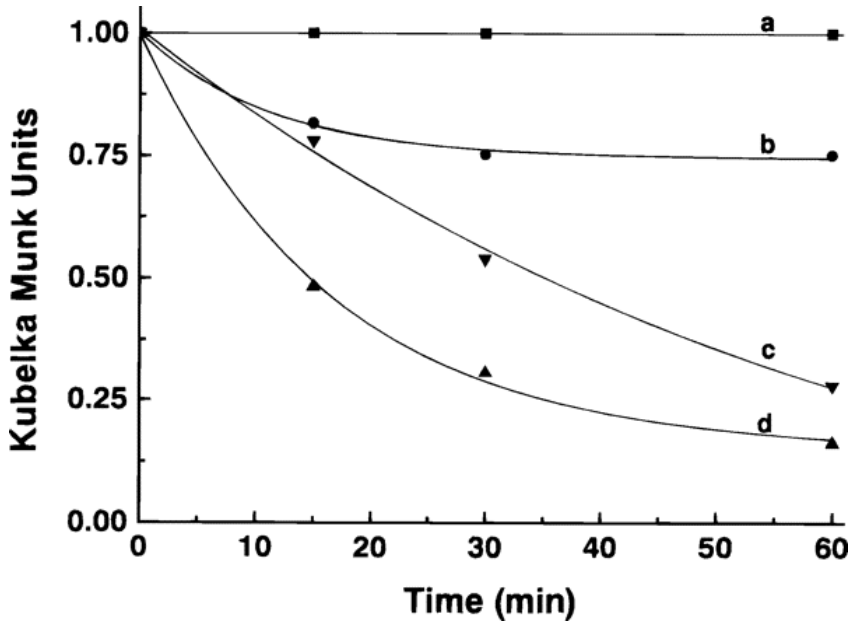

Figure 1.1 Normalized decay traces representing the degradation of AO7. "(a) The degradation of AO7 on alumina (air-equilibrated; 0.02 mmol of AO7/g of Al_2O_3), (b) AO7 on TiO_2 (0.02 mmol of AO7/g of TiO_2), (c) AO7 on TiO_2 at high coverage (0.10 mmol of AO7/g of TiO_2), and (d) AO7 on TiO_2 at low coverage (0.02 mmol of AO7/g of TiO_2). Sample b was degassed while the others were equilibrated in air before the photolysis" [18]. Reprinted with permission from [18]. Copyright 1996 American Chemical Society.

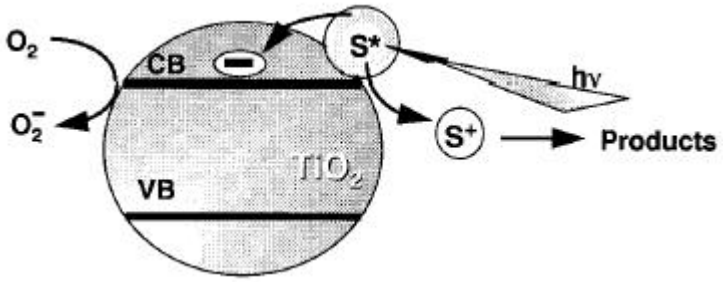

Figure 1.2 Illustration of photosensitized degradation of colored pollutant. Reprinted with permission from [18]. Copyright 1996 American Chemical Society.

Direct, photocatalyzed oxidation via near-UV illumination, $\lambda < 385$ nm, was not explored. In the absence of oxygen, only modest degradation of AO7 was observed, with the conversion occurring attributed to residual adsorbed oxygen, suggesting that the oxygen scavenges photoinjected electrons from the TiO_2 during the photo-driven degradation process. Psuedo-first order rate constants were evaluated by transforming the visible region diffuse reflectance (R) data to Kubelka-Munk units ($f(R) = (1-R)^2/2R$). For oxygen-assisted photobleaching, first order rate constants reported were 0.021 and 0.03 min^{-1} for initial high and low dye coverage respectively, on TiO_2.

Porada and Gade [19] examined the photodegradation in air of Acid Red 44 (AR44) adsorbed on TiO_2 from solutions of different initial dye concentrations by irradiation of 546 nm, 365 nm, and 311 nm wavelength light for determination of quantum yield. Diffuse reflectance spectroscopy was used to monitor the photodegradation of the dye. At the irradiation wavelengths of 365 and 313 nm, the degradation rates were approximately 3 and 4 times respectively the rate occurring with 546 nm illumination of the dye coated powder, suggesting photocatalyst activity of TiO_2. Porada and Gade probed the influence of TiO_2 on the self-sensitzed photodegradation of AR44 by monitoring the reflectance of samples with exposure to 546 nm light of dye coated MgO, a photo-inert support. The dye did not degrade measurably, and they concluded that the photodegradation only takes place in the presence of a photocatalyst. They did not determine whether the degradation in the presence of TiO_2 was indeed a photocatalytic phenomenon by examining the photodegradation of AR44 on MgO with illumination of near-UV light, the region of light absorption by TiO_2.

Stathatos, Tsiourvas and Lianos [20] prepared titanium dioxide films by dip coating glass slides in reverse-micellar solution containing titanium isopropoxide with subsequent

calcination. The films were then coated with Basic Blue 41 (BB41) or Basic Red 46 (BR46) to examine their photodegradation activity. They illuminated the dye-coated TiO_2 films with unfiltered broadband light from 350 to 800 nm and monitored absorption, i.e. concentration, changes by UV-visible transmission spectroscopy. Virtually complete conversion of BB41 after approximately 30 min of unfiltered illumination is reported, see Figure 1.3. Simultaneously using illumination by near-UV and visible light, the decomposition of adsorbed BR46 due to heterogeneous photocatalysis, direct photolysis, and dye charge injection (dye sensitization) into TiO_2 were not separable, although use of a 400 nm filter "substantially" decreased the conversion rate, suggesting a substantial photocatalytic mechanism [20]. In the absence of O_2, the observation of very limited dye conversion suggests that oxygen is a key electron scavenger leading to dye degradation.

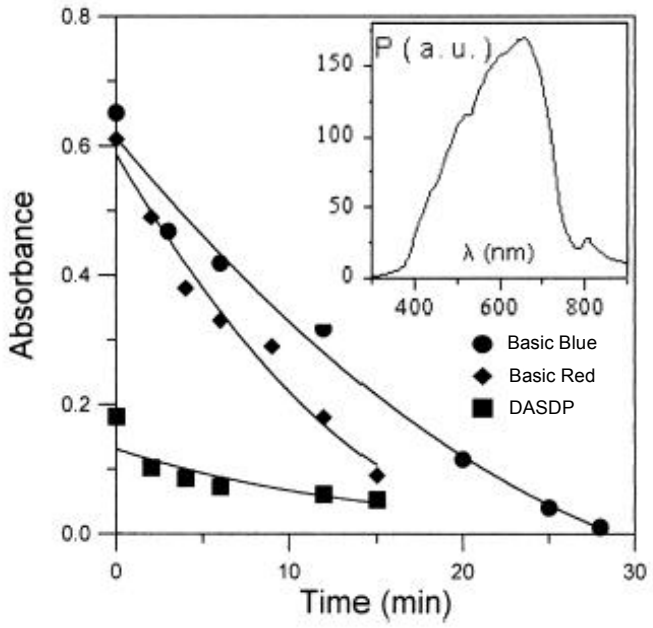

Figure 1.3 Changes in absorbance maxima of adsorbed dyes with UV illumination. Insert depicts lamp profile. Reprinted from [20], Copyright 1999, with permission from Elsevier.

Yang and coworkers [21] reported the photocatalytic oxidation in water of Acid Blue 9 (AB9) by TiO_2 with UV illumination (254 to 365 nm) using UV-visible spectroscopy. Heterogeneous photocatalysis was not explicitly confirmed. Liquid phase kinetics were affected by solution pH, with the rate of oxidation increasing as the pH decreased. A kinetic model first order, with respect to dye concentration, was deemed suitable for the liquid phase oxidation by these researchers, who stated that the apparent rate constants included contributions from the rate of mass transfer of the dye to the photocatalyst surface and the inherent surface reactions.

To examine the mechanism of reaction during UV illumination, the researchers monitored the degradation of AB9-coated TiO_2 powder by diffuse reflectance infrared Fourier transform spectroscopy (DRIFTS) in air. Yang and coworkers [21] did not explicitly discuss a sequential mechanism of oxidation, although chemical structural changes with UV illumination were outlined; "A remarkable decrease at peaks of 1580, 1407, and 1390 cm^{-1} was assigned as the degradation of cyclic conjugated C=N stretching and C-H bending from the ethyl group. It indicates that the excited holes and OH radicals attack $-CH_2-$ and $-C_2H_5$ bonds that are attached on the nitrogen atom. As a result, the color of AB9 dye fades quickly since the conjugated structures such as C=N and C=C bonds were broken by the photoredox process [21]." The researchers did not develop a kinetic model from the solid-state reflectance data, but did demonstrate complete conversion of the dye after 5 hours of UV illumination and negligible influence of deposition pH on the reaction rate in the air-solid system, see Figure 1.4. Data obtained by Yang and coworkers [21], shown in

Figure 1.5 below, for the solid-state oxidation of AB9 will be used to demonstrate that the kinetic models we develop can be applied to work done by other researchers.

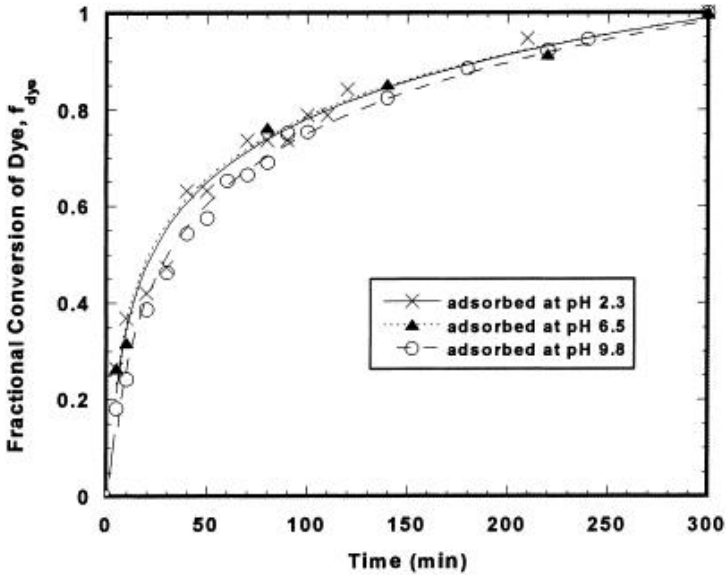

Figure 1.4 Fractional conversion of AB9 dye adsorbed at various pH values during photon illumination. Reprinted from [21], Copyright 2001, with permission from Elsevier.

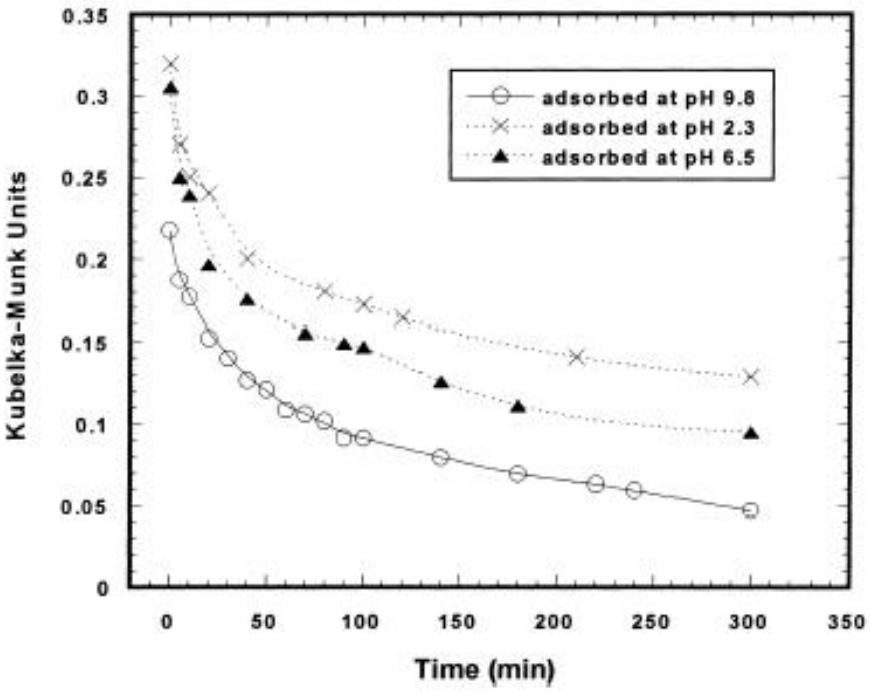

Figure 1.5 Solid-state concentrations of AB9 adsorbed to TiO_2 as a function of UV illumination time. Reprinted from [21], Copyright 2001, with permission from Elsevier.

A method to assess the photocatalytic activity of prepared TiO_2 thin films was developed by Doushita and Kawahara [22]. Acid Blue 9 (AB9) and Methylene Blue (MB) were combined separately with a polyvinyl alcohol (PVA) binder by dissolving 0.5 wt % PVA and 0.5 wt % dye in 40 g of hot water and 10 g of ethanol. The dye/PVA solution was spin coated onto the photocatalytic films. The authors indicate that the PVA binder and ethanol were used to prepare a homogeneous coating, with the PVA aiding in the uniform dispersion of dye and therefore coloration, and the ethanol lowering the solution surface tension to avoid striations as the samples were spin coated.

The coated films were illuminated with near-UV light, maximum wavelength of exposure of 352 nm, and UV-visible spectroscopy was used to monitor absorption changes

during UV exposure. Methylene Blue was an unsuccessful probe because color loss during UV exposure was reversible after exposure was halted. For the AB9/PVA/TiO_2 samples, the 600 to 700 nm peak of absorbance significantly decreased with near-UV illumination, while no absorption changes were found upon similar irradiation of AB9/PVA samples on (photo-inert) silica-coated glass. Doushita and Kawahara found that relative humidity greatly influenced the reaction, concluding that increasing humidity increased the formation of hydroxyl and peroxy radicals, therefore increasing the conversion rate of dye. Doushita and Kawahara [22] proposed a one-dimension model in the dye-PVA layer to explain the photodegradation of dye, including in the model the diffusion of oxidizing radicals and a first order reaction mechanism for dye discoloration, dependent on radicals present in the system. Curiously, no attempt was made to fit this model to their experimental data.

Zhi, Wang and Fujishima [23] report the novel use of vividly colored and fluorescent dyes as indicators to detect coating flaws in self-cleaning photocatalytic surfaces and the underlying precoat layer, respectively. A precoating agent, used to prevent TiO_2 from reacting with the substrate surface, containing approximately 0.01 to 0.05 wt % fluorescent dye was visually detectable with black-light illumination, and therefore the absence of the precoat film was also detectable. The fluorescence of this layer, detected using a Shimadzu Model UV-60 double-beam spectrophotometer, diminished with black-light (300 to 400 nm) illumination when the photocatalytic layer was applied, but was virtually unaffected without the presence of TiO_2. In this case, the photocatalyst adjacent to the dye layer gave rise to dye bleaching when illuminated. Vivid dyes were combined with TiO_2 to compose the photocatalytic layer, allowing for visual detection to reveal gaps in the photocatalyst coating. UV-visible spectra of precoat-photocatalytic combination layers containing both

Methlylene Blue and NK-719, a cyanine dye, showed a 50% decrease in absorption after 15 min and 1 hour respectively. Zhi and coworkers did not apply a kinetic model or reaction mechanism to these degradations, nor did they probe the activity of the photocatalytic layer after the indicator dyes were removed.

Shang, Chai and Zhu [24] synthesized composite films of polystyrene (PS)-TiO_2 and PS-TiO_2/CuPc (copper phthalocyanine) containing a ratio of 2.0 wt % of TiO_2 or TiO_2/CuPc to PS. They demonstrated the photocatalytic degradation of polystyrene (PS) by 310 to 750 nm wavelength exposure from fluorescent lamps. After 250 hours of exposure, the dye-sensitized composite exhibited higher weight loss (6.9 wt %) for PS-TiO_2/CuPc with illumination than the PS-TiO2 composite (4.1 wt %). With irradiation, a gas phase concentration increase of CO_2 was observed, with the PS-TiO_2/CuPC system releasing more CO_2 than the PS-TiO_2 composites. The researchers concluded that rapid initial CO_2 generation was due to the reaction of oxidative species produced at the TiO_2 surface with nearby polymer chains. The CO_2 generation rate then decreased with illumination as the PS was destroyed, which the authors presumed was because the photodegradation rate was dependent on the slow desorption and diffusion of the photooxidants to the now more remote PS. No data or experiments were reported on photoreactions in the absence of TiO_2, but the homogeneous photodegradation of PS was assumed negligible by the researchers as the PS has high chemical stability and is nonbiodegradable.

Kemmitt and coworkers [25] deposited titania and titania/silica films on aluminum plates, ceramic tiles, soda glass and WO_3-doped soda glass. They compared the photocatalytic activity of the coatings by monitoring the oxidation in air of rhodamine dye. Following the drying of a dye solution on the films, the oxidation of rhodamine dye during

340 nm light exposure was quantified using fluorescence spectroscopy. They stated that rhodamine can autocatalyse its own oxidation by promoting electrons from its lowest excited state into the conduction band of TiO_2. The autocatalyzed reaction contributions were neglected by using 340 nm light for the photocatalytic oxidation, because rhodamine "weakly" absorbs at this wavelength [25]. The resulting photocatalytic fluorescence decays, for all samples, "were fit to a biexponential decay function, the first component displaying a variable and small time (rate) constant while the second component showed little variation with a time (rate) constant of approximately 10 min^{-1} [25]". The first rate constant, 0.28-2.90 min^{-1}, was attributed to the photocatalysed decomposition leading to decolorization, while the larger rate constant, 10 min^{-1}, was assumed due to the non-photocatalytic decomposition of rhodamine leading to fluorescence. A single exponential decay rate constant of approximately 10 min^{-1} was reported for control experiments involving UV-induced (340 nm) decomposition of rhodamine on uncoated substrates, affirming the authors' assumption that the larger rate constant was due to non-photocatalytic decomposition.

1.2.2 Photodegradation of Soot and Other Stains

Lee and Choi [15] examined the solid-phase photocatalytic degradation with near-UV illumination in air of flame-deposited hexane soot. The soot was deposited, ~2 μm thickness, on TiO_2 films adhered to glass plates. Two near-UV exposure methods were used; (1) front illumination from the soot layer side, which blocked some of the UV radiation from reaching the TiO_2, and (2) back illumination through the glass to the TiO_2 layer. The black soot layer was completely removed after approximately 30 hours of back

illumination. The researchers used scanning electron microscopy (SEM) to monitor a soot layer near the edge of the photocatalytic film, see Figure 1.6 below for the geometry of the system. SEM revealed that a gap between the edges of the soot layer and the TiO_2 layer increased beyond 80 μm with UV illumination, verifying migration of active oxidant species.

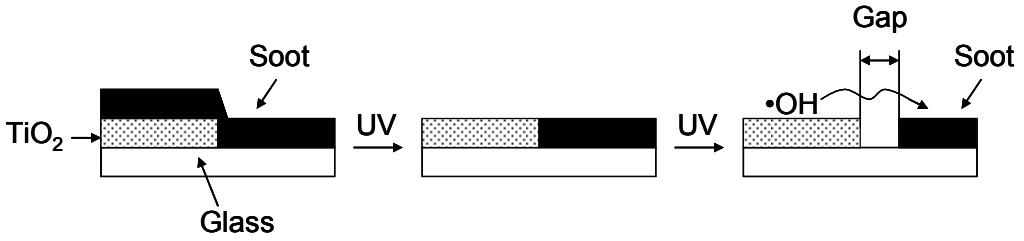

Figure 1.6 Photocatalytic degradation of soot as examined by Lee and Choi [15]. Schematic drawn similar to illustration by Lee and Choi. Adapted with permission from [15]. Copyright 2002 American Chemical Society.

The rate of gap distance increase slowed with time as the gap became larger, which the authors assumed was because of the increase distance required for the OH radicals to travel. Although the researchers describe the photooxidants as traveling along the surface, they agree that "the through-air diffusion (of oxidants) within the soot layer thickness could be an efficient mechanism as well [15]".

The *direct*, *lateral*, and *remote* photocatalytic oxidation of soot by a thick TiO_2 film is demonstrated by visual evidence reported by Lee, McIntyre and Mills [16] using a simple series of experiments. *Direct* photocatalytic oxidation occurs at the catalyst surface to degrade an adsorbed contaminant with UV illumination. *Lateral* oxidation of a pollutant is "attributed to the spill-over of a photogenerated, highly oxidizing species" and *remote* photocatalytic oxidation occurs "via a through air diffusion mechanism far from their

(oxidizing species) place of photogeneration" [16]. The *direct* and *lateral* destruction of soot was demonstrated in the same experiment; soot was applied to a photocatalytic layer containing a gap. With far-UV illumination (λ = 254 nm) the soot layer slowly disappeared, first on the surface of the TiO_2 layer (*direct* removal) and then in the 0.7 mm gap created between the TiO_2 layers (*lateral* removal). The *remote* oxidation was examined by illuminating, through the quartz slide to which it was attached, a soot layer positioned over a photocatalytic layer. The researchers report visual evidence showing that only soot directly above the TiO_2 layer, separated by a 175 μm air gap, is removed with far-UV illumination.

Palmitic acid (PA) is secreted by glands of the skin and is a model contaminant because of its stability and abundance; it is a major component of fingerprints. Romeas and coworkers [34] examined the properties of photocatalytic films prepared by dip-coating glass in a solution of 80 wt % TiO_2 and 20 wt % photostable binder of unknown composition. Glass slides, coated first with TiO_2 and then with 50 μg cm^{-2} PA, were illuminated with 315-400 nm light. The PA film thickness was approximately 580 nm as calculated from PA density at 335 K. The removal of the palmitic acid with UV illumination gradually improved the transparency of the layer, according to visual estimates. Adherent intermediate products of the palmitic acid degradation were identified by dissolving the treated film in sodium hydroxide aqueous solution and analyzing the solution by HPLC. Gas phase intermediate products were collected on an activated charcoal cartridge, desorbed into a solution of dichloromethane and analyzed by GC-MS. Romeas et al. [34] detected 39 intermediate products for the palmitic acid degradation including alkanes, alcohols, aldehydes, ketones, and acids. An apparent zero-order rate constant of 0.60 +/- 0.12 μmol h^{-1} was reported for the PA film degradation. Control experiments

revealed that without either UV irradiation or TiO_2 photocatalyst, no degradation of the palmitic acid occurred.

Photocatalytic films were coated with a water-repellent agent, a (fluoroalkyl)silane (FAS-17), to create a film described as superhydrophobic by Nakajima et al [35]. Water-surface contact angle measurements were used to monitor the photocatalytic rate of decomposition of FAS-17 with UV irradiation from blacklight bulbs. A decrease in contact angle from 140^o to 0^o, and therefore increased wettability, occurred with UV exposure of a 71.4 wt % TiO_2 film initially coated with FAS-17. The FAS-17 coating was removed after approximately 100 hours of illumination, monitored by contact angle. An outdoor test was also performed, and the contact angle of a FAS-17 film containing no TiO_2 also decreased from about 140^o to approximately 100^o with 1800 hours of outdoor exposure, which the authors attributed to the deposition of stains on the surface from atmospheric pollutants. Nakajima et al. [35] report that a "bare TiO_2 surface is expected to contaminate readily because of the high surface energy of TiO_2 relative to the low surface energy of contaminants".

Vicente and coworkers [14] prepared thin TiO_2 photocatalytic films by dip-coating soda lime glass slides in a solution of titanium tetrabutoxide. Calcination for 30 minutes at 300^oC created scratch resistant films. Film thickness was controlled by withdrawal rate, with the average thickness of the TiO_2 film being 125 nm. Stearic acid layers were then applied to the TiO_2 coated slides by dip-coating in solutions of ethanol with stearic acid concentrations between 5 g L^{-1} to 60 g L^{-1}. Destruction via 312 nm irradiation of a stearic acid layer on a TiO_2 film was measured to quantify the film photocatalytic activity. A decrease in thickness of the stearic acid film with UV exposure was monitored with infrared

transmission spectroscopy, specifically tracking absorption due to C-H stretching vibrations at 2910 cm^{-1}. Vincente et al. [14] found that the stearic acid layers were essentially removed after approximately 125 min of exposure to 312 nm light. The thickness of the stearic acid layers was not explicitly reported, only thickness normalized to the initial thickness was given. Additional TiO_2 coatings, up to three layers, did not exhibit noticeably different photocatalytic activity. The effect of stain thickness was also examined; doubling the stearic acid concentration of the initial solution from 20 g L^{-1} to 40 g L^{-1} approximately doubled the complete removal time of the film from 100 to about 200 minutes.

Photocatalytic TiO_2 films, 300 +/- 100 nm thick, were prepared by Sitkiewitz and Heller [13]. A solid model contaminant was applied to the TiO_2 film by spin coating a 0.5 g mL^{-1} solution of stearic acid in isopropyl alcohol to produce a 200 nm stearic acid layer. A filtered high pressure mercury lamp (365 nm) was the light source in this study. Gas phase samples of product intermediates were collected and analyzed by GC-MS. Adherent intermediate products were rinsed from the glass slides with acetonitrile and analyzed by FTIR. Over 4 hours of illumination, Sitkiewitz et al. report that the CO_2 production rate during stearic acid degradation increases with increasing H_2O partial pressure and is proportional to the square-root of irradiance (intensity was varied from 0.08 to 6.0 mW cm^{-2}). Only CO_2 and H_2O were detected in the gas phase upon photocatalytic degradation of stearic acid. Increasing oxygen pressure from 0% to 21% increases CO_2 production until atmospheric concentration was reached, with no further increase using 21% to 100% oxygen. Only small amounts of CO_2 were produced with illumination of the stearic acid/TiO_2 film in the absence of O_2, which reinforces their proposed reaction mechanism in which O_2 is needed to create oxygen ($\bullet O_2^-$) radicals. The photocatalyst deactivated when

there was no H_2O present in the gas phase only when the irradiation flux was greater than 2 mW cm^{-2}. Sitkiewitz et al. concluded that at higher reaction rates, H_2O was not replenished fast enough through the stearic acid film to supply the surface with H_2O to continue the reaction.

Minabe et al. [12] coated stearic acid onto photocatalytic films from a saturated solution to give a net weight of 44 μg cm^{-2}. Photodegradation of the stearic acid occurred with exposure to 365 nm light. The reaction was monitored in the gas phase by GC, and FTIR was used to monitor solid phase intermediate products of films deposited on CaF_2 slides. Minabe et al. [12] report pseudo-zero order photooxidation kinetics for up to 20 hours of UV illumination with a weight change rate of 0.75 μg cm^{-2} h^{-1}. Complete removal of the stearic acid layer after 80 hours of UV exposure was not achieved. The role of relative humidity on CO_2 production rate, the major gas phase product, in the photooxidation of stearic acid was probed, and Minabe et al. report an oxidation rate of 20 nmol C cm^{-2} h^{-1} at relative humidity above 90% vs. 48 nmol C cm^{-2} h^{-1} in an atmosphere below 10% relative humidity. Minabe et al. report that their stearic acid photodegradation rate constant at low humidity was an order of magnitude greater than that of Sitkiewitz et al. [13], which they attribute to differences in morphology of the TiO_2 films.

Mills et al. [36] suggest the use of Pilkington Activ™ TiO_2 coated glass as a standard for photocatalytic work done with supported catalyst films, just as Degussa P25 has been used as a standard for TiO_2 powders. With FTIR they assessed the photocatalytic activity of Activ™ using degradation of stearic acid applied to the TiO_2 layer under irradiation of UV light (254 nm and 365 nm). In separate experiments, contact angles measurements were used to examine the photo-induced superhydrophilic nature of the

photocatalytic surface with irradiation of 254 nm. The authors report that the photocatalytic degradation of stearic acid does not appear to be dependent on stearic acid concentration initially; it follows apparent zero-order kinetics until it deviates from this kinetic model as it approaches the last 10-20% of completion. The stearic acid film was photocatalytically degraded at a reported rate of 1.9 nm h^{-1} (0.17 μg cm^{-2} h^{-1}) by illumination of 365 nm light. The importance of oxygen (O_2) in the reaction, to create electron rich oxygen radicals, is apparent because in the absence of oxygen the photocatalytic destruction of stearic acid did not proceed within detectable limits. Mills et al. report a reduced photocatalytic oxidation rate in a "dry" atmosphere, three times lower than under humid conditions.

1.3 References

[1] Tang, W.Z., Z. Zhang, H. An, M.O. Quintana and D.F. Torres, *TiO_2/UV Photodegradation of Azo Dyes in Aqueous* Solutions. Environmental Technology 1997, **18**: p. 1-12.

[2] Lachheb, H., E. Puzenat, A. Houas, M. Ksibi, E. Elaloui, C. Guillard and J.-M. Herrmann, *Photocatalytic degradation of various types of dyes (Alizarin S, Crocein Orange G, Methyl Red, Congo Red, Methylene Blue) in water by UV-irradiated titania*. Applied Catalysis B: Environmental 2002, **39**: p. 75-90.

[3] Lizama, C., J. Freer, J. Baeza, and H.D. Mansilla, *Optimized photodegradation of Reactive Blue 19 on TiO_2 and ZnO suspensions*. Catalysis Today 2002, **76**: p. 235-246.

[4] Sauer, T., G.C. Neto, H.J. Jose and R.F.P.M. Moreira, *Kinetics of photocatalytic degradation of reactive dyes in a TiO_2 slurry reactor*. Journal of Photochemistry and Photobiology A: Chemistry 2002, **149**: p. 147-154.

[5] Zielinska, B., J. Grzechulska, R.J. Kalenczuk and A.W. Morawski, *The pH influence on photocatalytic decomposition of organic dyes over A11 and P25 titanium dioxide*. Applied Catalysis B: Environmental 2003, **45**: p. 293-300.

[6] Gratzel, M., K.R. Thampi, and J. Kiwi, *Methane Oxidation at Room Temperature and Atmospheric Pressure Activated by Light via Polytungstate Dispersed on Titania*. Journal of Physical Chemistry 1989, **93**(10): p. 4128-4132.

[7] Dibble, L.A. and G.B. Raupp, *Fluidized-Bed Photocatalytic Oxidation of Trichloroethylene in Contaminated Airstreams*. Environmental Science and Technology 1992, **26**(3): p. 492-495.

[8] Luo, Y. and D.F. Ollis, *Heterogeneous Photocatalytic Oxidation of Trichloroethylene and Toluene Mixtures in Air: Kinetic Promotion and Inhibition, Time-Dependent Catalyst Activity*. Journal of Catalysis 1996, **163**: p. 1-11.

[9] Lim, T.H., S.M. Jeong, S.D. Kim and J. Gyenis, *Photocatalytic decomposition of NO by TiO_2 particles*. Journal of Photochemistry and Photobiology A: Chemistry 2000, **134**(3): p. 209-217.

[10] Gonzalez-Garcia, N., J.A. Ayllon, X. Domenech and J. Peral, *TiO_2 deactivation during the gas-phase photocatalytic oxidation of dimethyl sulfide*. Applied Catalysis B: Environmental 2004, **52**: p. 69-77.

[11] Heller, A, *Chemistry and Applications of Photocatalytic Oxidation of Thin Organic Films*. Accounts of Chemical Research 1995, **28**(12): p. 503-508.

[12] Minabe, T., D.A. Tryk, P. Sawunyama, Y. Kikuchi, K. Hashimoto and A. Fujishima, *TiO_2-mediated photodegradation of liquid and solid organic compounds*. Journal of Photochemistry and Photobiology A: Chemistry 2000, **137**: p. 53-62.

[13] Sitkiewitz, S. and A. Heller, *Photocatalytic oxidation of benzene and stearic acid on sol-gel derived TiO_2 thin films attached to glass*. New Journal of Chemistry 1996, **20**(2): p. 233-241.

[14] Vicente, J.P, T. Gacoin, P. Barboux, J.-P. Boilot, M. Rondet and L. Gueneau, *Photocatalytic decomposition of fatty stains by TiO_2 thin films*. International Journal of Photoenergy 2003, **5**: p. 95-98.

[15] Lee, M.C. and W. Choi, *Solid Phase Photocatalytic Reaction on the Soot/TiO_2 Interface: The Role of Migrating OH Radicals*. Journal of Physical Chemistry B 2002, **106**(45): p. 11818-11822.

[16] Lee, S.-K., S. McIntyre and A. Mills, *Visible illustration of the direct, lateral and remote photocatalytic destruction of soot by titania*. Journal of Photochemistry and Photobiology A: Chemistry 2004, **162**: p. 203-206.

[17] Poulios, I., P. Spathis, A. Grigoriadou, K. Delidou and P. Tsoumparis, *Protection of Marbles Against Corrosion and Microbial Corrosion with TiO_2 Coatings*. Journal of Environmental Science and Health Part A - Toxic/Hazardous Substances & Environmental Engineering 1999, **34**(7): p. 1455-1471.

[18] Vinodgopal, K, D.E. Wynkoop and P.V. Kamat, *Environmental Photochemistry on Semiconductor Surfaces: Photosensitized Degradation of a Textile Azo Dye, Acid Orange 7, on TiO_2 Particles Using Visible Light*. Environmental Science and Technology 1996, **30**(5): p. 1660-1666.

[19] Porada, T. and R. Gade, *Determination of the Quantum Yield for the Self-sensitized Photodegradation of Acid Red 44 Adsorbed on TiO_2*. Zeitschrift fur Physikalische Chemie – International Journal of Research in Physical Chemistry & Chemical Physics 1999, **210**(1): p. 113-126.

[20] Stathatos, E., D. Tsiourvas and P. Lianos, *Titanium dioxide films made from reverse micelles and their use for the photocatalytic degradation of adsorbed dyes*. Colloids and Surfaces A: Physicochemical and Engineering Aspects 1999, **149**: p. 49-56.

[21] Yang, T.C.-K., S.-F. Wang, S.H.-Y. Tsai and S.Y. Lin, *Intrinsic photocatalytic oxidation of the dye adsorbed on TiO_2 photocatalysts by diffuse reflectance infrared Fourier transform spectroscopy*. Applied Catalysis B: Environmental 2001, **30**: p. 293-301.

[22] Doushita, K. and T. Kawahara, *Evaluation of Photcatalytic Activity by Dye Decompostion*. Journal of Sol-Gel Science and Technology 2001, **22**: p. 91-98.

[23] Zhi, J.F., H.B. Wang and A. Fujishima, *Development of Photocatalytic Coating Agents with Indicator Dyes*. Industrial and Engineering Chemistry Research 2002, **41**(4): p. 726-731.

[24] Shang, J., M. Chai and Y. Zhu, *Photocatalytic Degradation of Polystyrene Plastic under Fluorescent Light*. Environmental Science and Technology 2003, **37**(19): p. 4494-4499.

[25] Kemmitt, T., N.I. Al-Salim, M. Waterland, V.J. Kennedy and A. Markwitz, *Photocatalytic titania coatings*. Current Applied Physics 2004, **4**: p. 189-192.

[26] Childs, L.P. and D.F. Ollis, *Is Photocatalysis Catalytic?* Journal of Catalysis, 1980. **66**: p. 383-390.

[27] Serpone, N. and E. Pelizzetti, *Photocatalysis: Fundamentals and Applications* 1989, New York, NY: John Wiley & Sons, Inc. 3-7. Photocatalysis already defined by J. Plotnikov in his book Allgemeine Photochemie, 2nd ed., Walter de Gruyter, West Berlin, 1936, pp. 362-375.

[28] Hufschmidt, D., L. Liu, V. Seizer and D. Bahnemann, *Photocatalytic water treatment: fundamental knowledge required for its practical application*. Water Science and Technology 2004, **49**(4): p. 135-140.

[29] Prairie, M.R., L.R. Evans, B.M. Stange and S.L. Martinez, *An Investigation of TiO_2 Photocatalysis for the Treatment of Water Contaminated with Metals and Organic Chemicals*. Environmental Science and Technology 1993, **27**(9): p. 1776-1782.

[30] Matsuda, S., H. Hatano and A. Tsutsumi, *Ultrafine particle fluidization and its application to photocatalytic NO_x treatment*. Chemical Engineering Journal 2001, **82**: p. 183-188.

[31] Muszkat, L., L. Feigelson, L. Bir and K.A. Muszkat, *Photocatalytic degradation of pesticides and bio-molecules in water*. Pest Management Science 2002, **58**: p. 1143-1148.

[32] Augugliaro, V., C. Baiocchi, A.B. Prevot, E. Garcia-Lopez, V. Loddo, S. Malato, G. Marci, L. Palmisano, M. Pazzi and E. Pramauro, *Azo-dyes photocatalytic degradation in aqueous suspension of TiO_2 under solar irradiation*. Chemosphere 2002, **49**: p. 1223-1230.

[33] Arslan, I. and I.A. Balcioglu, *Degradation of commercial reactive dyestuffs by heterogeneous and homogeneous advanced oxidation processes: a comparative study*. Dyes and Pigments 1999, **43**: p. 95-108.

[34] Romeas, V., P. Pichat, C. Guillard, T. Chopin and C. Lehaut, *Degradation of palmitic (hexadecanoic) acid deposited on TiO_2-coated self-cleaning glass: kinetics of disappearance, intermediate products and degradation pathways*. New Journal of Chemistry 1999, **23**: p. 365-373.

[35] Nakajima, A, K. Hashimoto, T. Watanabe, K. Takai, G. Yamauchi and A. Fujishima, *Transparent Superhydrophobic Thin Films with Self-Cleaning Properties*. Langmuir 2000, **16**(17): p. 7044-7047.

[36] Mills, A., A. Lepre, N. Elliott, S. Bhopal, I.P. Parkin and S.A. O'Neill, *Characterisation of the photocatalyst Pilkington Activ^{TM}: a reference film photocatalyst?* Journal of Photochemistry and Photobiology A: Chemistry 2003, **160**: p. 213-224.

2 DYE-COATED SAMPLE PREPARATION AND PHOTOREACTOR

In this study, a laboratory photoreactor equipped with 8 GE Blacklight Blue 20W lamps with peak emission at 365 nm was the source for near-UV exposure of dye-coated Degussa P25 titanium dioxide (TiO_2) particles as well as the dye coated photo-inert aluminum oxide (Al_2O_3) particles used for control experiments. Nearly ambient temperature was maintained by fans located near the lamps within the photoreactor. The average UVA (320 to 390 nm) intensity of exposure for all experiments measured with a Traceable® UV Light Meter was 1.3 mW cm^{-2}. Dyes were deposited onto catalyst particles and inert supports in aqueous solution, and the coated particles were captured by centrifugation, dried, and hand ground to powder before near-UV exposure. Sub-monolayer initial dye coverage of support particles was used. Two methods, Indirect and Direct Analysis, were employed to examine the degradation of organic dyes with exposure to near-UV.

During exposure with the Indirect method, samples were subject to ambient humidity and powder samples were shaken in uncovered Petri dishes during the photoreaction in attempt to achieve uniform near-UV exposure of particles. Separate samples for each exposure time were used. Reaction products were dissolved from the support particles into basic aqueous solution, support particles were removed by centrifugation and the resulting solution was analyzed by UV-visible transmission spectroscopy to examine the photoreaction progress. The experimental system and results for this method are discussed in Chapter 3.

The Direct Analysis method allowed for the examination of the same sample throughout the reaction with UV exposure. Dye-coated sample powder was pressed into a sealable

sample holder with a quartz window which allowed for UV exposure and analysis by diffuse reflectance UV-visible spectroscopy. The experimental system and results for this method are discussed in Chapter 4.

2.1 Dye-Coated Sample Preparation

The photocatalytic degradation of four organic dyes was examined by illuminating dye-coated TiO_2 (semiconductor) and Al_2O_3 (insulator) particles with near-UV light in a photoreactor. The following sections detail the chemicals used, estimation of dye coverage on supports, and the preparation of dye-coated samples.

2.1.1 Organic Dyes

Acid Blue 9 (Erioglaucine), Acid Orange 7 (Orange II), Reactive Black 5 (Remazol Black B) and Reactive Blue 19 (Remazol Brilliant Blue R) were purchased from Fisher Scientific and used as received. Dye properties are given in Table 2.1, and Figure 2.1, Figure 2.2, Figure 2.3 and Figure 2.4 depict the dye chemical structures of Acid Blue 9, Acid Orange 7, Reactive Black 5 and Reactive Blue 19 respectively.

Table 2.1 Dyes

dye	CAS No.	molecular formula	molecular and formula[a] weight	MP (°C)	Absorbance (nm)[b]
Acid Blue 9	3844-45-9	$C_{37}H_{34}N_2Na_2O_9S_3$	792.9, 782.9	283[b]	625 - 406
Acid Orange 7	633-96-5	$C_{16}H_{11}N_2NaO_4S$	350.3, 350.32	164[a]	483
Reactive Black 5	17095-24-8	$C_{26}H_{26}N_5NaO_{19}S_6$	927.9, 991.8	> 300[b]	597
Reactive Blue 19	2580-78-1	$C_{22}H_{14}N_2Na_2O_{11}S_3$	624.5, 624.52		592

[a] as reported by Fisher Scientific in certificate of analysis for chemical lot received

[b] as reported by Sigma-Aldrich for CAS No.

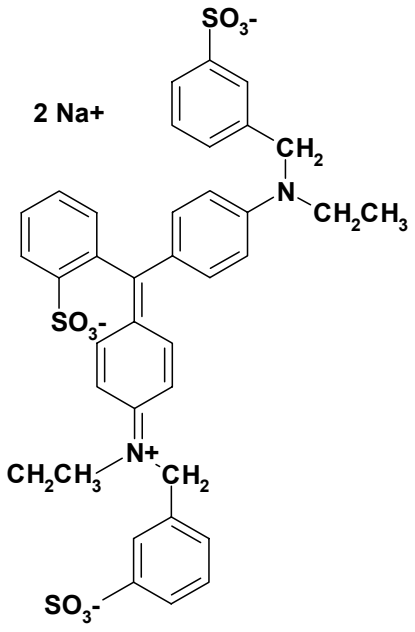

Figure 2.1 Acid Blue 9

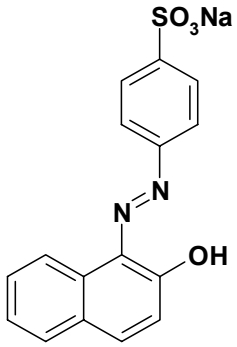

Figure 2.2 Acid Orange 7

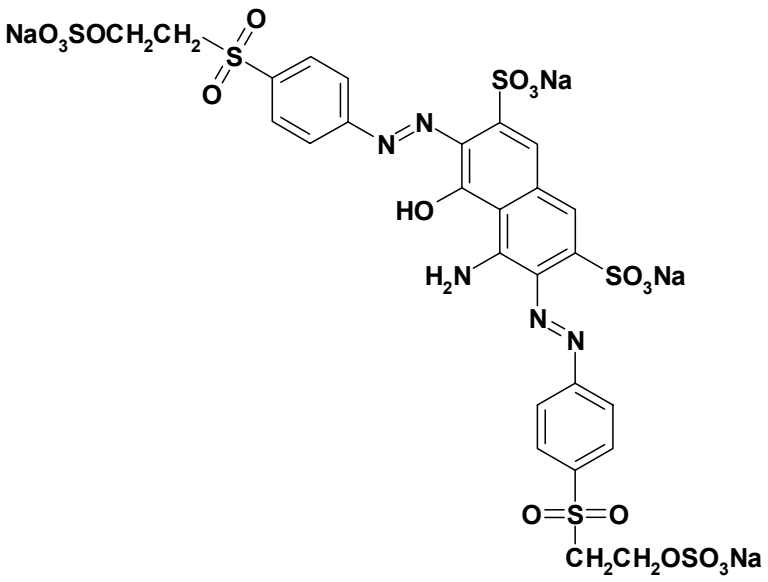

Figure 2.3 Reactive Black 5

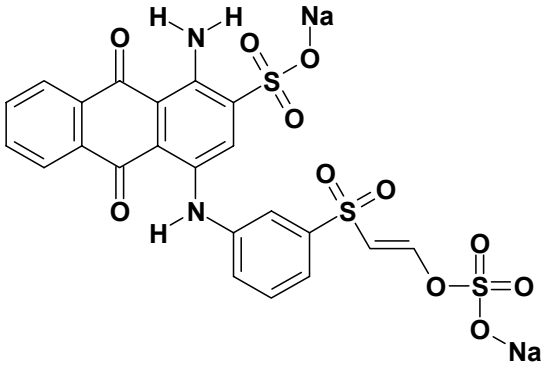

Figure 2.4 Reactive Blue 19

2.1.2 Catalyst and Inert Support

The photocatalyst, Degussa P25 titanium dioxide, was a gift from the Degussa Corporation and was used as received. The company's specifications on the product include a primary particle size of 21 nm and a BET surface area of 50 +/- 15 $m^2 g^{-1}$. Aluminum oxide was the photo inert support employed, with Aeroxide® Alu C also received as a gift

from the Degussa Corporation and used unaltered. The vendor reports typical BET surface area of 100 +/- 15 m^2 g^{-1} for the Al_2O_3 product and an average primary particle size of 13 nm.

2.1.3 Dye Coverage Calculations

The dye coverage on the support particles, titanium dioxide and aluminum oxide, was calculated assuming that the dye molecules sit on the surface of the support particles and on other dye molecules, if multiple layers, as flat circles. The size of the dye molecules was estimated by adding together the average bond lengths, as shown in Table 2.2, forming the main body of the molecule, for example see Figure 2.5.

Table 2.2 Estimation of dye molecular diameters.

bond/molecule	length (Å)	Acid Blue 9	Acid Orange 7	Reactive Black 5	Reactive Blue 19
benzene[a]	2.78	2	2	2	3
C-C in benzene[a]	1.39	1			1
C-C[b]	1.53	3		1	
C-N[b]	1.46	2	2	2	2
C-O[b]	1.42			1	1
C-S[b]	1.82	1	1	2	2
C=C[b]	1.34				1
N=N[b]	1.24		1	1	
S-O[c]	1.70		1	2	2
estimated molecular diameter (Å):		16.28	13.24	19.71	22.45

[a] McMurry, J. Organic Chemistry, 3rd Edition; Brooks/Cole Publishing: Pacific Grove, CA, 1992; pp 533, 536.

[b] "Characteristic Bond Lengths in Free Molecules", CRC Handbook of Chemistry and Physics, 84th Edition, 2003, p. 9-44.

[c] Sum of covalent radii taken from: Shriver, D. F.; Atkins, P.; Langford, C. H. Inorganic Chemistry, 2nd Edition; W. H. Freeman and Co: New York, NY, 1994; pp 58.

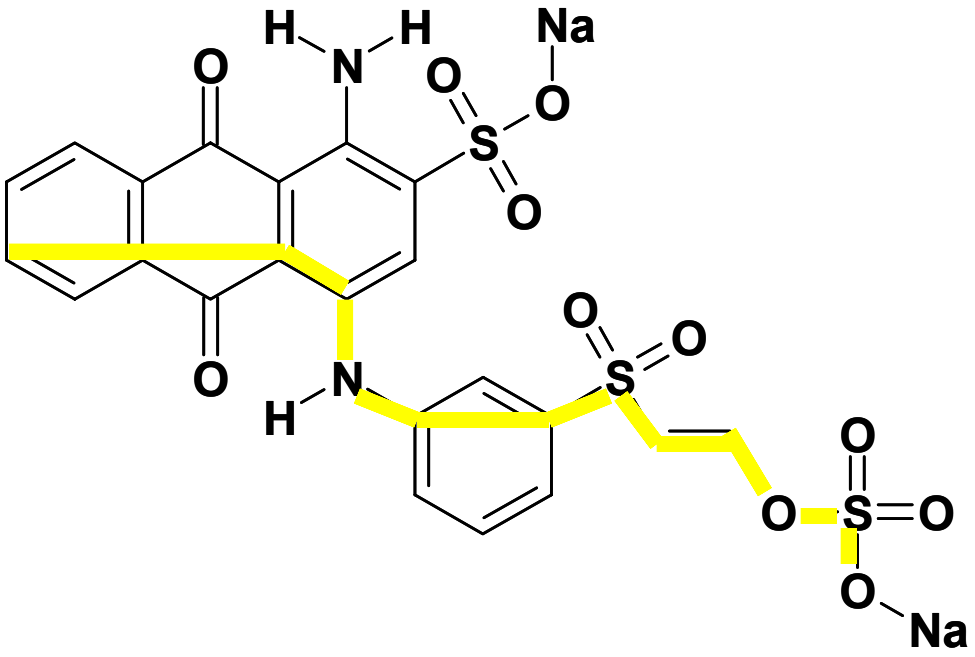

Figure 2.5 Estimation of Reactive Blue 19 size. Main body of molecule shown in thick yellow line.

The average diameter of the dye molecules is approximately 18 angstroms, giving a surface area of $\pi r^2_{molecule} = 2.5 \times 10^{-18}$ m^2 for circular geometry for one molecule or 1.5×10^6 m^2 for one mole. The molar surface area of 1.5×10^6 m^2 was obtained by multiplying the surface area for one molecule by Avogadro's number, therefore the spaces created if circular molecules are arranged without overlap are not accounted for. The average molecular weight of the four dye molecules is 670, therefore the average surface area per g of dye is 2200 m^2. To achieve a monolayer coverage, average concentrations of 0.023 g or 3.4×10^{-5} mol dye per g TiO_2 and 0.045 g or 1.0×10^{-4} mol dye per g Al_2O_3 are required. For our experiments, 0.005 g dye was used in combination with 1.5 g of TiO_2, producing an average dye coverage of approximately 14% of a monolayer for all photocatalytic studies according to these estimates. For the control experiments, 0.005 g dye was used in combination with

0.75 g of Al_2O_3 to achieve the same percent monolayer dye coverage of the support as in the photocatalytic studies.

2.1.4 Preparation of Dye-Coated TiO_2 and Al_2O_3 Particles

The dye coated TiO_2 and Al_2O_3 particles used to examine photodegradation were prepared as follows:

1) Aqueous solutions of the 0.005 g dye and 100 mL of deionized water were placed in clean centrifuge bottles along with a magnetic stir bar. The solution container was closed to prevent evaporation, and covered with aluminum foil to prevent exposure to light.
2) The dye solution was stirred with magnetic stir bar for approximately 30 min to aid dye dissolution.
3) Support particles, TiO_2 or Al_2O_3, were added in the amount of 1.5 g or 0.75 g respectively.
4) The suspension was stirred in the dark overnight for at least 12 h, as reported by Yang et al. [1], to allow the dye adsorption/desorption equilibrium on the support particles to be reached.
5) The magnetic stir bar was removed and the suspensions were centrifuged for 1 h at 10,000 rpm.
6) The water, with what little, if any, dye remaining in solution, was poured off of the dye-coated particles.
7) The dye-coated sample residue was then placed in an oven-safe granite mortar or ceramic dish and dried in a dark oven at 85^{o}C for 4.5 h.

8) The sample was allowed to cool in the dark for 30 min and then ground by hand with a marble or ceramic pestle for 5 min. The sample was stored in an airtight container in the dark until used in UV exposure experiments.

2.1.5 Dye-Coated Powder Samples Prepared

The samples prepared and referred to throughout the following chapters are given in Table 2.3 below.

Table 2.3 Dye-coated powder samples prepared

dye	sample	dye (g)	TiO_2 (g)	Al_2O_3 (g)
Acid Blue 9	ABa	0.0054	1.50	
	ABb	0.0051	1.51	
	ABc	0.0053	1.56	
	AAB	0.0056		0.795
Acid Orange 7	AOa	0.0057	1.51	
	AOb	0.0055	1.52	
	AOc	0.0056	1.53	
	AAO	0.0053		0.770
Reactive Black 5	RBka	0.0058	1.51	
	RBkb	0.0053	1.50	
	RBkc	0.0054	1.56	
	ARBk	0.0055		0.758
Reactive Blue 19	RBa	0.0052	1.51	
	RBb	0.0052	1.51	
	RBc	0.0050	1.53	
	ARB	0.0055		0.760

2.2 Photoreactor

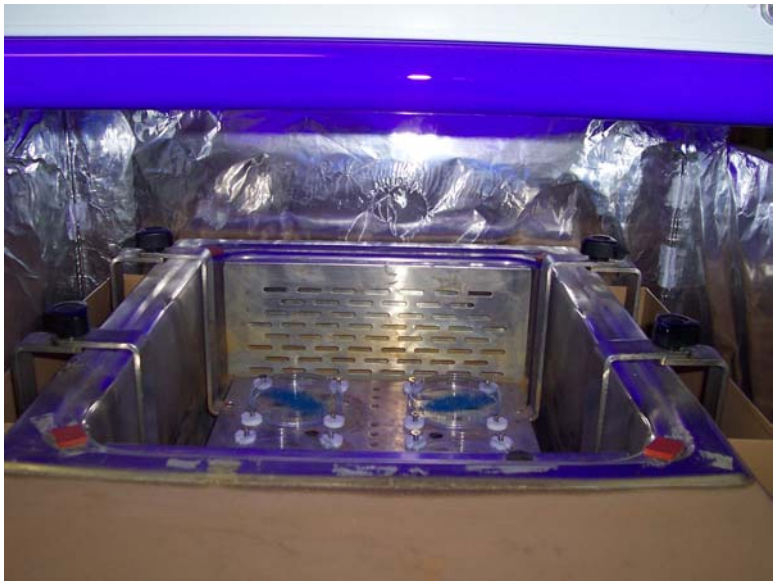

Figure 2.6 Photoreactor with shaker.

Dye-coated TiO_2 and Al_2O_3 powders were illuminated with near-UV light, peak emission at 365 nm, in the photoreactor shown in Figure 2.6. The same reactor was used for the Indirect Analysis and Direct Analysis methods. The reactor houses 8 GE Blacklight Blue 20W lamps arranged side by side to create a light source roughly 0.6 m long, the length of each lamp, by 0.4 m wide. Fans are located near the ends of the lamps within the reactor and operated whenever the lamps were on to maintain temperatures close to average room temperature within the photoreactor. A shaker, which had a platform that could be shook in a circular motion at variable speeds or kept stationary, was placed inside the reactor. The platform, on which samples could be placed, was 0.3 m from the lamps. Four Petri dish holders were mounted to the platform; at each of these locations the light intensity was measured with a Traceable® UV Light Meter. For all experiments, the reactor was turned on 15 min before exposure of samples began to obtain a steady illumination power output

that was then measured with the light meter immediately before UV exposure began, and again before the reactor was turned off for the day. The average UVA intensity for all experiments reported was 1.3 mW cm^{-2}. Black felt cloth was used as a cover for the reactor when the lamps were on to protect both the samples during exposure as well as people in the laboratory.

2.3 References

[1] Yang, T.C.-K., S.-F. Wang, S.H.-Y. Tsai and S.Y. Lin, *Intrinsic photocatalytic oxidation of the dye adsorbed on TiO_2 photocatalysts by diffuse reflectance infrared Fourier transform spectroscopy*. Applied Catalysis B: Environmental 2001, **30**: p. 293-301.

3 EXPERIMENTAL: INDIRECT ANALYSIS

Because visible stain removal was the goal of this research, we chose to examine, by UV-visible spectroscopy, the disappearance of the original colored dye with near-UV illumination by comparison with unexposed controls. The Indirect Analysis approach to examining the photocatalytic degradation of organic dyes by TiO_2, evident by color removal, involved exposing dye-coated particles to UV, desorbing reaction products into aqueous solution, and then using the resulting solution for UV-visible spectroscopic analysis. The method was indirect in that for each illumination time examined, a different sample was needed and the spectroscopic analysis was not done on the sample as exposed, but on an altered (dissolved) state of the sample. A benefit of this approach to examining the system is that the analysis method, transmission UV-visible spectroscopy, is a technique commonly used in laboratories around the world and widely available to most scientists. The Direct Analysis method, discussed in Chapter 4, relies on diffuse reflectance UV-visible spectroscopy, is not as commonly used, nor easily used in a field measurement. This chapter explains the Indirect Analysis method used for exposure of dye-coated TiO_2 particles, sample preparation for UV-visible spectroscopy and UV-visible analysis and data analysis. Experimental results are presented in two forms: (1) digital photography images depicting color removal with UV illumination of the dye-coated TiO_2 powders, and (2) UV-visible spectra showing changes in absorbance with UV exposure.

3.1 UV Illumination of Dye-Coated TiO_2 Powders

Dye-coated TiO_2 powders were illuminated with near-UV light in the reactor described in Chapter 2. The samples analyzed by this method include ABa, ABb, AOa,

AOb, RBka, RBkb, RBa and RBb. The dye-coated powders were exposed the day after the samples were dried and ground by hand, and therefore the second day following the initial preparation of dye/catalyst suspensions. The photoreactor was turned on for 15 min prior to sample illumination, and the light intensity of all four Petri dish holder locations was measured prior to and after exposure. For UV illumination, approximately 0.13 g of the dye-coated TiO_2 sample was spread onto the bottom of a sterile polystyrene Petri dish. The Petri dishes used were 8.5 cm in diameter, although the sample did not cover the entire dish. Powder samples were shaken, with the shaker set at 250 rpm according to its dial, in uncovered Petri dishes during the photoreaction in attempt to achieve uniform UV exposure of particles. Uniform UV illumination was not achieved for all illumination times examined. Non-uniform UV illumination was visually evident because the color removal was not uniform and the particles would clump and stick to the Petri dish, which did not allow the particles to rotate. The particles clumped and stuck to the Petri dish more noticeably at the longer exposure times. This could be because with increased UV exposure and the slight heating that consequentially occurred, the particles were more likely to stick together and to the Petri dish surface, essentially being dried to the surface. Another possibility is that the non-uniform UV illumination, and therefore non-uniform color removal, occurred for all illumination times, but was visually more apparent as the color removal increased with UV exposure. During UV exposure, samples were subject to ambient humidity, and nearly ambient temperature was maintained by fans located near the lamps within the photoreactor. Separate portions of the original powder samples were reacted for various illumination times in the same position in the photoreactor for time

periods of 0, 5, 10, 20, 40, 60, 90, 120 and 240 min. All exposed samples were removed from the Petri dishes and stored in the dark in airtight glass vials.

3.2 Results: Images of Color Removal

Photographs taken with a Kodak EasyShare CX6330 3.1 mega-pixel camera of the dye-coated TiO_2 powders illuminated with UV light for the indicated periods from 0 to 4 hr are shown in Figure 3.1 and Figure 3.2. Change in color is immediately evident as the illumination time progresses from 0 to 5 min of UV exposure. Color removal is readily apparent by comparing the unexposed sample to the sample exposed for 4 hr. As mentioned in the previous section, samples exposed for longer periods had less uniform illumination and therefore less uniform reaction occurring throughout the sample, evident in the colored and white speckles in the samples illuminated for 4 hr.

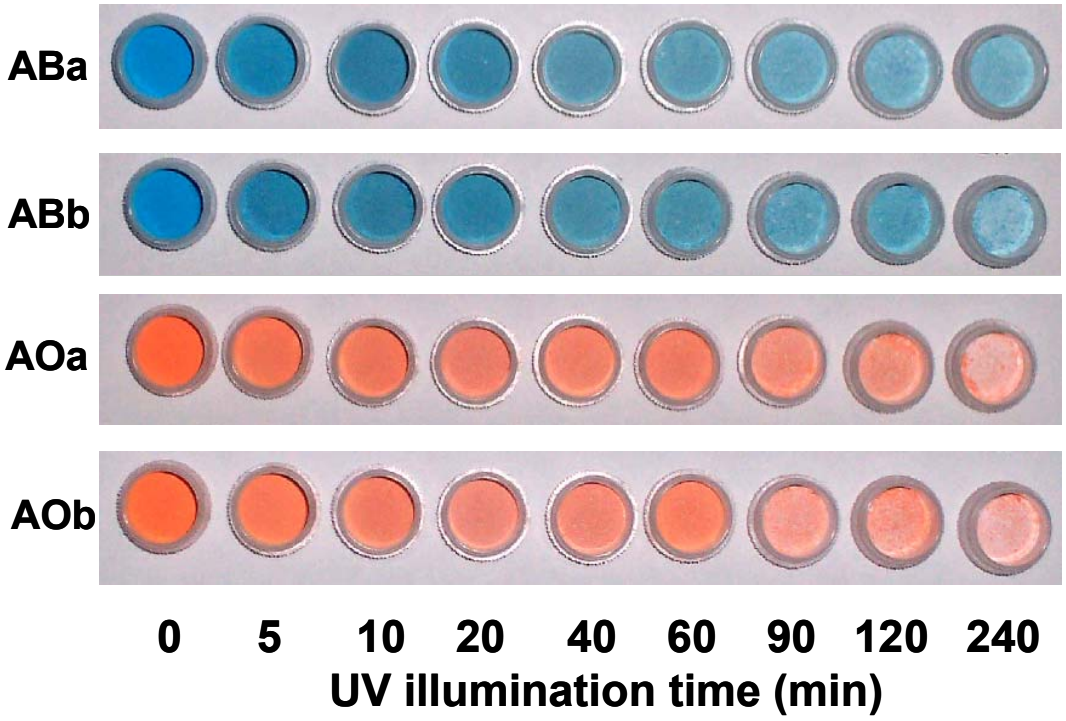

Figure 3.1 Indirect Analysis: Color removal of Acid Blue 9 and Acid Orange 7 on TiO_2.

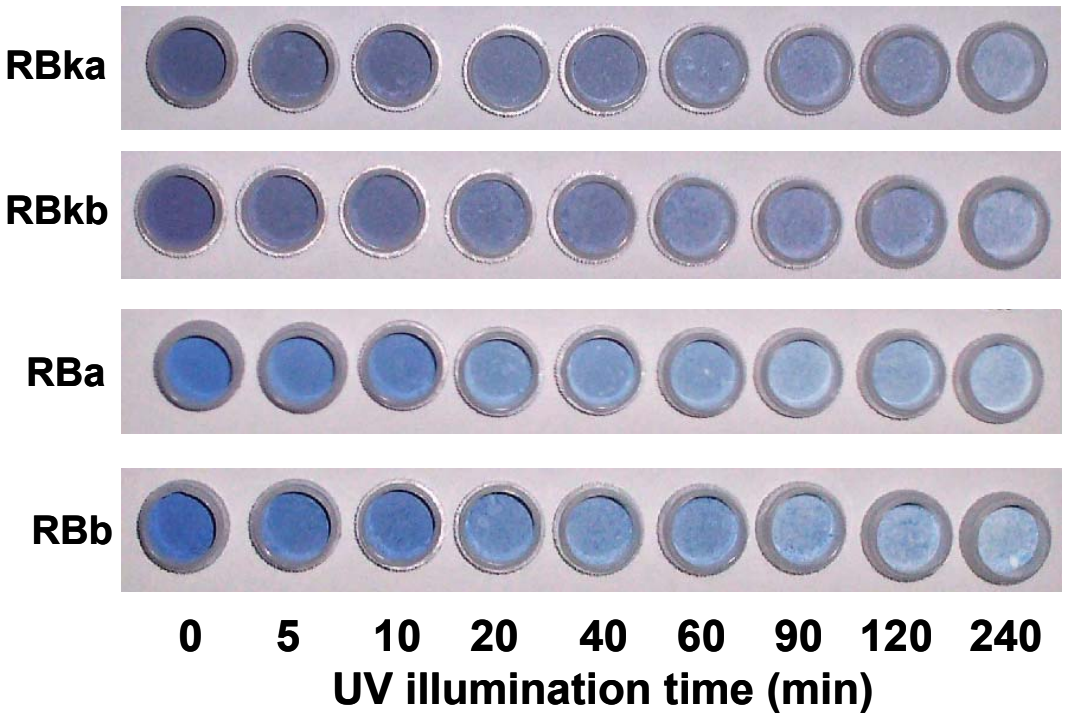

Figure 3.2 Indirect Analysis: Color removal of Reactive Black 5 and Reactive Blue 19 on TiO_2.

3.3 Preparation of Solutions for UV-visible Transmission Spectroscopy

Reaction products were desorbed from the TiO_2 support into aqueous solution to examine changes in dye concentration with near-UV illumination by UV-visible transmission spectroscopy. Suspensions were prepared in disposable polypropylene centrifuge tubes comprising 30 mg of dye-coated TiO_2 sample, 3 mL of deionized water and 20 μL 1 N sodium hydroxide aqueous solution. The dye and reaction products contribute very little to the entire weight of the powder sample, and therefore the same weight was used to compare samples within a set. A set refers to samples originating from the same unexposed dye-coated TiO_2 sample. The sodium hydroxide concentration used, not taking into account any contributions from the reaction products, made the suspension pH 12. A suspension was prepared for each of the 9 UV illumination times within a set. The suspensions were shaken in the dark for at least 20 hr to allow the reaction products to desorb from the photocatalyst. The white TiO_2 particles were then separated from the dye solution by centrifugation at 10,000 rpm for 45 min. The solutions were stored in the dark until spectroscopic analysis, which was done the same day.

3.4 UV-visible Transmission Spectroscopy

The disappearance of the original colored dye and changes in colored intermediate concentrations with near-UV illumination by comparison with unexposed controls was monitored by UV-visible transmission spectroscopy. The photo-oxidation kinetics of the dye-solid systems was investigated with a Jasco V-550 UV-visible spectrophotometer. A mixture of 3 mL deionized water and 20 μL 1 N sodium hydroxide aqueous solution was used as the reference in the two beam system. Absorbance (Abs) measurements of sample

solutions in methacrylate cuvettes, 1 cm pathlength (b), were taken from 200 to 800 nm. Analysis of the data obtained is given in the next subsection.

3.4.1 UV-visible Transmission Spectroscopy Data Analysis

Data analysis, based on the Beer-Lambert law (Abs=αbC), was performed by first determining a wavelength of maximum Abs for each dye to be used for analysis of the calibration data as well as the sample data. Baseline corrected Abs was obtained by subtracting the baseline drawn by connecting the endpoints of the peak of highest absorbance, shown in Figure 3.3 as the dashed line, from the sample Abs at the chosen wavelength. The molar absorptivity (α_D), units of L mol^{-1} cm^{-1}, of each dye was determined by fitting a straight line through zero to data of baseline corrected Abs at the chosen wavelength versus molar concentration (C) of calibration solutions prepared in pH 12 sodium hydroxide aqueous solutions. The wavelengths and molar absorptivities for each dye are given in Table 3.1. Spectra of Acid Blue 9 and Reactive Black had multiple peaks of Abs, and Table 3.1 gives α_D at two wavelengths for each of these dyes.

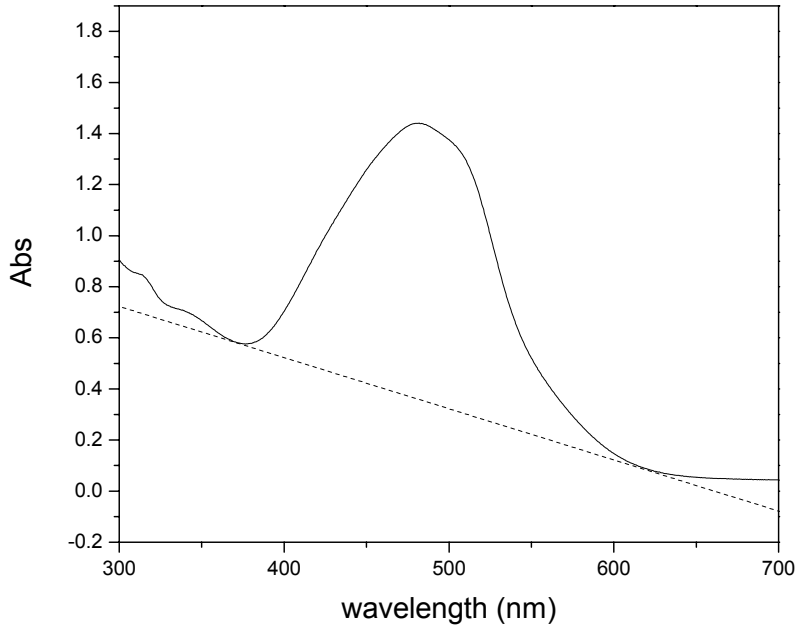

Figure 3.3 Spectral baseline.

Table 3.1 Wavelengths of maximum absorbance and molar absorptivities for dyes

dye	wavelength (nm)	α_D (L mol^{-1} cm^{-1})
Acid Blue 9	629 408	37852 4432
Acid Orange 7	485	8346
Reactive Black 5	617 317	24116 14101
Reactive Blue 19	596	4618

3.4.2 Results: UV-visible Transmission Spectra

UV-visible spectroscopy was used to monitor changes in unreacted dye concentration with near-UV illumination compared to unexposed controls. UV-visible spectroscopy is not a technique used to obtain detailed information about the chemical structure of a sample or chemical changes that are occurring with reaction. The technique is useful to examine the disappearance of a species with reaction, as well as to determine if

new species are being formed that absorb within the UV-visible region. Baseline corrected spectra obtained for all samples are shown in Figure 3.4 through Figure 3.11. These spectra show that the general trend with UV exposure is a decrease in the original dye concentration, seen by comparing the Abs for the wavelengths given in Table 3.1 of unexposed samples to the succession of exposed samples. Some of the closely spaced decay curves in Abs are out of sequence with exposure time, but this is likely an artifact of error occurring in the exposure and analysis method. The inconsistencies in order of Abs decay with UV illumination time are not consistent in duplicate experiments, supporting the theory that experimental error led to the non-ideal results. Another explanation for the non-sequential Abs, discussed in more detail in Chapter 5, is that intermediates could form that also absorb light in the same region, but then decompose with further exposure. With the images in section 3.2, we have shown that color removal of organic dyes is possible with the presumed photocatalytic reaction occurring on TiO_2. To explain the change in dye concentration with reaction, kinetic models using the spectroscopic data were developed and are tested and discussed in Chapters 5 and 6.

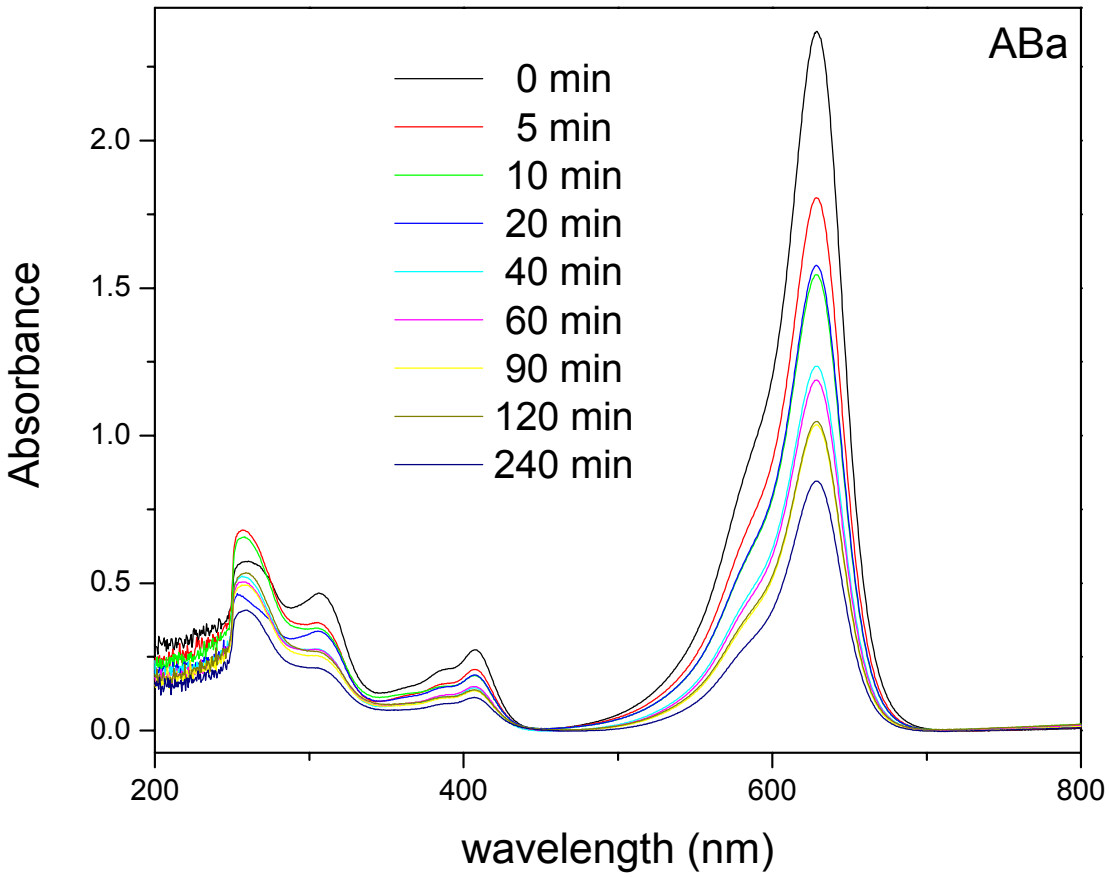

Figure 3.4 Indirect Analysis: UV illumination from 0 to 4 hr of Acid Blue 9 on TiO_2 (ABa)

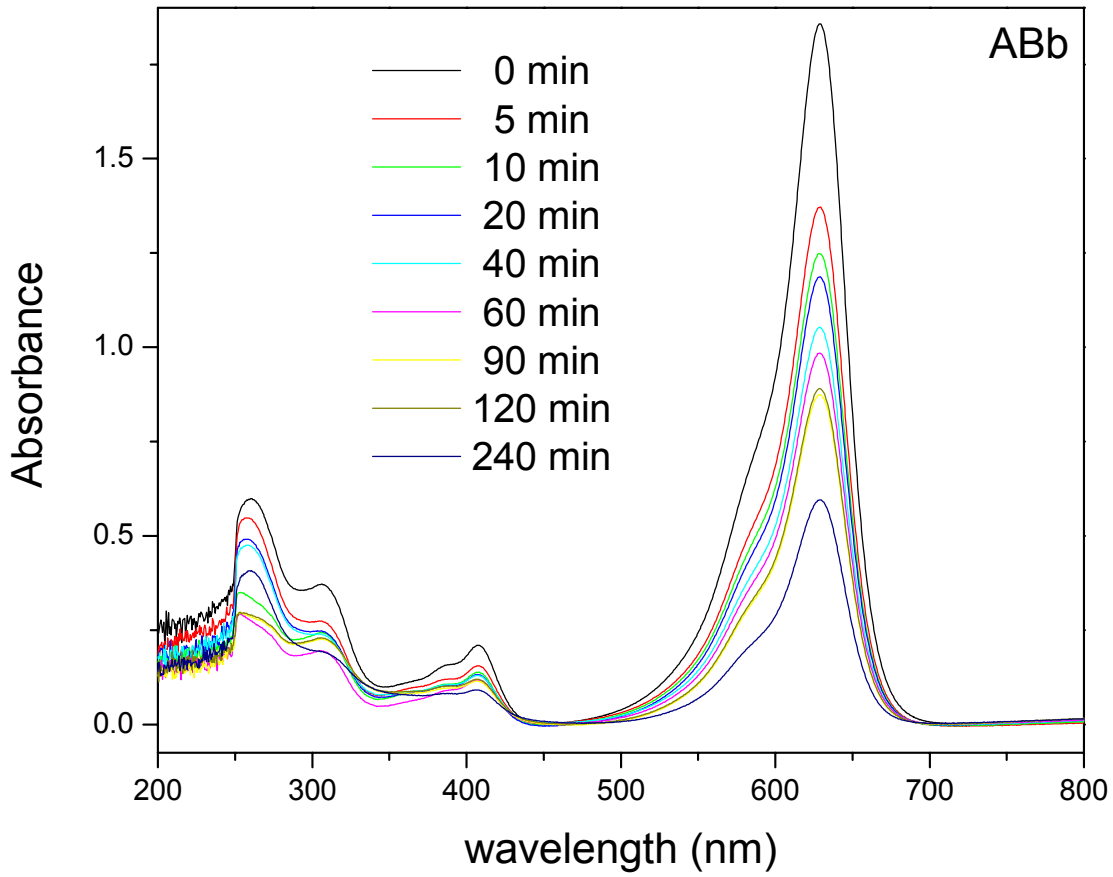

Figure 3.5 Indirect Analysis: UV illumination from 0 to 4 hr of Acid Blue 9 on TiO_2 (ABb)

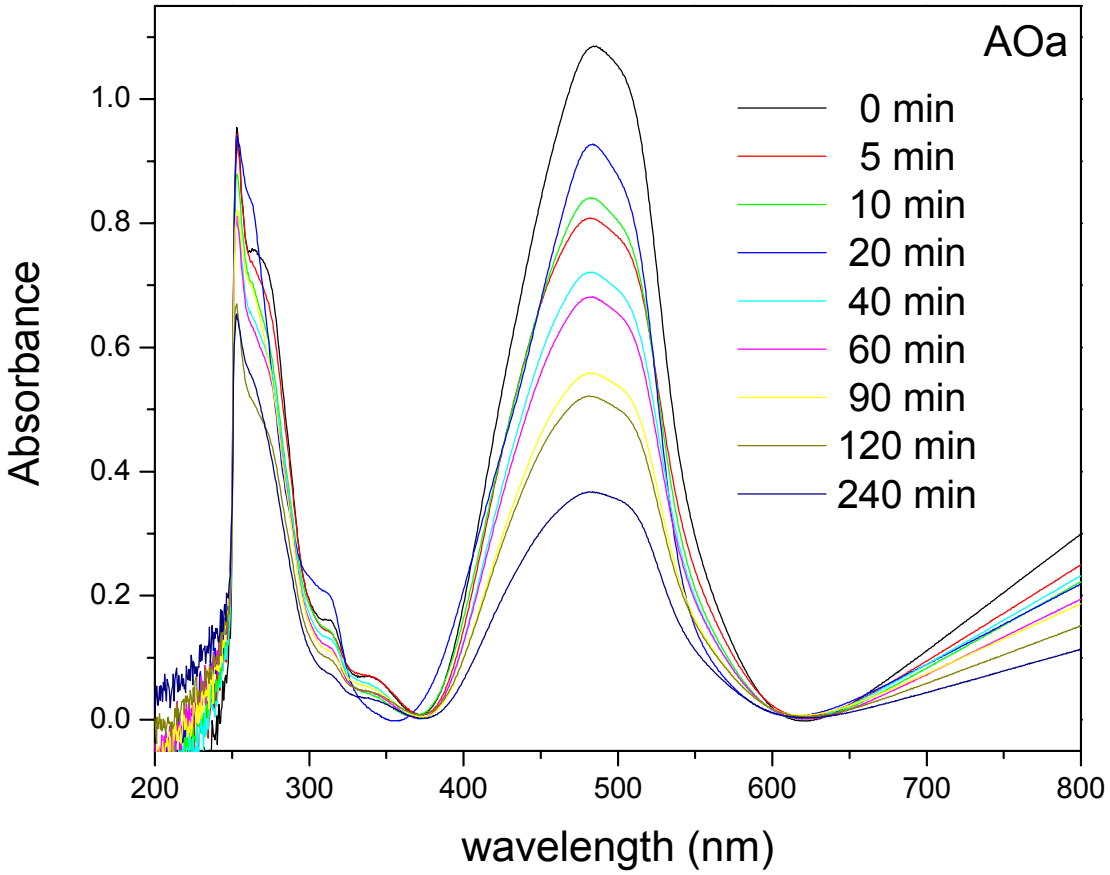

Figure 3.6 Indirect Analysis: UV illumination from 0 to 4 hr of Acid Orange 7 on TiO_2 (AOa)

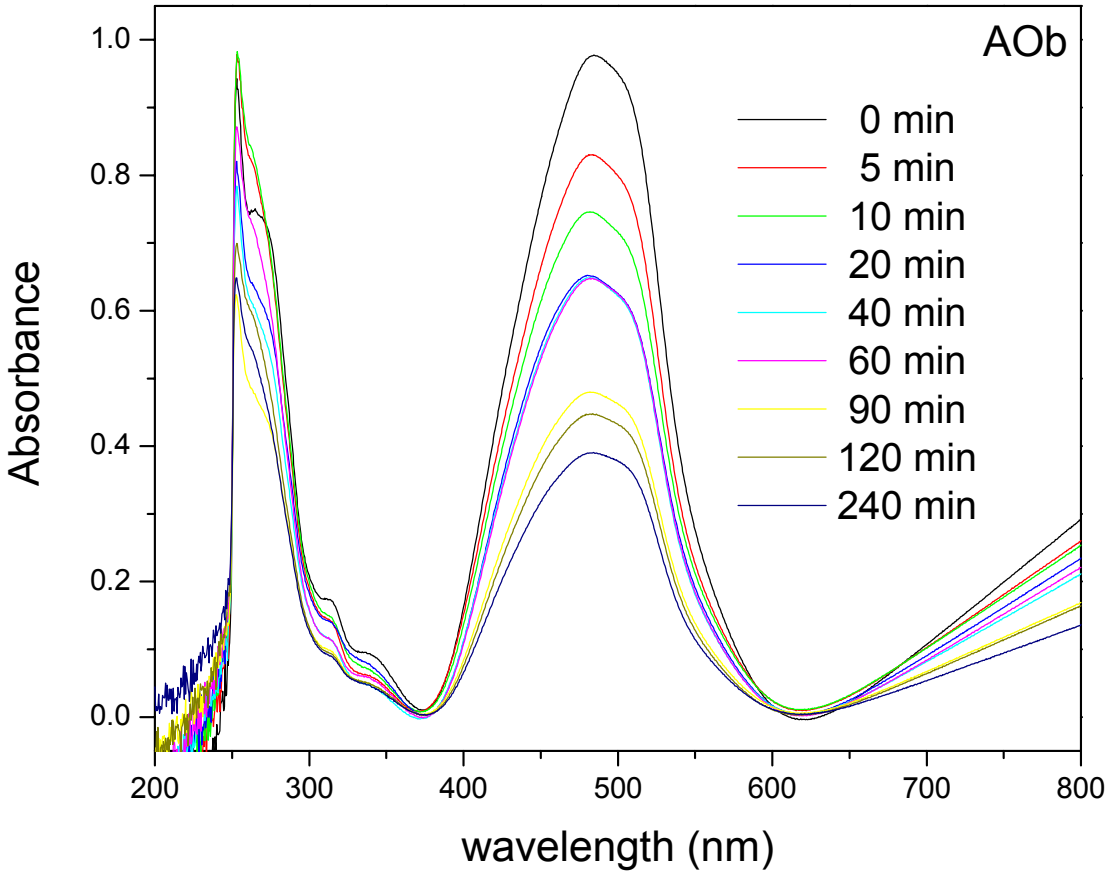

Figure 3.7 Indirect Analysis: UV illumination from 0 to 4 hr of Acid Orange 7 on TiO_2 (AOb)

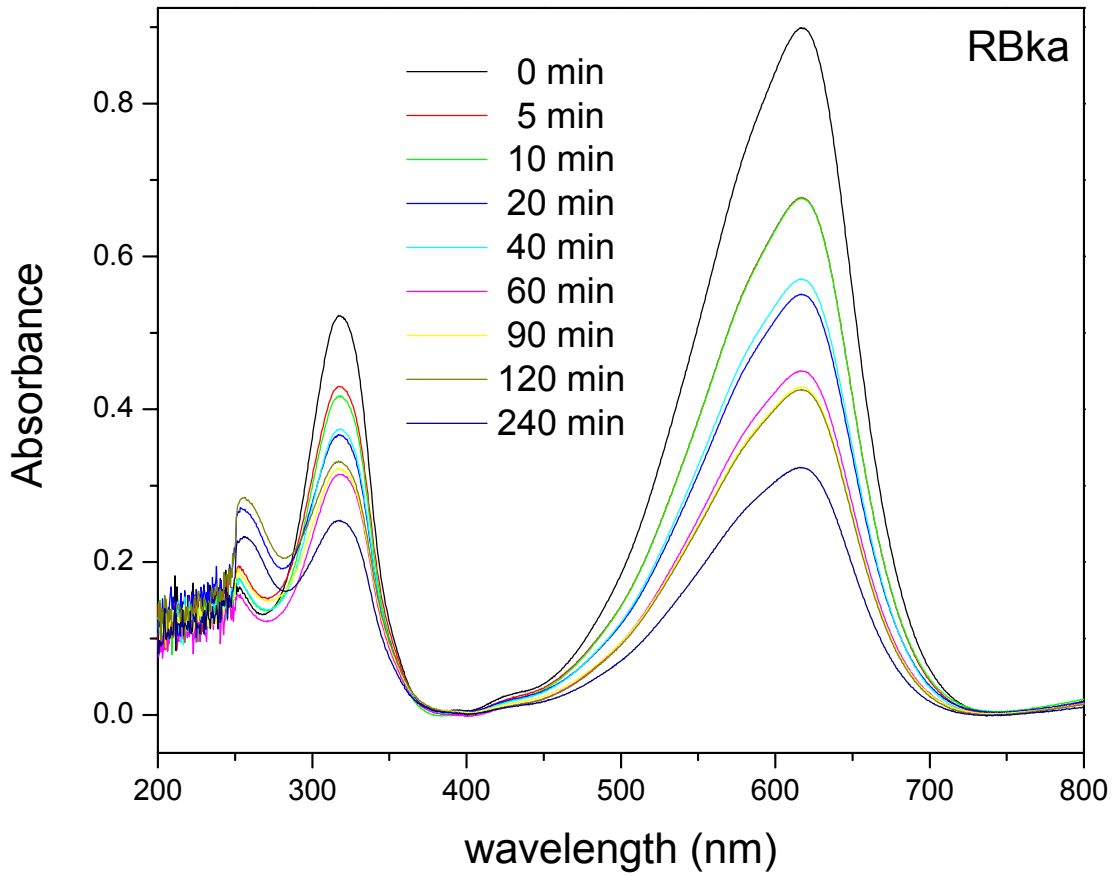

Figure 3.8 Indirect Analysis: UV illumination from 0 to 4 hr of Reactive Black 5 on TiO_2 (RBka)

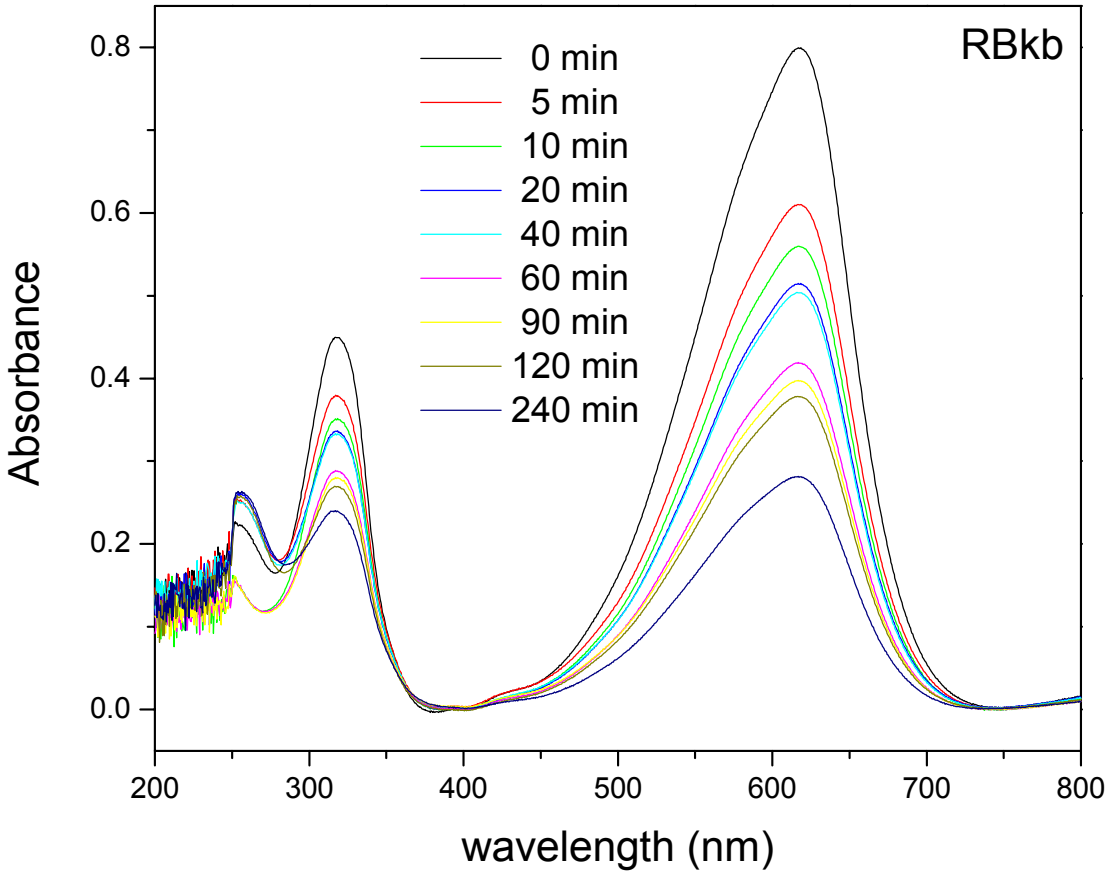

Figure 3.9 Indirect Analysis: UV illumination from 0 to 4 hr of Reactive Black 5 on TiO_2 (RBkb)

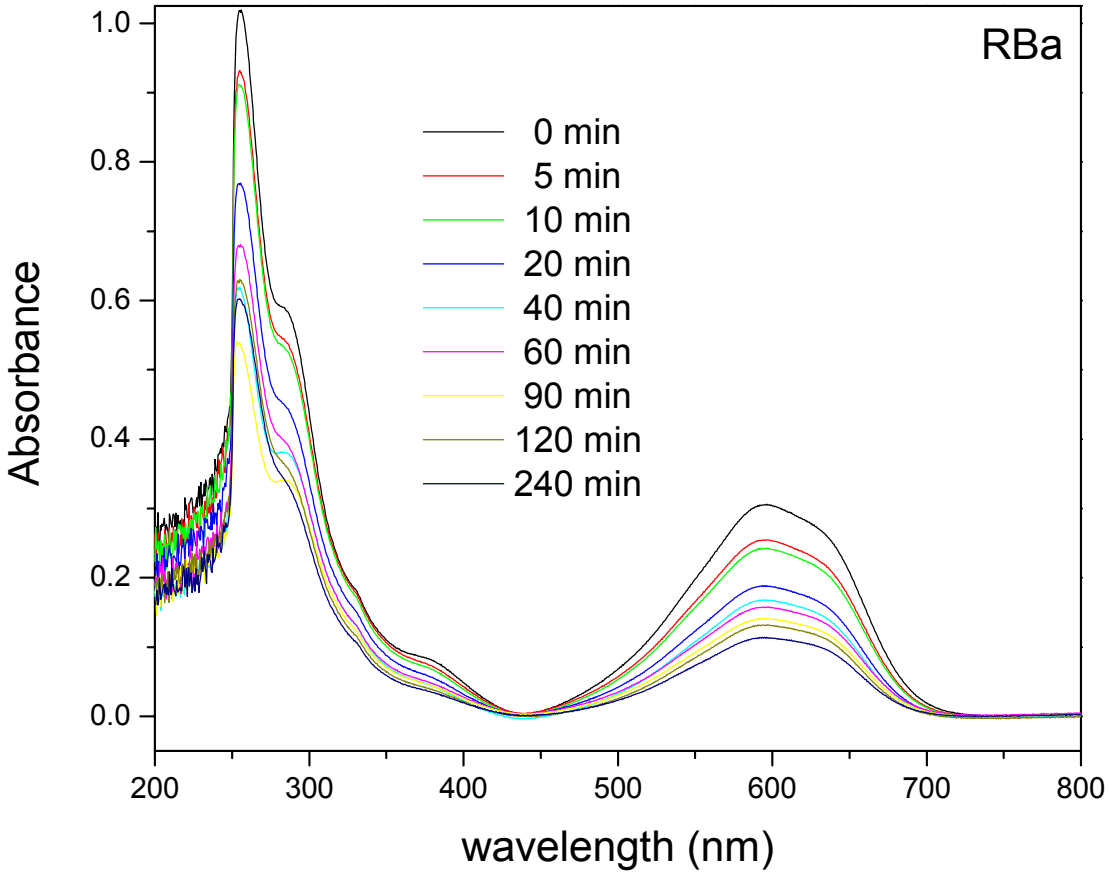

Figure 3.10 Indirect Analysis: UV illumination from 0 to 4 hr of Reactive Blue 19 on TiO_2 (RBa)

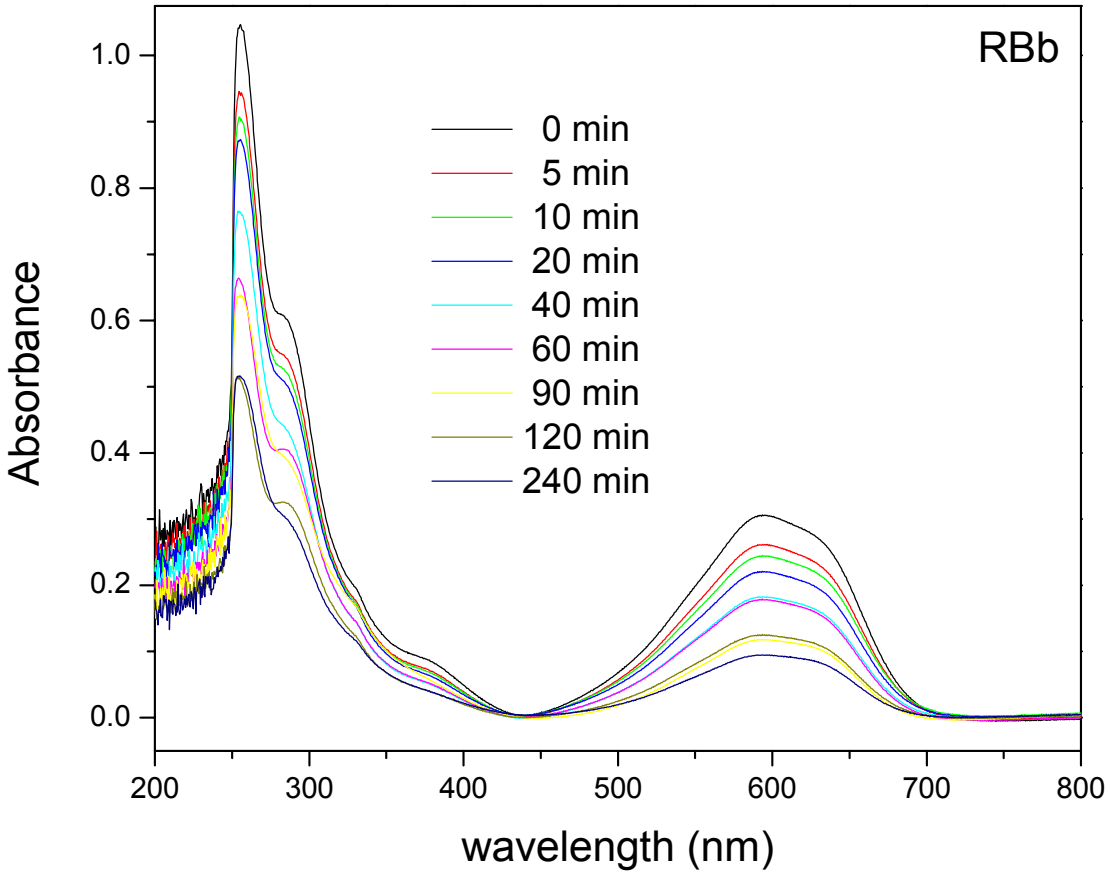

Figure 3.11 Indirect Analysis: UV illumination from 0 to 4 hr of Reactive Blue 19 on TiO_2 (RBb)

4 EXPERIMENTAL: DIRECT ANALYSIS

The Indirect Analysis approach (Chapter 3) to examining the photocatalytic degradation of adsorbed organic dyes was developed first. The method used equipment that was readily available, but involved multiple steps leading to the final analysis of the reaction with the possibility of inconsistencies and error existing with each step. Using the Direct Analysis method of the present chapter, it was possible to follow dye concentration changes in the same sample with UV illumination, and the reaction could be examined in the adsorbed state in which it occurred. The method involved illuminating dye-coated TiO_2 powders pressed into a closed sample holder with near-UV light through a quartz window, then monitoring changes in dye concentration by diffuse reflectance UV-visible spectroscopy. The term in-situ is not used here because the sample holder and sample were taken out of the photoreactor, theoretically stopping the reaction, for analysis by diffuse reflectance. The exposure and analysis method is described, with explanation of how the reflectance data was transformed and graphical representation of spectra obtained. Visual evidence of color removal is shown in photographs taken as UV illumination time progressed.

4.1 UV Illumination and Diffuse Reflectance UV-visible Spectroscopy of Dye-Coated TiO_2 Powders

Dye-coated TiO_2 powders were illuminated with near-UV light in the reactor described in Chapter 2. Samples analyzed by this method include ABa, ABc, AOa, AOc, RBkb, RBkc, RBa and RBc. The reflectance measurements were taken using a Jasco V-550 UV-visible spectrophotometer with an ISV-469 integrating sphere attachment. The integrating sphere attachment allows for the collection of light reflected in all directions.

The reaction and analysis was performed using 90 mg of dye-coated TiO_2 powder pressed into a powder sample holder (PSH-001) purchased from Jasco. The sample holder was a circular piece of quartz glass 0.014 m in diameter housed in a metal frame, with a plunger attached to a cap screwed on by hand to press the powder into a stationary position. When the holder is completely closed, the maximum sample thickness allowed is 0.001 m (1 mm). Photocatalytic reactions are induced by the absorption of light by the catalyst particle of light with energy equal to or greater than its bandgap, promoting an electron from the valence band to the conduction band. The photoexcited electron (e^-) is then available for reduction reactions and the photoproduced hole (h^+) created is available for oxidation reactions, if the inefficient process of electron/hole recombination does not occur. The bandgap of TiO_2, predominantly in its anatase form, is about 3.2 eV [1-3] or approximately 385 nm, therefore photocatalysis can occur with absorption of light of wavelength less than or equal to 385 nm. The reactor illuminates samples with near-UV light most intense at 365 nm, an ideal lamp reactor for TiO_2 photocatalysis studies. During the Direct Analysis method, the goal was to allow the reaction to occur in the reactor, to stop the reaction after the period of illumination by removal from the reactor, and then to analyze the samples by UV-visible diffuse reflectance spectroscopy. The diffuse reflectance spectra obtained were limited to the range from 390 nm to 800 nm for the Acid Blue 9, Reactive Black 5 and Reactive Blue 19 samples so that the photocatalytic reaction would not be propagated during the analysis. The spectra obtained for Acid Orange 7 was extended to 380 nm to include a feature that changed near 390 nm, and the range was shortened to end at 700 nm. Transformation of the reflectance data to obtain concentration information is given in the following subsection.

4.1.1 UV-visible Diffuse Reflectance Data Analysis

The reflectance data obtained was percent reflectance relative to a white standard reflectance plate made of nonabsorbing material that optimally diffuses light. P. Kubelka and F. Munk developed a theory for the diffuse reflectance of powdered samples published in 1931 and 1948, referenced by Fuller and Griffiths in 1978 [4]. Equation 4.1 is the Kubelka-Munk equation for an "infinitely thick" layer [4], where R_∞ is the absolute reflectance of the layer, s is the scattering coefficient and k is the molar absorption coefficient.

$$f(R_\infty) = \frac{(1-R_\infty)^2}{2R_\infty} = \frac{k}{s}$$

Equation 4.1 Kubelka-Munk equation

The absolute reflectance can not be obtained because a standard that diffuses all light has not yet been developed, so the ratio (R_∞') of the reflectance obtained for the sample to the standard is used. The data obtained from the Jasco instrument was this ratio in percent form, therefore R_∞' was easily obtained. P. Kortum published work in 1963, referenced by Fuller and Griffiths [4], showing that for samples of low concentration on supports or in media with low absorption in the spectroscopic region analyzed; k and thus $f(R_\infty)$ vary linearly with concentration, C. Thus,

$$k = 2.303\alpha C$$

Equation 4.2 Molar absorption coefficient

where α is the molar absorptivity and C is the molar concentration. Therefore the reflectance data obtained can be related to sample concentrations in much the same way as absorbance is by the Beer-Lambert law, by Kubelka-Munk (KM) units described in Equation

4.3, where $b' = 2.303/s$. All of the reflectance data was transformed to *KM* units, so that the data could be treated in a manner similar to the absorbance (Abs) data obtained by the Indirect Analysis method when kinetic modeling was done. The transformed spectra are shown in the following subsection.

$$KM = f(R'_\infty) = \frac{(1 - R'_\infty)^2}{2R'_\infty} = \frac{k}{s} = \alpha b' C$$

Equation 4.3 Kubelka-Munk units

4.1.2 Results: UV-visible Diffuse Reflectance Spectra

The reflectance spectra obtained, converted to *KM* units for all of the dye-coated TiO_2 samples studied by the Direct Analysis method, are depicted in Figure 4.1 through Figure 4.8 on the following pages. All of the samples show a sequential profile decrease in *KM* units, and thus a decrease in dye concentration in succession with UV illumination time. It is important to note, and it will be discussed in more detail in Chapter 5, that the spectral features of the unexposed samples for all dyes are slightly different than the spectra for the exposed samples within a set. Both of the unexposed Acid Blue 9 coated TiO_2 samples, shown in Figure 4.1 and Figure 4.2, have lower *KM* units in the region between 440 nm and 490 nm than the illuminated samples. Also, there is a more pronounced peak at 410 nm for the unreacted sample than the reacted samples. The Acid Orange 7 samples illuminated for 0 min and 1 min in Figure 4.3 and Figure 4.4 both have what appears to be a peak within a peak, but this feature disappears with more UV exposure. A pronounced point with a shoulder exists in the unexposed Reactive Black 5 coated TiO_2 samples, represented in Figure 4.5 and Figure 4.6, but this feature disappears with the photocatalyzed reaction. The *KM* units at approximately 440 nm for both of the Reactive Blue 19 samples, shown in

Figure 4.7 and Figure 4.8 with no UV exposure in the reactor are lower than the *KM* units for the samples illuminated for 1 min. The Reactive Blue 19 samples also have a peak with a shoulder at 600 nm that disappears with illumination. Possible reasons for these differences in spectral features will be discussed in the kinetic modeling chapters.

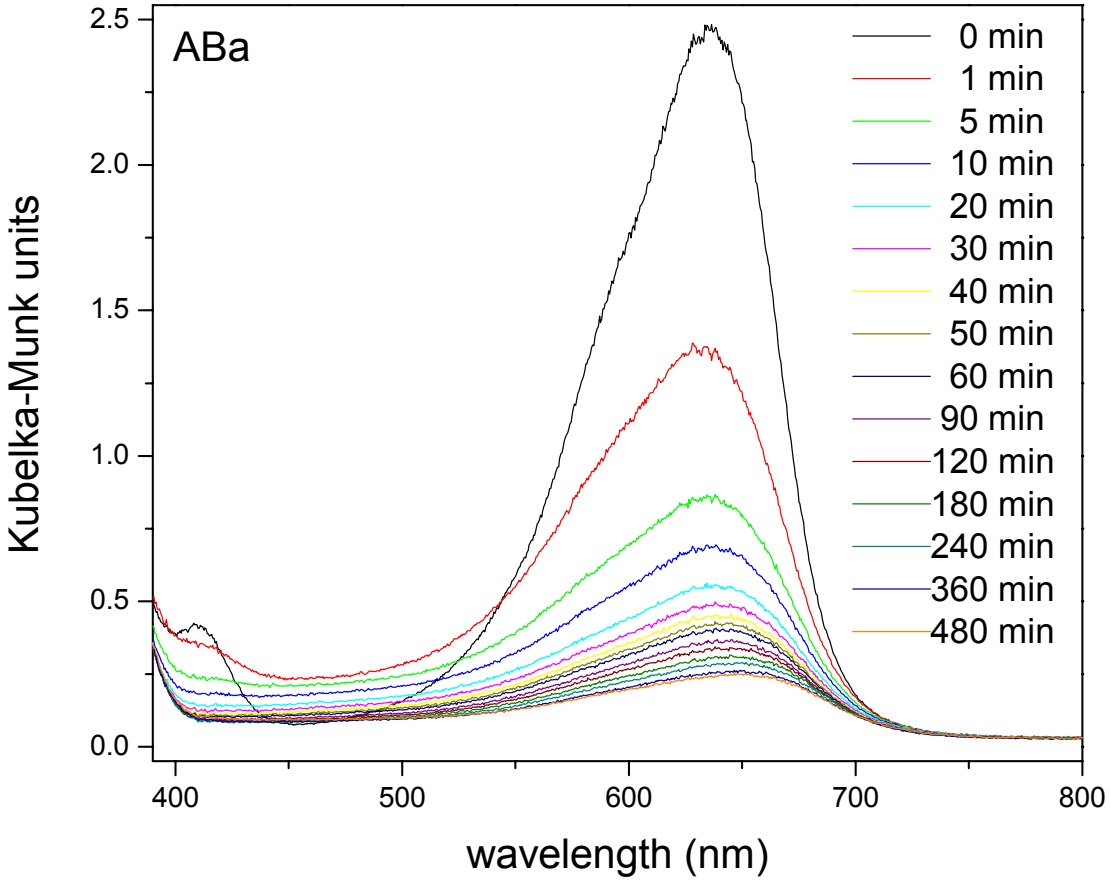

Figure 4.1 Direct Analysis: UV illumination from 0 to 8 hr of Acid Blue 9 on TiO_2 (ABa)

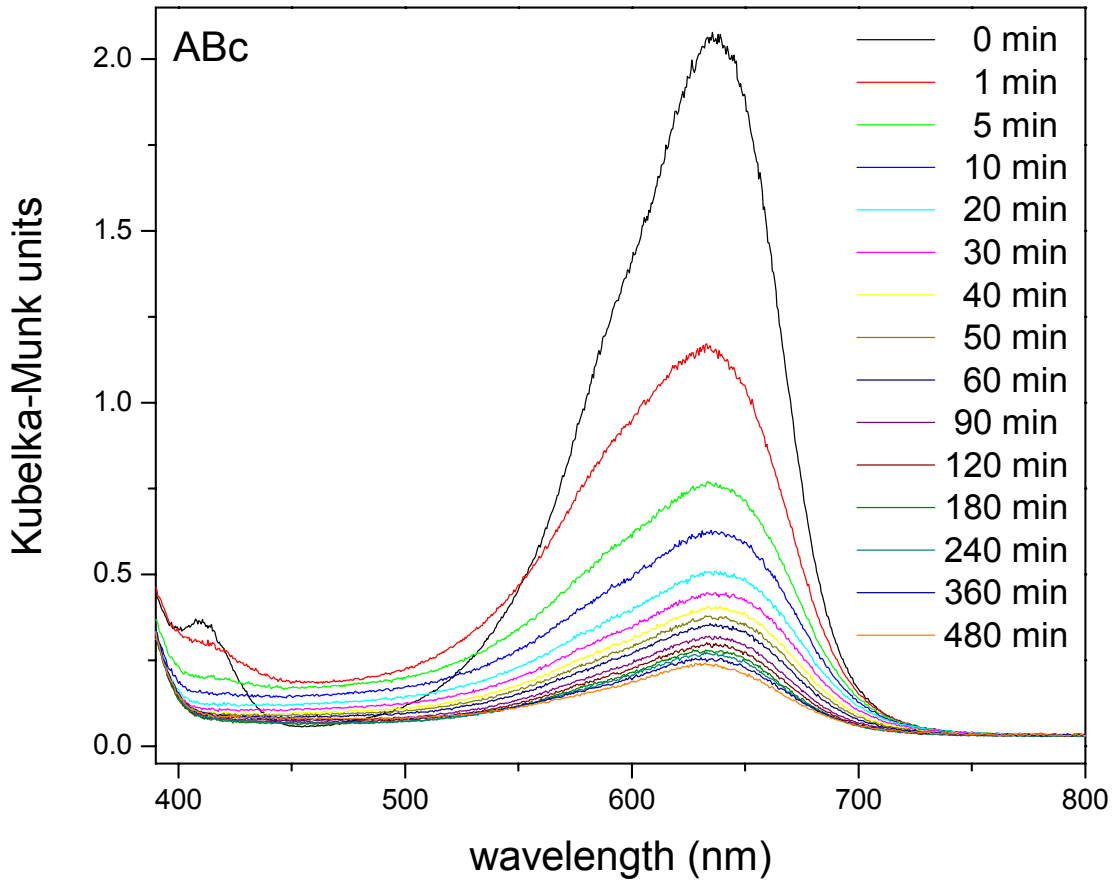

Figure 4.2 Direct Analysis: UV illumination from 0 to 8 hr of Acid Blue 9 on TiO_2 (ABc)

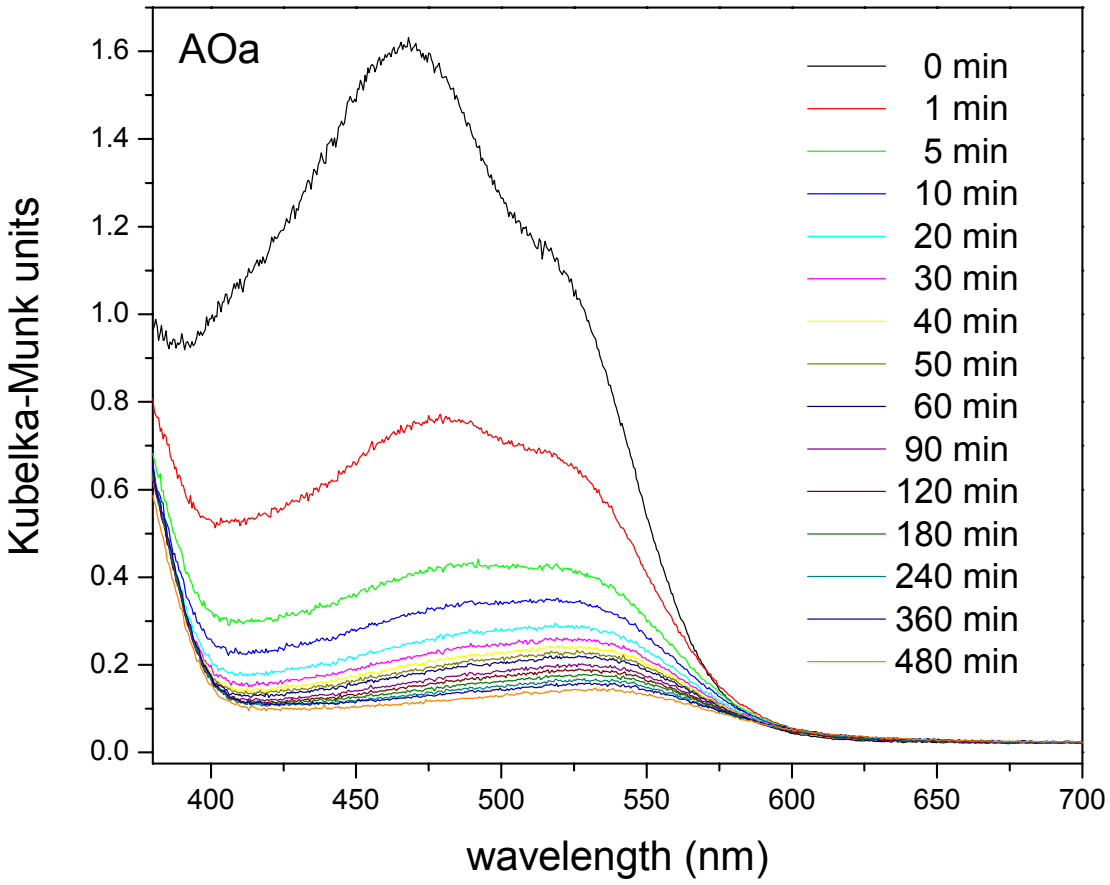

Figure 4.3 Direct Analysis: UV illumination from 0 to 8 hr of Acid Orange 7 on TiO_2 (AOa)

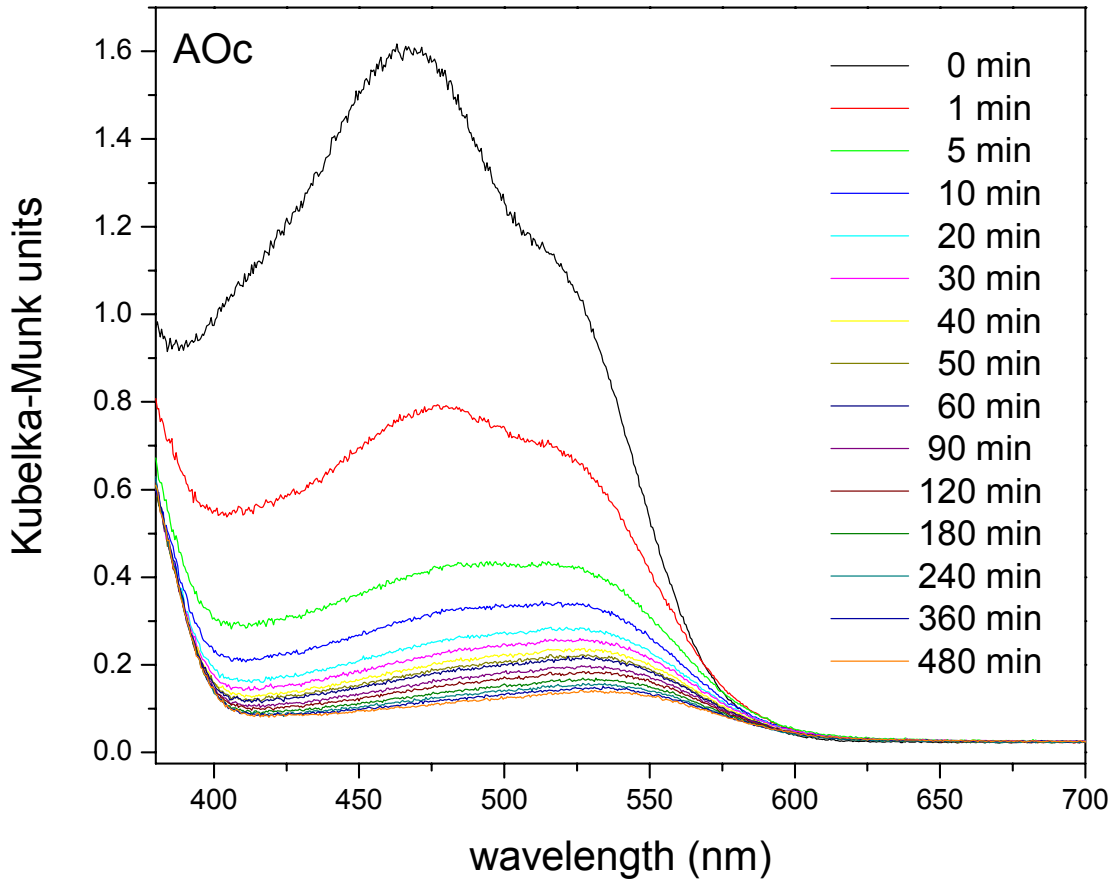

Figure 4.4 Direct Analysis: UV illumination from 0 to 8 hr of Acid Orange 7 on TiO_2 (AOc)

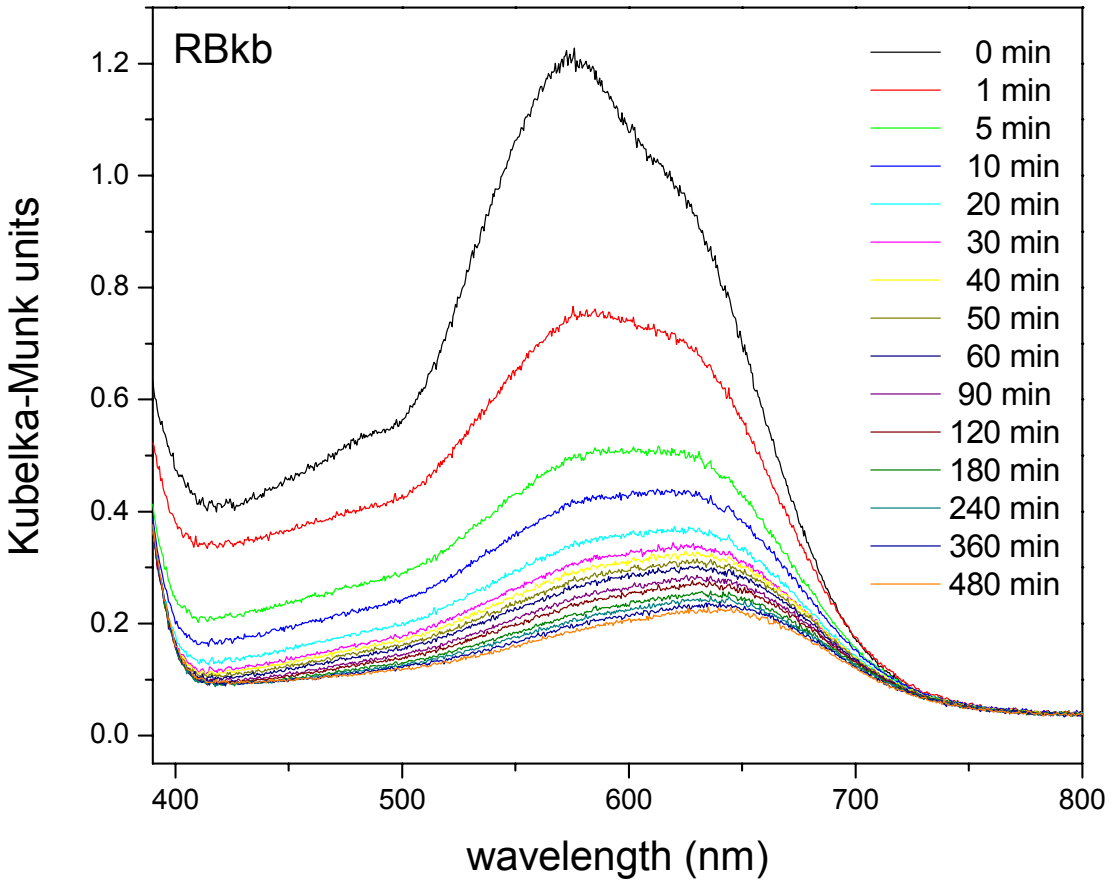

Figure 4.5 Direct Analysis: UV illumination from 0 to 8 hr of Reactive Black 5 on TiO_2 (RBkb)

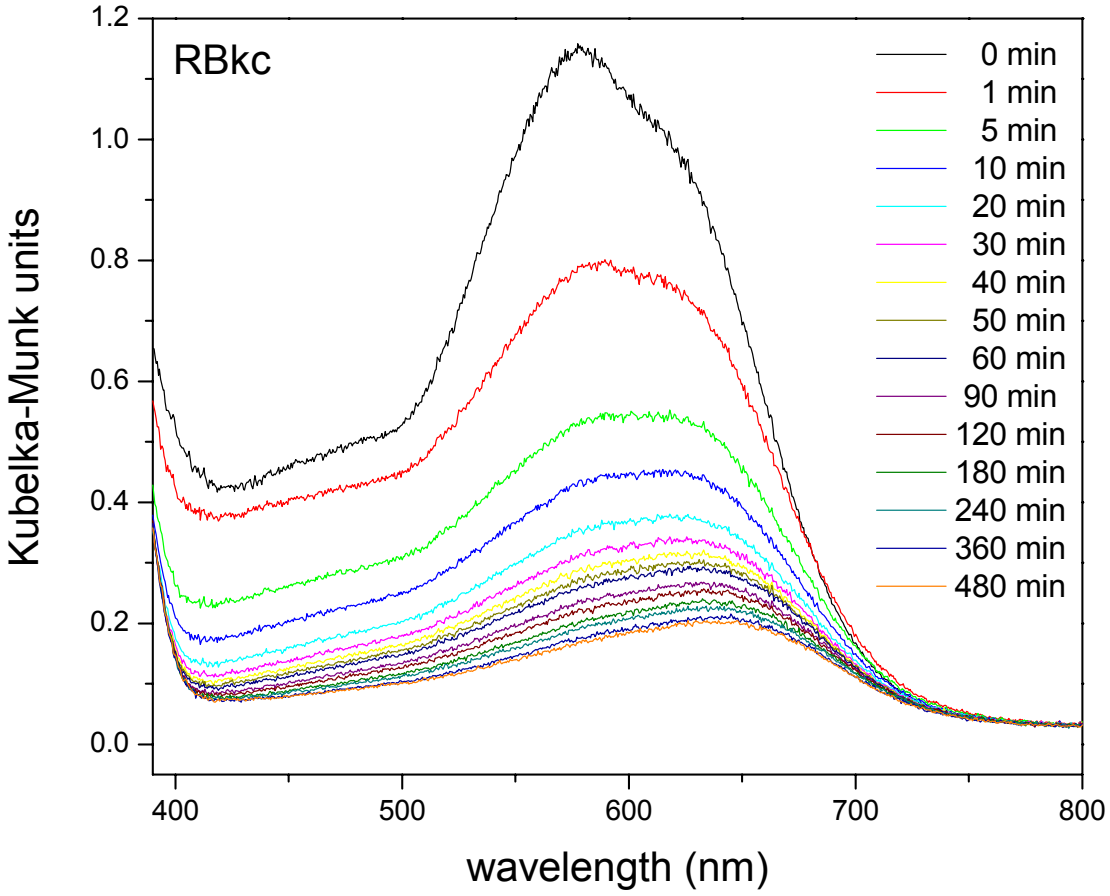

Figure 4.6 Direct Analysis: UV illumination from 0 to 8 hr of Reactive Black 5 on TiO_2 (RBkc)

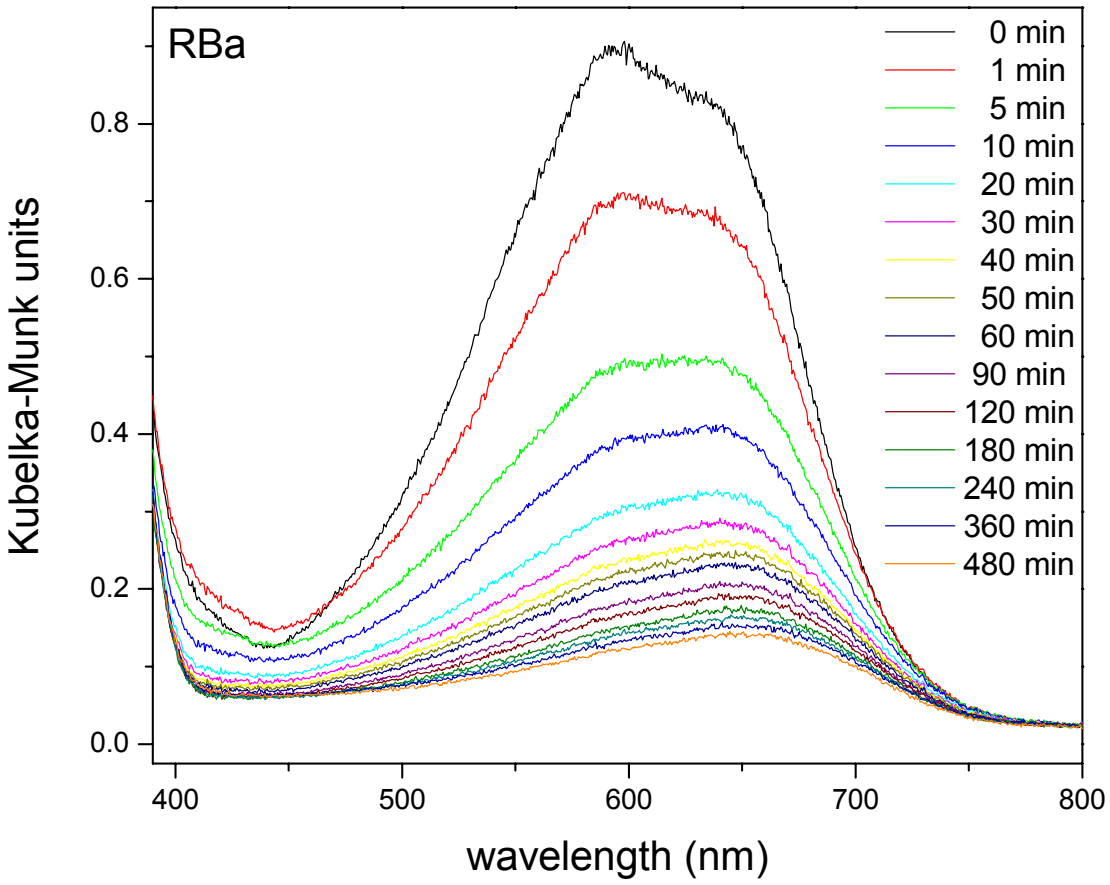

Figure 4.7 Direct Analysis: UV illumination from 0 to 8 hr of Reactive Blue 19 on TiO_2 (RBa)

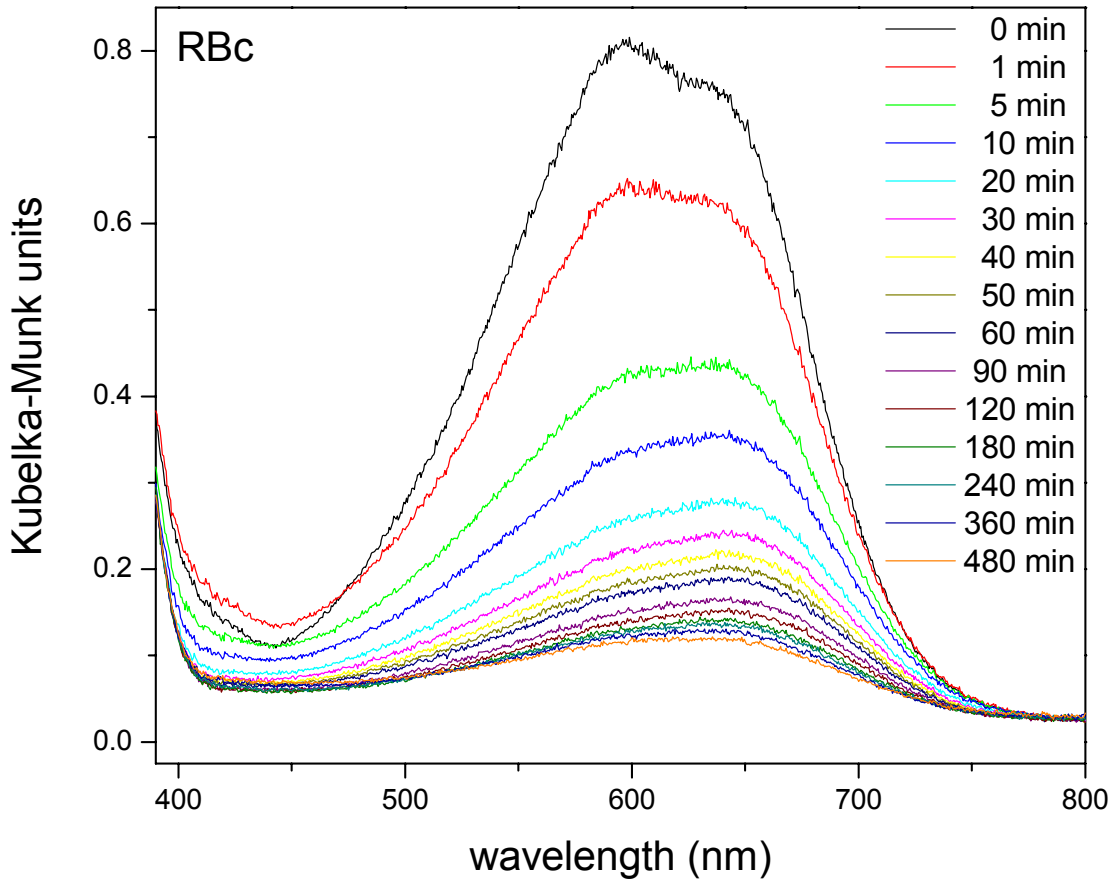

Figure 4.8 Direct Analysis: UV illumination from 0 to 8 hr of Reactive Blue 19 on TiO_2 (RBc)

4.2 Results: Images of Color Removal

Visual evidence of color removal with UV illumination of dye-coated TiO_2 powders is shown in Figure 4.9 and Figure 4.10. The photographs, taken with a Kodak EasyShare CX6330 3.1 mega-pixel camera, show each of the eight samples (ABa, ABc, AOa, AOc, RBkb, RBkc, RBa and RBc) before UV illumination and after 8 hr of exposure. The removal of color was the driving force for this work, as it is applicable to self-cleaning surfaces.

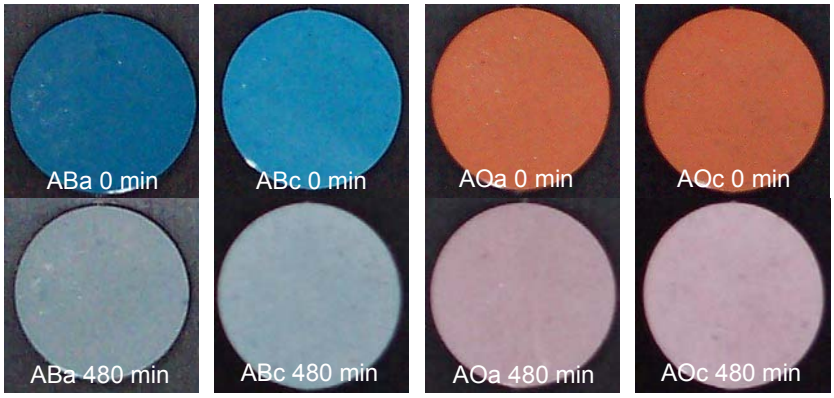

Figure 4.9 Visual evidence of color removal with UV illumination of Acid Blue 9 and Acid Orange 7 coated TiO_2 powders

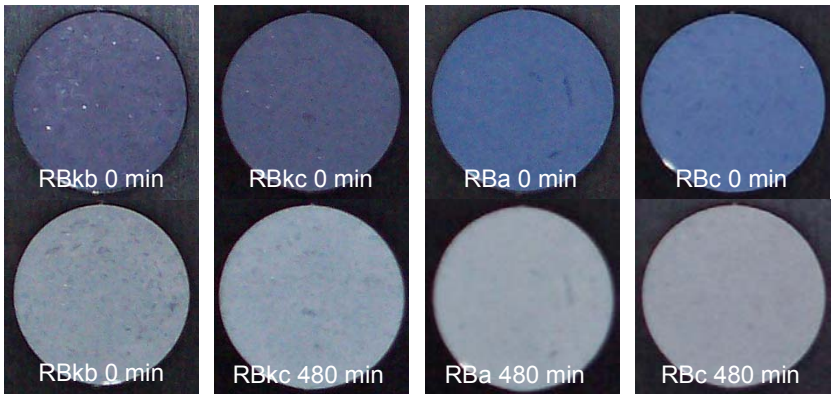

Figure 4.10 Visual evidence of color removal with UV illumination of Reactive Black 5 and Reactive Blue 19 coated TiO_2 powders

4.3 References

[1] Lee, S.-K., S. McIntyre and A. Mills, *Visible illustration of the direct, lateral and remote photocatalytic destruction of soot by titania*. Journal of Photochemistry and Photobiology A: Chemistry 2004, **162**: p. 203-206.

[2] Zielinska, B., J. Grzechulska, R.J. Kalenczuk and A.W. Morawski, *The pH influence on photocatalytic decomposition of organic dyes over A11 and P25 titanium dioxide*. Applied Catalysis B: Environmental 2003, **45**: p. 293-300.

[3] Hufschmidt, D., L. Liu, V. Seizer and D. Bahnemann, *Photocatalytic water treatment: fundamental knowledge required for its practical application*. Water Science and Technology 2004, **49**(4): p. 135-140.

[4] Fuller, M.P. and P.R. Griffiths, *Diffuse Reflectance Measurements by Infrared Fourier Transform Spectrometry*. Analytical Chemistry 1978, **50**(13): p. 1906-1910.

5 MODELING PHOTOCATALYZED DYE DEGRADATION: SERIES REACTION MECHANISM

Literature reports that photocatalytic dye oxidation reactions in liquid systems can be described by first order reaction models with respect to dye concentration [1-4]. Lachheb et al. [1] successfully fit their data for the photocatalytic degradation of five dyes (Methylene Blue, Orange G, Alizarin S, Methyl Red, Congo Red) in water to a first order reaction model. The average first order rate constant for four of the dyes, excluding Congo Red, was 0.0504 min^{-1}. The standard deviation for the first order rate constants obtained for the photocatalytic degradation of Methylene Blue, Orange G, Alizarin S and Methyl Red was 10% of the average rate constant for all four dyes, which is similar to the standard deviation (11%) of the molecular weights of these dyes. The rate constant obtained for the degradation of Congo Red was approximately half the value of the average for the other four dyes, while the molecular weight of the dye was about twice the average of the others, suggesting that the size of a molecule plays a role in its photocatalytic degradation rate. Tanaka et al. [2] concluded that the mechanism for the photocatalytic degradation of azo dyes in water was an oxidative process and that the first order rate constants for six dyes varied less than a factor of three. Tarasov et al. [3] report first order kinetic models for the photocatalytic oxidation of Methylene Blue, Direct Green 6, Acid Yellow 42 and Acid Yellow 11 in aqueous systems, stating that the rate of color removal depends on the dye and the intensity of UV illumination. Yang et al [4] fit the photodegradation of Acid Blue 9 by TiO_2 in an aqueous system at various pH conditions to a first order reaction model with respect to dye concentration, shown in their Figure 5. The researchers also examined the

solid state system of Acid Blue 9-coated TiO_2 by diffuse reflectance Fourier transform infrared spectroscopy, virtually eliminating mass transfer effects, but did not report a kinetic model to fit their data. Using our kinetic analysis, the reflectance data obtained by Yang et al. [4] will also be fit to our models developed, to determine if work done by other researchers is consistent with ours. The conditions of the experiments by Yang et al. [4] vary from the experiments reported in this study, for example the intensity of UV illumination was 15 mW cm^{-2} compared to 1.3 mW cm^{-2}, but the trends of the reaction data should be similar.

5.1 First Order Single Step Reaction

The reaction data obtained in this study was modeled to the single step first order reaction of dye going to product(s) with a batch reactor model, shown in Equation 5.1 with C_D indicating dye concentration, t is time and k' is the first order rate constant. The absorbance (Abs) data obtained by the Indirect Analysis method was transformed to dye concentration using the Beer-Lambert law, assuming that the Abs was due only to the dye. The reflectance data was fit in a similar manner using Kubelka-Munk units, described in Chapter 4.

$$\frac{dC_D}{dt} = -k'C_D$$

Equation 5.1 First order batch reactor model

Figure 5.1 is an example of this fit for data obtained by the Indirect Analysis method for the photocatalytic color removal of Acid Blue 9 on TiO_2. The data does not fall on a straight line and therefore does not fit this simple first order reaction model for the entire period of UV illumination examined. Instead, the semilog plot of Abs vs. time shows two regions,

(dashed lines) suggesting a two step reaction model. Literature reports [1-4] that the photocatalytic degradation of organic dyes fits a first order reaction model with respect to dye concentration, which is consistent with the results found in this study, although we report a two step reaction mechanism to explain our photocatalytic oxidation data.

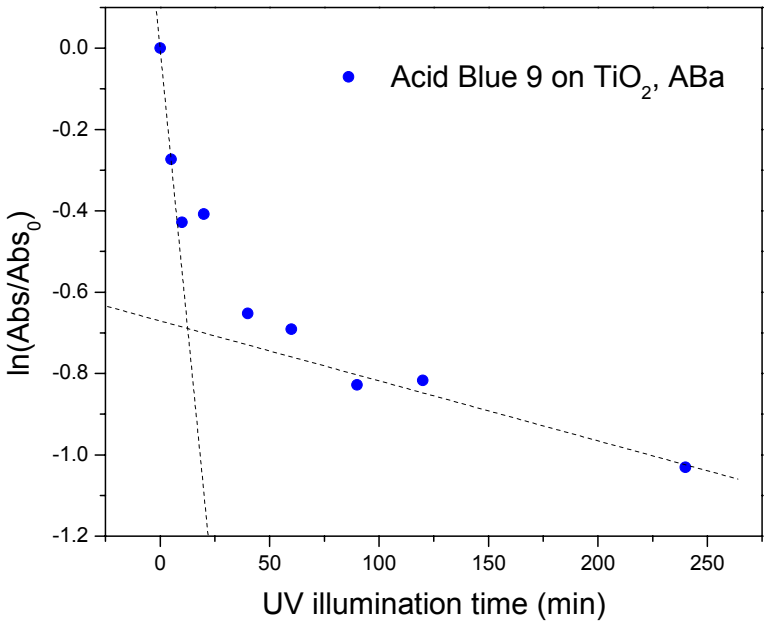

Figure 5.1 Single step first order reaction model

5.2 Series Reaction Mechanism

The series reaction mechanism is described by the reaction below:

$$\text{dye} \xrightarrow{k_1} \text{intermediate} \xrightarrow{k_2} \text{colorless products}$$

Reaction 5.1

If it is assumed that the reactions consuming the dye and intermediate are first order, the intermediate concentration is described by C_I, the initial dye concentration is $C_{D(0)}$ and that

no intermediate exists at t=0, then the batch reactor models for change in C_D and C_I with respect to time can be described by solving the differential equations shown in Equation 5.2 and Equation 5.3 below.

$$\frac{dC_D}{dt} = -k_1 C_D \quad \Rightarrow \quad C_D = C_{D(0)} \exp(-k_1 t)$$

Equation 5.2

$$\frac{dC_I}{dt} = k_1 C_D - k_2 C_I \quad \Rightarrow \quad C_I = \left(\frac{k_1 C_{D(0)}}{k_2 - k_1}\right)\left(\exp(-k_1 t) - \exp(-k_2 t)\right)$$

Equation 5.3

Absorbance and reflectance measured was the sum of contributions from the dye and intermediate(s), therefore the Beer-Lambert law (Abs=αbC) (Chapter 3) and the definition of Kubelka-Munk units discussed in Chapter 4 (KM=$\alpha b'C$) were used with the concentration equations to obtain models for Abs (Equation 5.4) and KM (Equation 5.5). The molar absorptivity of dye and intermediate are denoted by α_D and α_I respectively, and Abs_0 and KM_0 are the initial absorbance and transformed reflectance, respectively, of the unexposed sample.

$$\left(Abs_{model}(t)\right) = Abs_0\left(\left(\frac{\alpha_I}{\alpha_D}\frac{k_1}{k_2 - k_1}\right)\left(\exp(-k_1 t) - \exp(-k_2 t)\right) + \exp(-k_1 t)\right)$$

Equation 5.4

$$\left(KM_{model}(t)\right) = KM_0\left(\left(\frac{\alpha_I}{\alpha_D}\frac{k_1}{k_2 - k_1}\right)\left(\exp(-k_1 t) - \exp(-k_2 t)\right) + \exp(-k_1 t)\right)$$

Equation 5.5

To fit the data obtained to these models, the parameter values for k_1, k_2 and α_I/α_D need to be determined.

5.3 Series Reaction Mechanism Parameter Evaluation

The apparent parameters (k_1, k_2 and α_I/α_D) were determined by examining the limiting values of Abs_{model} and KM_{model} with respect to t. For the small time limit, the exponential terms were expanded to the first two terms in the series, resulting in Equation 5.6 below. Rearranging this equation, result shown in Equation 5.7, we began the parameter values evaluation by performing a linear regression, by the method of least squares, of our data at short illumination times plotted as $((Abs_{observed}/Abs_0)-1)$ or $((KM_{observed}/KM_0)-1)$ versus t. The slope obtained was then used with the information obtained from the long time limit to solve for the parameters. Data obtained for 0 to 5 min of UV exposure was fit to Equation 5.7, using two exposure times for the Indirect Analysis experiments and three for the Direct Analysis experiments.

$$\left(\frac{\mathrm{Abs}_{\mathrm{observed}}}{\mathrm{Abs}_0}\ \mathrm{or}\ \frac{KM_{\mathrm{observed}}}{\mathrm{KM}_0}\right) = (1-\mathrm{k}_1\mathrm{t}) + \left(\frac{\alpha_I \mathrm{k}_1}{\alpha_D(\mathrm{k}_2-\mathrm{k}_1)}\right)(1-\mathrm{k}_1\mathrm{t}-1+\mathrm{k}_2\mathrm{t})$$

Equation 5.6 Short time asymptote (expanded solution)

$$for\ t \to 0: \quad \left(\left(\frac{\mathrm{Abs}_{\mathrm{observed}}}{\mathrm{Abs}_0}\ or\ \frac{KM_{\mathrm{observed}}}{KM_0}\right)-1\right) = \left(\frac{\alpha_I}{\alpha_D}-1\right)\mathrm{k}_1\mathrm{t}$$

Equation 5.7 Short time asymptote

The series reaction model equations, Equation 5.4 and Equation 5.5, can be simplified for longer times, assuming k_1 is greater than k_2, to the equation below:

$$\left(\frac{Abs_{observed}}{Abs_0}\ or\ \frac{KM_{observed}}{KM_0}\right)=\left(\frac{-\alpha_I k_1}{\alpha_D(k_2-k_1)}\right)\exp(-k_2 t)$$

Equation 5.8

Then by taking the natural log of both sides, the equation below is obtained:

$$for\ t\to\infty\ and\ k_1>k_2:\quad \ln\left(\frac{Abs_{observed}}{Abs_0}\ or\ \frac{KM_{observed}}{KM_0}\right)=(-k_2 t)+\ln\left(\frac{-\alpha_I k_1}{\alpha_D(k_2-k_1)}\right)$$

Equation 5.9 Long time behavior

Data obtained for near-UV illumination times of 90 min or more was fit to the long time equation to obtain k_2 from the slope of the best fit line. The value for k_2 obtained was then used simultaneously with the value of the intercept and the slope obtained from the limit for short times to solve for the other parameters, k_1 and α_I/α_D, as shown below:

$$k_2 = slope_{large\ t}$$

Equation 5.10

$$k_1=\frac{k_2\exp(\text{intercept}_{\text{large t}})+\text{slope}_{\text{small t}}}{\exp(\text{intercept}_{\text{large t}})-1}$$

Equation 5.11

$$\left(\frac{\alpha_I}{\alpha_D}\right)=\left(\frac{slope_{small\ t}}{k_1}+1\right)$$

Equation 5.12

For the Indirect Analysis, three illumination times were fit for the long time limit and six were fit for the reflectance data. This method of parameter evaluation was performed for each set of experiments, with a set including all the illumination times of the same initial dye-coated sample. For our model, the values of α_D and α_I were not needed explicitly, only

the ratio of α_I to α_D was needed, which was obtained by the limiting values analysis. Therefore, the calibration study was unnecessary for determination of rate constants. Parameters obtained by the analysis described are given in the next section and it will be shown that the data validates the assumption that k_1 is greater than k_2.

5.4 Results: Series Reaction Mechanism Parameters

The initial conditions, Abs_0 or KM_0, and apparent parameters obtained for the Indirect Analysis data acquired by transmission spectroscopy are given in Table 5.1, and those determined for the Direct Analysis data obtained by diffuse reflectance spectroscopy are given in Table 5.2 below. The tables show values obtained for the ratio of molar absorptivity of intermediate to dye and the two rate constants (k_1 and k_2) for each set of experiments (indicated by label of original dye-coated sample) as well as the averages for these values obtained for duplicate experiments and standard deviation (SD) of the results. The tables also show what percentage the SD is of the average value, allowing for easier comparison of the deviation between data sets. The wavelengths used for parameter evaluation and testing of the fit to the series reaction model for data obtained by both experimental methods were the wavelengths of maximum absorbance given in Chapter 3; 629 nm for Acid Blue 9 data, 485 nm for Acid Orange 7, 617 nm for Reactive Black 5 and 596 nm for Reactive Blue 19 data.

Table 5.1 Series Reaction Mechanism parameters for Indirect Analysis data

	Indirect Analysis		average	SD	SD / average
	ABa	**ABb**			
Abs_0	2.3709	1.8564			
α_I/α_D	0.5035	0.6203	0.5619	0.0584	10%
k_1 (min^{-1})	0.0962	0.1380	0.1171	0.0209	18%
k_2 (min^{-1})	0.00148	0.00279	0.00214	0.000655	31%
	AOa	**AOb**			
Abs_0	1.0841	0.9770			
α_I/α_D	0.6558	0.5332	0.5945	0.0613	10%
k_1 (min^{-1})	0.149	0.0646	0.107	0.0422	40%
k_2 (min^{-1})	0.00283	0.00131	0.00207	0.000760	37%
	RBka	**RBkb**			
Abs_0	0.8992	0.7994			
α_I/α_D	0.5741	0.6084	0.5912	0.0171	3%
k_1 (min^{-1})	0.116	0.121	0.1185	0.0025	2%
k_2 (min^{-1})	0.00199	0.00235	0.00217	0.000180	8%
	RBa	**RBb**			
Abs_0	0.3050	0.3052			
α_I/α_D	0.5069	0.4576	0.4822	0.0247	5%
k_1 (min^{-1})	0.0672	0.0535	0.0604	0.0069	11%
k_2 (min^{-1})	0.00141	0.00173	0.00157	0.000160	10%

Table 5.2 Series Reaction Mechanism parameters for Direct Analysis data

	Direct Analysis		average	SD	SD / average
	ABa	**ABc**			
KM_0	2.4324	2.0042			
α_I/α_D	0.1511	0.1572	0.1541	0.0031	2%
k_1 (min^{-1})	0.1674	0.1615	0.1644	0.0029	2%
k_2 (min^{-1})	0.00104	0.000406	0.00072	0.000317	44%
	AOa	**AOc**			
KM_0	1.4911	1.4713			
α_I/α_D	0.1236	0.1188	0.1212	0.0024	2%
k_1 (min^{-1})	0.178	0.175	0.176	0.0018	1%
k_2 (min^{-1})	0.000902	0.000933	0.00092	0.000015	2%
	RBkb	**RBkc**			
KM_0	0.9956	0.9907			
α_I/α_D	0.2793	0.2703	0.2748	0.0045	2%
k_1 (min^{-1})	0.14517	0.13349	0.13933	0.0058	4%
k_2 (min^{-1})	0.000572	0.000756	0.000664	0.000092	14%
	RBa	**RBc**			
KM_0	0.8880	0.8132			
α_I/α_D	0.2078	0.1821	0.1950	0.0129	7%
k_1 (min^{-1})	0.121	0.122	0.1218	0.0007	1%
k_2 (min^{-1})	0.000960	0.000569	0.00076	0.000196	26%

Results for experiments preformed by the Direct Analysis method showed better reproducibility than results for the Indirect Analysis method, but this was expected, as discussed in Chapter 4, and the reason the method was developed and used for examining the photocatalytic degradation of solid organic dyes on TiO_2. The apparent first order rate constants were similar for the first step of the proposed mechanism, k_1, for all dyes examined by the same experimental system. This suggests that the photocatalytic degradation of organics initially occurs by a similar mechanism, e.g. hydrogen abstraction by hydroxyl radical. The rate constant, k_1, averaged 0.101 min^{-1} (SD=0.0336) for the eight

reported photocatalytic degradation experiments examined by the Indirect system and averaged 0.151 min^{-1} (SD=0.0215) for the eight Direct Analysis experiments. The average apparent first order rate constant for the second step, k_2, for all dyes was found to be 0.00199 min^{-1} (SD=0.00057) by the Indirect Analysis approach and 0.000767 min^{-1} (SD=0.000214) by Direct Analysis. Therefore, the average value determined by both experimental methods for all dyes for k_1 was 0.126 min^{-1} (SD=0.0376) and for k_2 was 0.00138 min^{-1} (SD=0.00075). This average value of k_1 is more than 90 times greater than k_2, therefore validating our assumption that k_1 is greater than k_2 used in the analysis of the limiting behaviors. The parameters were obtained by simple fits to the reaction data. The parameters could have been determined using an algorithm for the data to perform a non-linear curve fit to the model equation, for Abs or *KM* units, but as shown in the next section, the simple method of determination works well.

5.5 Results: Data Fit to Series Reaction Model

The series reaction mechanism, of colored dye converting to colored intermediate and then to colorless product, can be used to describe the photocatalytic degradation of adsorbed organic dyes to TiO_2. The term intermediate could be used to describe multiple intermediates absorbing light in the visible region, and there could actually be multiple colorless products. The spectroscopic analysis methods used, transmission and reflectance UV-visible, gave a measure of the total concentration of light-absorbing species and therefore the term intermediate refers to any and all light-absorbing species in the visible region that are not the dye and the term product refers to any and all species not absorbing visible light. The parameters determined for each experimental set were used to apply the

model equations, Equation 5.4 and Equation 5.5, to the data. The results, grouped by dye, for the Indirect Analysis method are given in graphical form in subsection 5.5.1 and the model fit to the data sets obtained by the Direct Analysis method are given in subsection 5.5.2. These graphs show that the series reaction mechanism is a plausible description of the photocatalytic degradation of organic dyes. The results will be further discussed in section 5.7.

5.5.1 Indirect Analysis

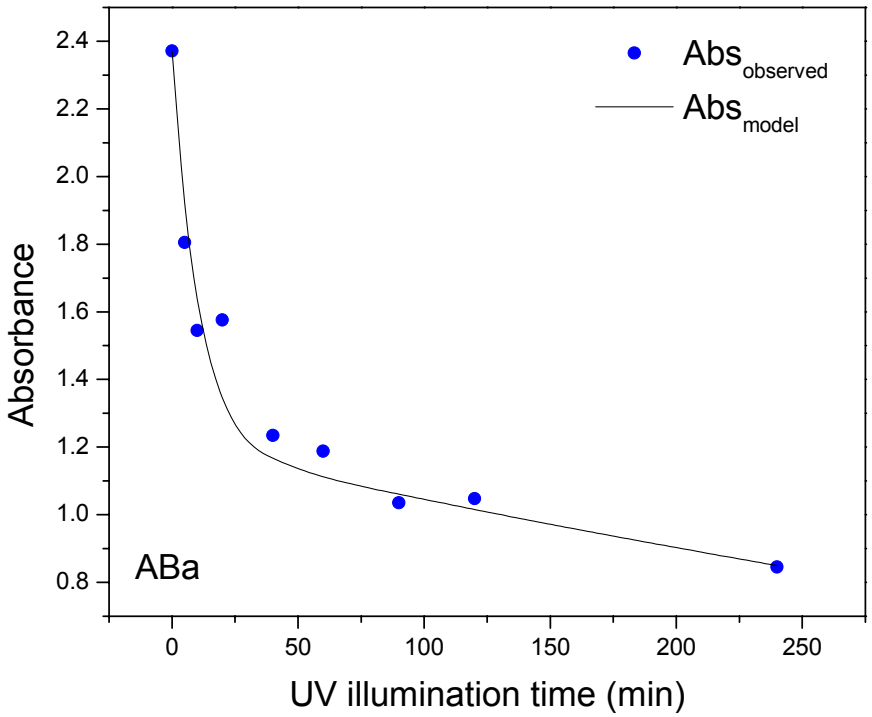

Figure 5.2 Series Reaction Model: Indirect Analysis of Acid Blue 9 on TiO_2 (ABa)

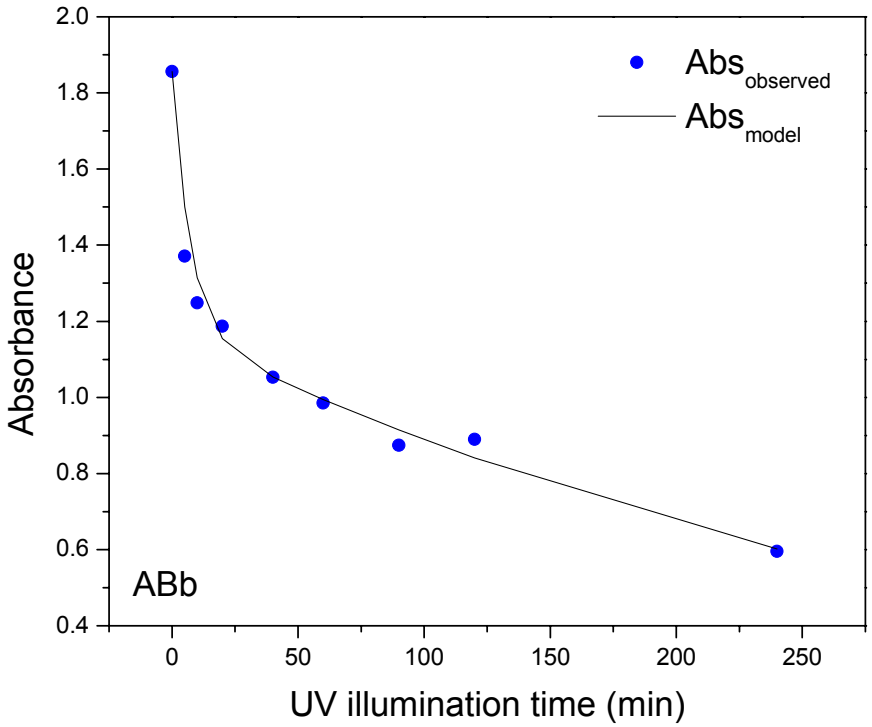

Figure 5.3 Series Reaction Model: Indirect Analysis of Acid Blue 9 on TiO_2 (ABb)

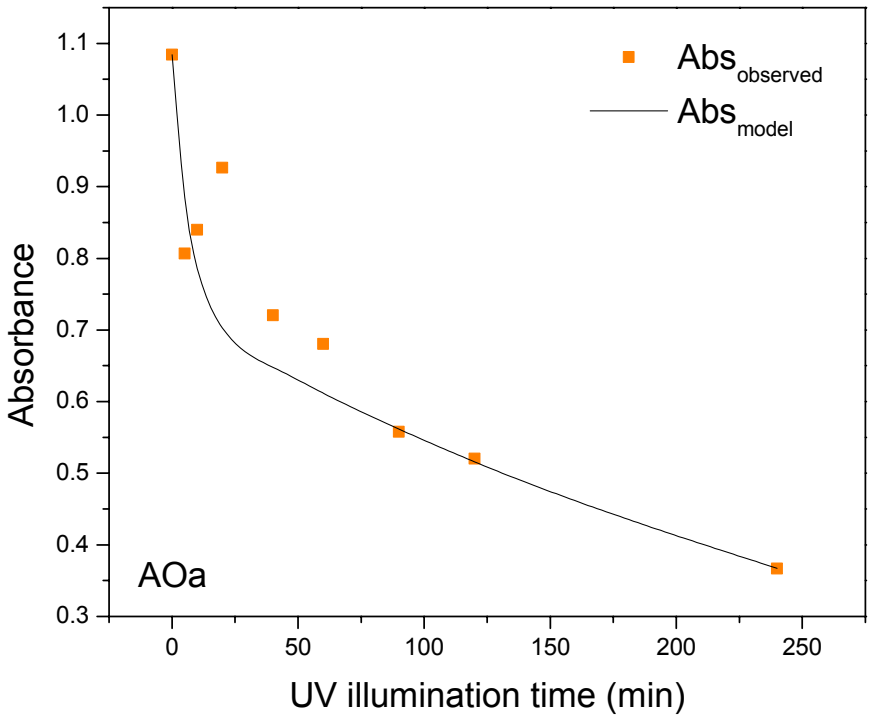

Figure 5.4 Series Reaction Model: Indirect Analysis of Acid Orange 7 on TiO_2 (AOa)

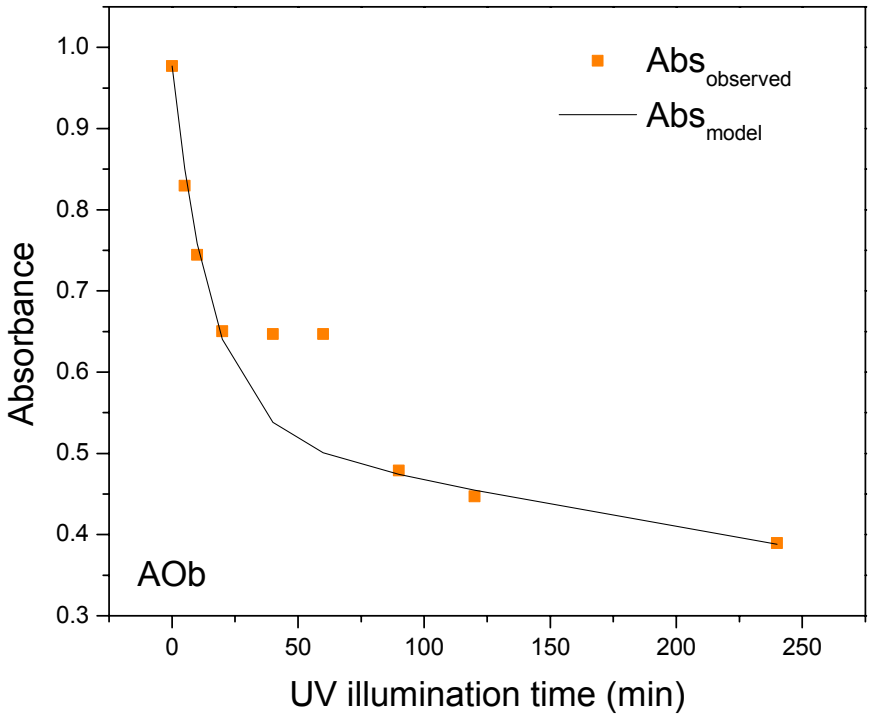

Figure 5.5 Series Reaction Model: Indirect Analysis of Acid Orange 7 on TiO_2 (AOb)

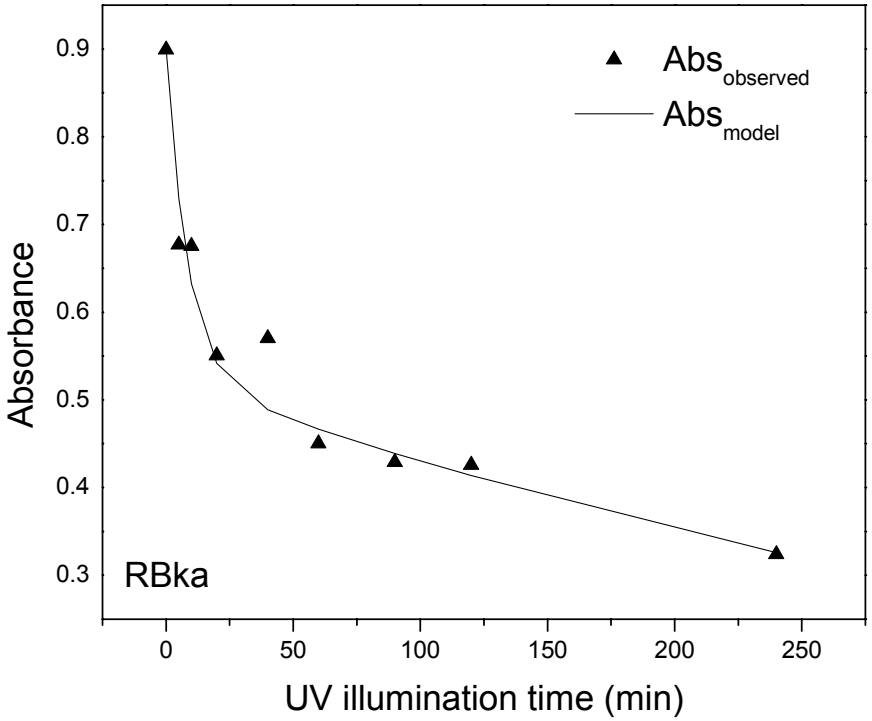

Figure 5.6 Series Reaction Model: Indirect Analysis of Reactive Black 5 on TiO_2 (RBka)

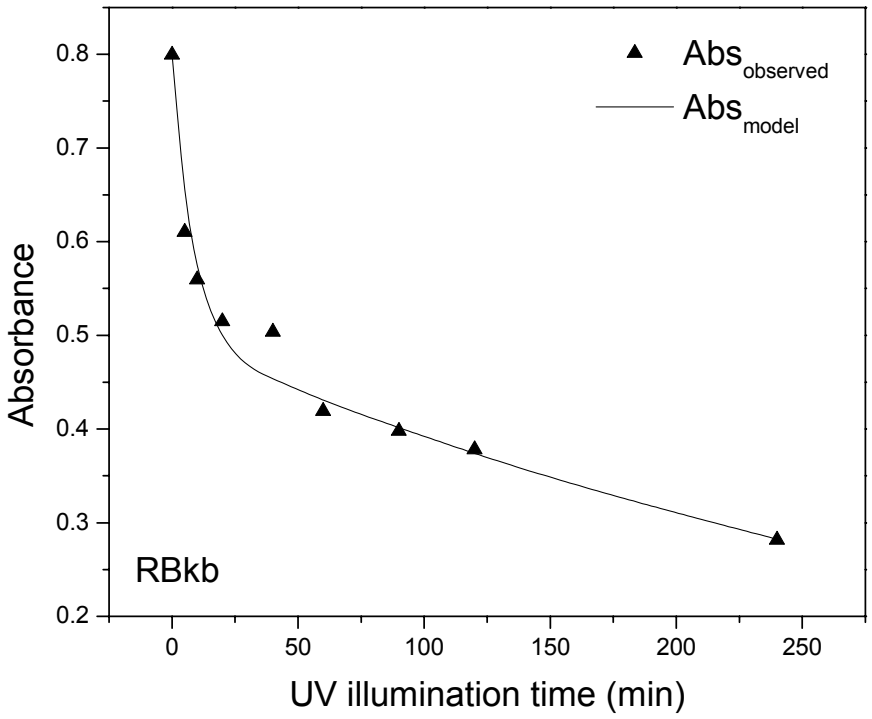

Figure 5.7 Series Reaction Model: Indirect Analysis of Reactive Black 5 on TiO_2 (RBkb)

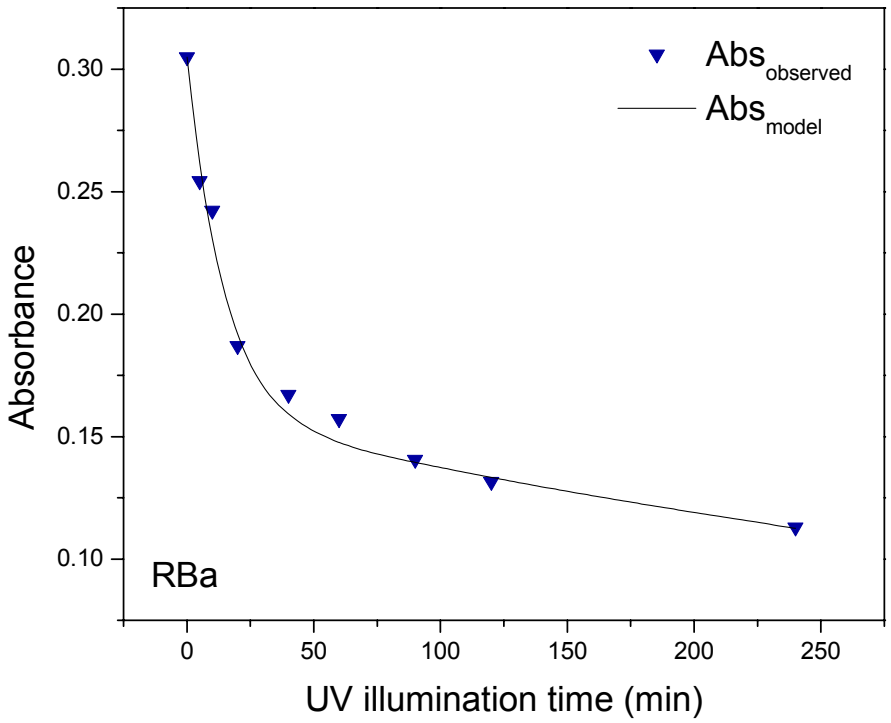

Figure 5.8 Series Reaction Model: Indirect Analysis of Reactive Blue 19 on TiO_2 (RBa)

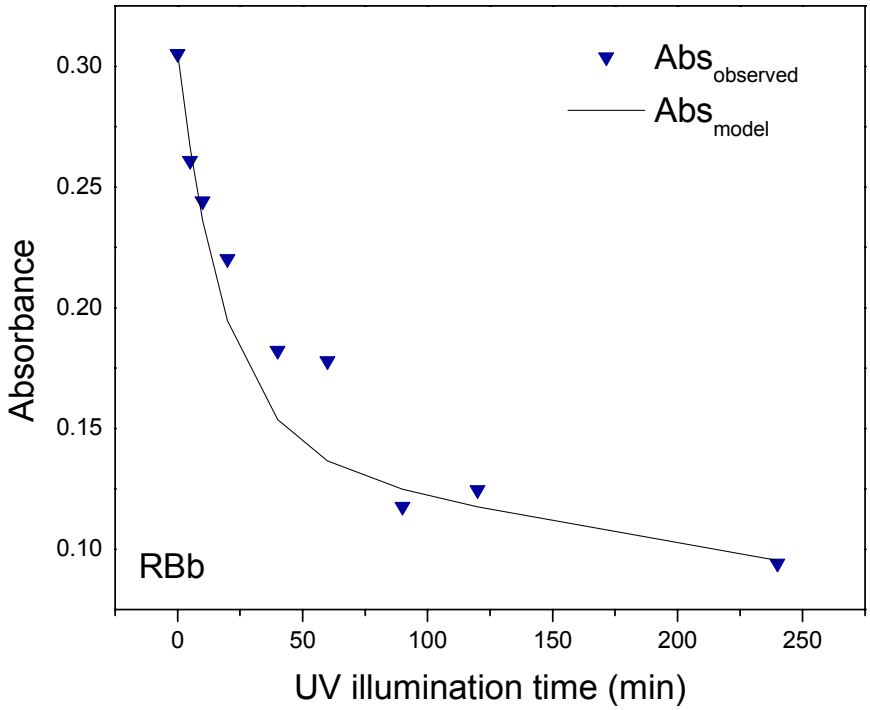

Figure 5.9 Series Reaction Model: Indirect Analysis of Reactive Blue 19 on TiO_2 (RBb)

5.5.2 Direct Analysis

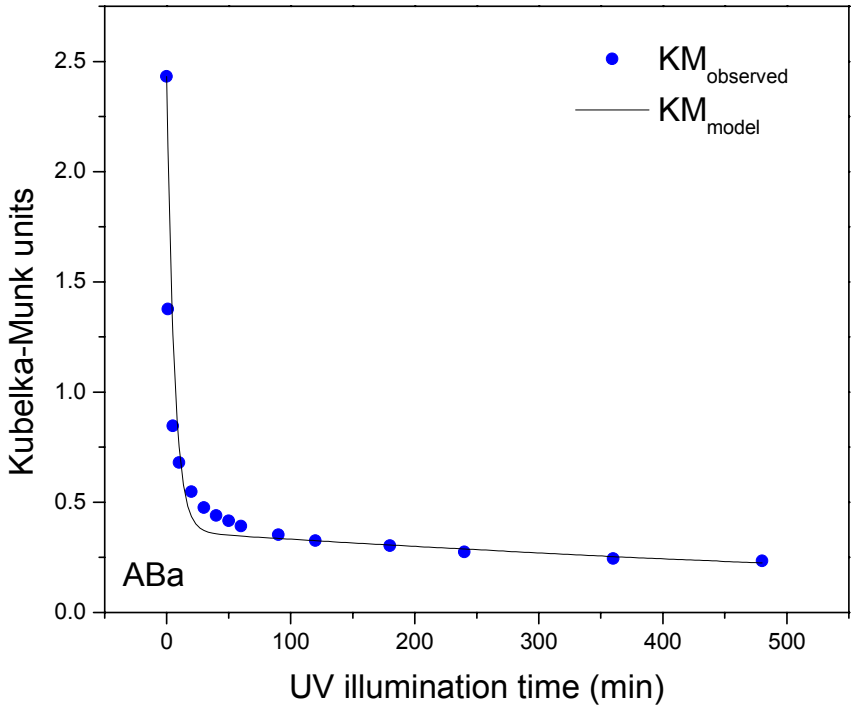

Figure 5.10 Series Reaction Model: Direct Analysis of Acid Blue 9 on TiO_2 (ABa)

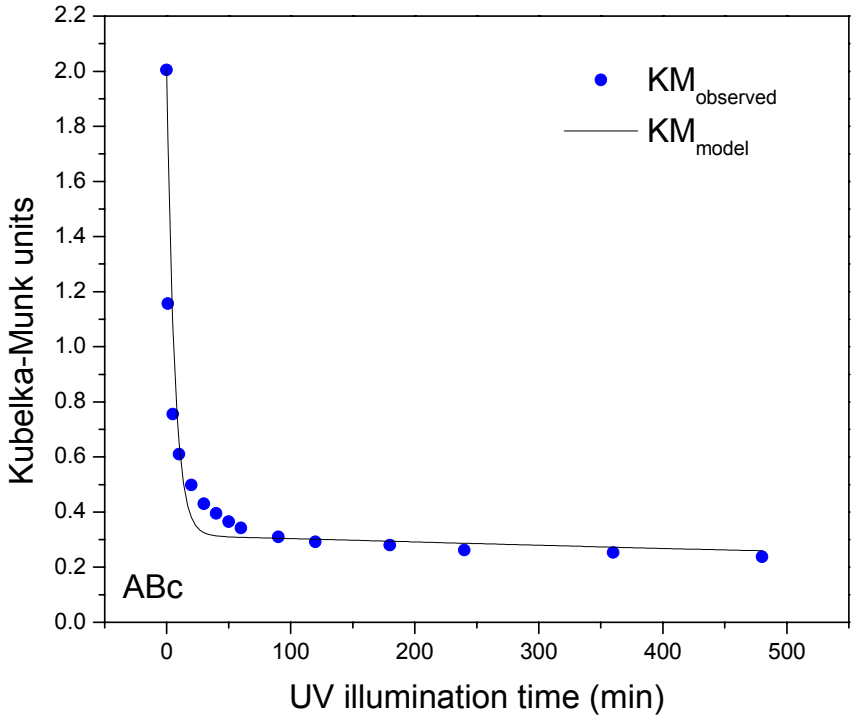

Figure 5.11 Series Reaction Model: Direct Analysis of Acid Blue 9 on TiO_2 (ABc)

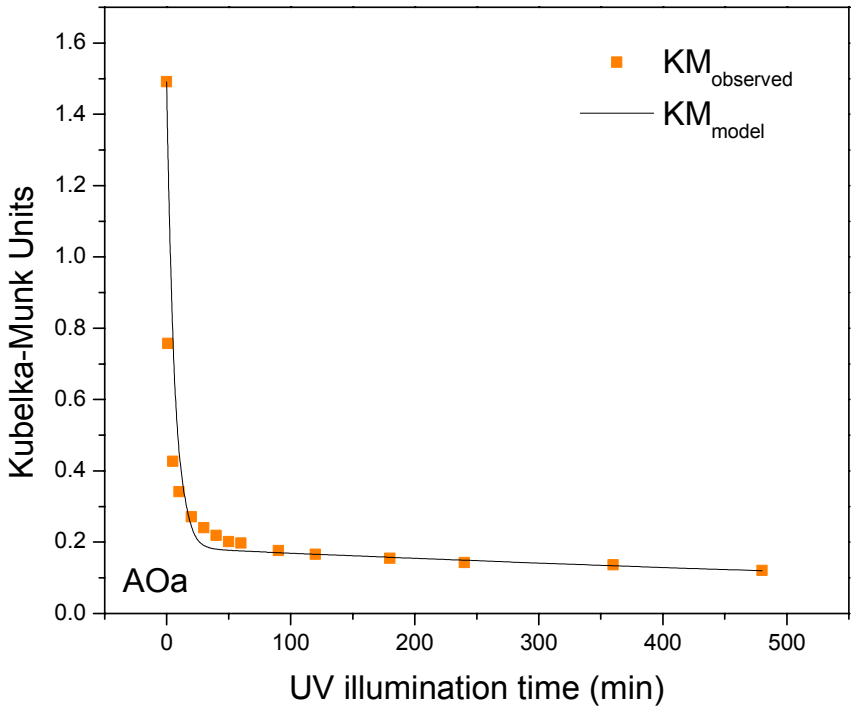

Figure 5.12 Series Reaction Model: Direct Analysis of Acid Orange 7 on TiO_2 (AOa)

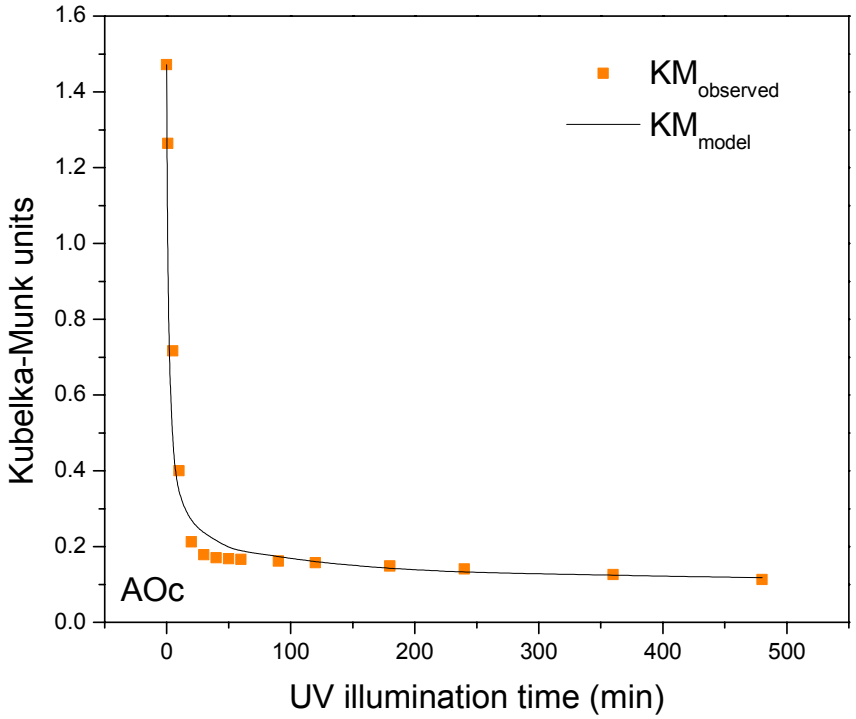

Figure 5.13 Series Reaction Model: Direct Analysis of Acid Orange 7 on TiO_2 (AOc)

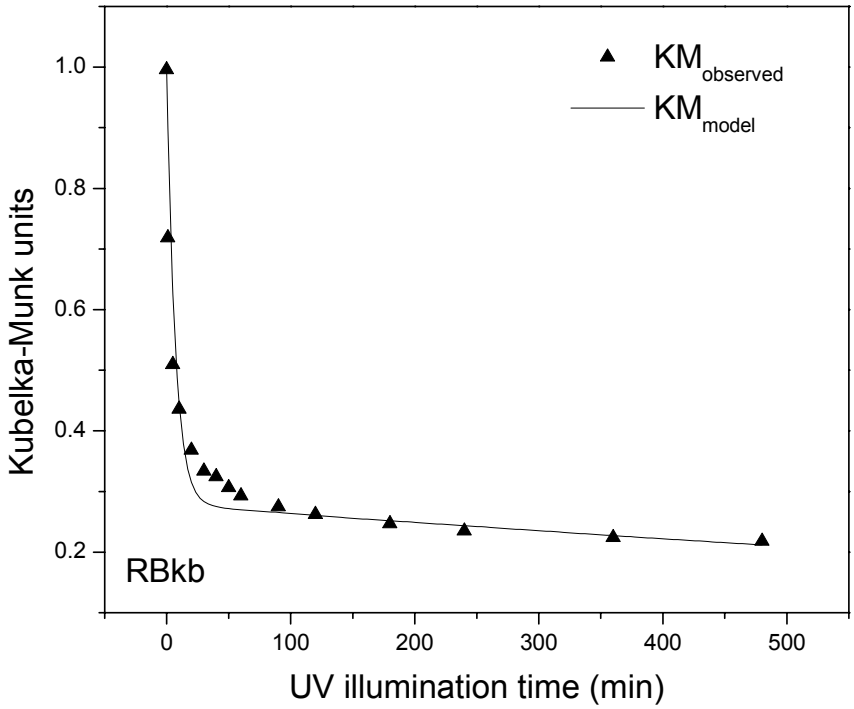

Figure 5.14 Series Reaction Model: Direct Analysis of Reactive Black 5 on TiO_2 (RBkb)

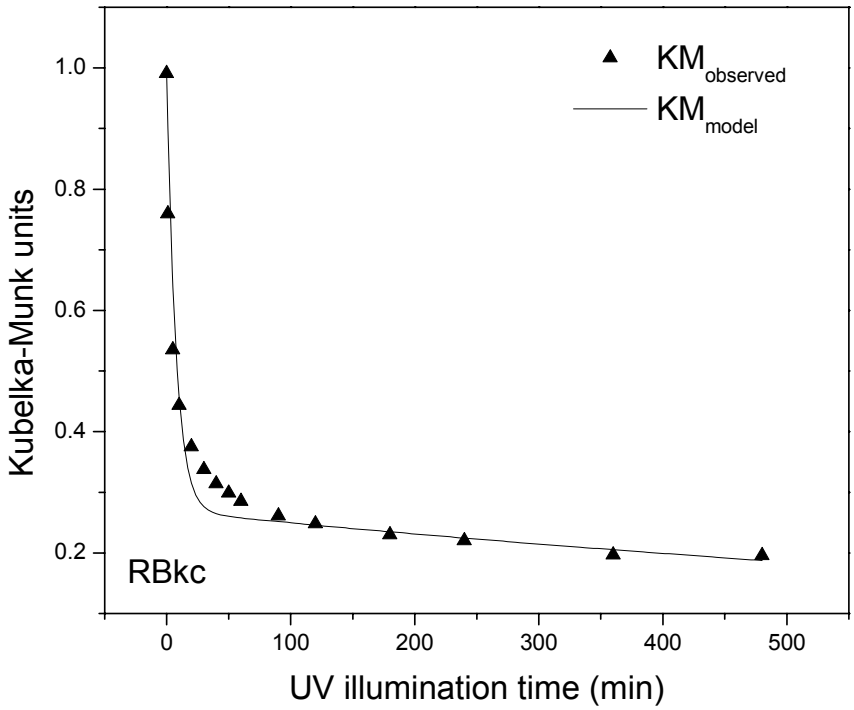

Figure 5.15 Series Reaction Model: Direct Analysis of Reactive Black 5 on TiO_2 (RBkc)

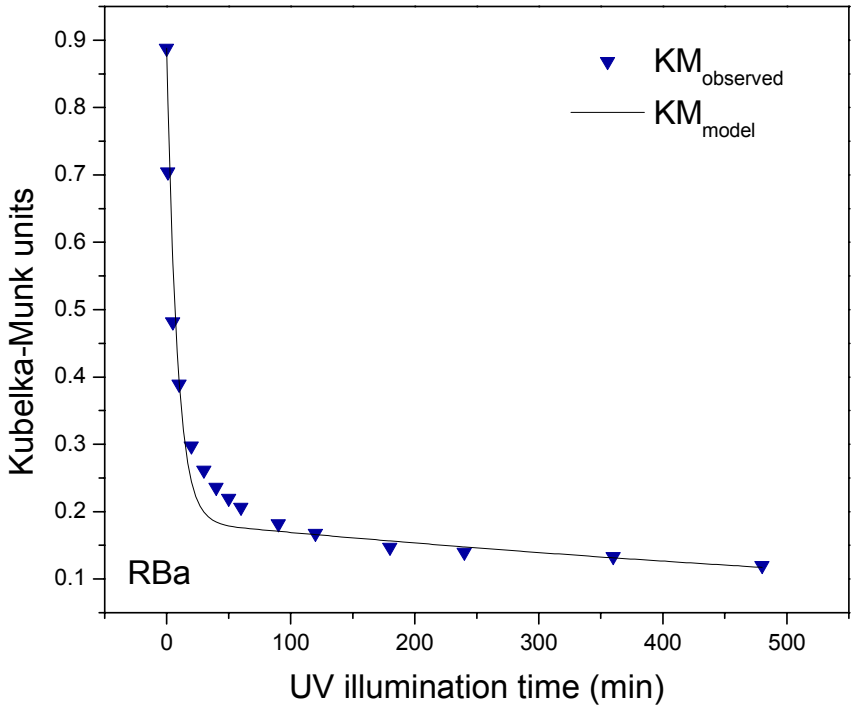

Figure 5.16 Series Reaction Model: Direct Analysis of Reactive Blue 19 on TiO_2 (RBa)

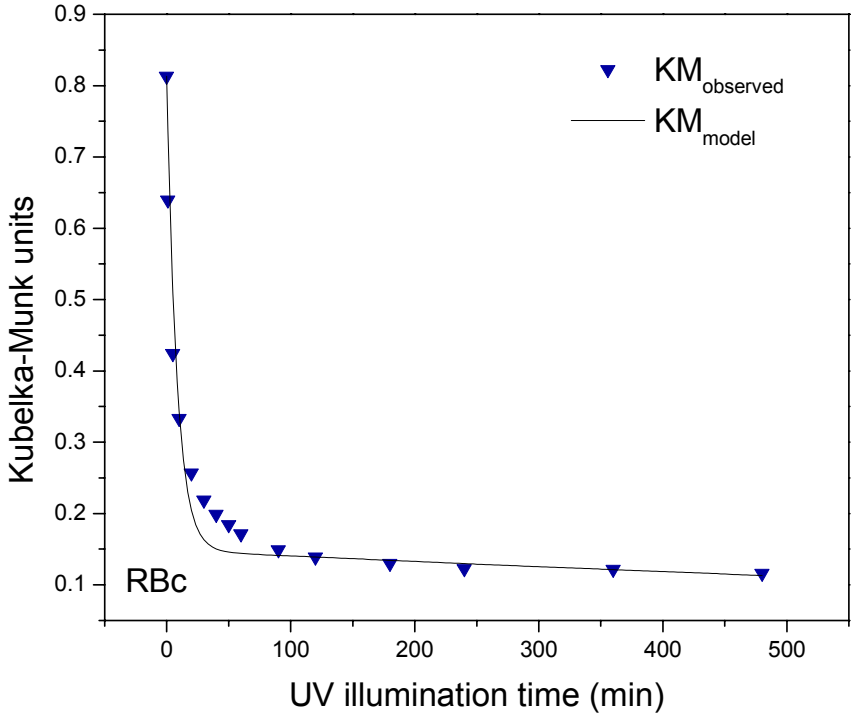

Figure 5.17 Series Reaction Model: Direct Analysis of Reactive Blue 19 on TiO_2 (RBc)

5.6 Series Reaction Model Fit to Data of Other Researchers

Previously, Yang et al.[4] reported the photocatalytic oxidation of Acid Blue 9 adsorbed on TiO_2 examined by diffuse reflectance infrared Fourier transform spectroscopy (DRIFTS). An aqueous solution of 10 ppm dye of pH 2.3 was prepared in which a concentration of 1.5 g L^{-1} of TiO_2, predominately in anatase form, was added and stirred overnight for the adsorption to occur. The Acid Blue 9 coated TiO_2 particles were then collected by filteration and dried. The powder was then placed in a sample holder for in situ analysis by DRIFTS during exposure to 15 mW cm^{-2} of UV. The series reaction model was successfully applied to results reported by Yang et al. [4] by analysis of their Fig. 8 data, as shown in Figure 5.18 below, producing a k_1 of 0.0868 min^{-1} and k_2 of 0.00168 min^{-1} by the parameter evaluation method described in section 5.3, comparable to our results.

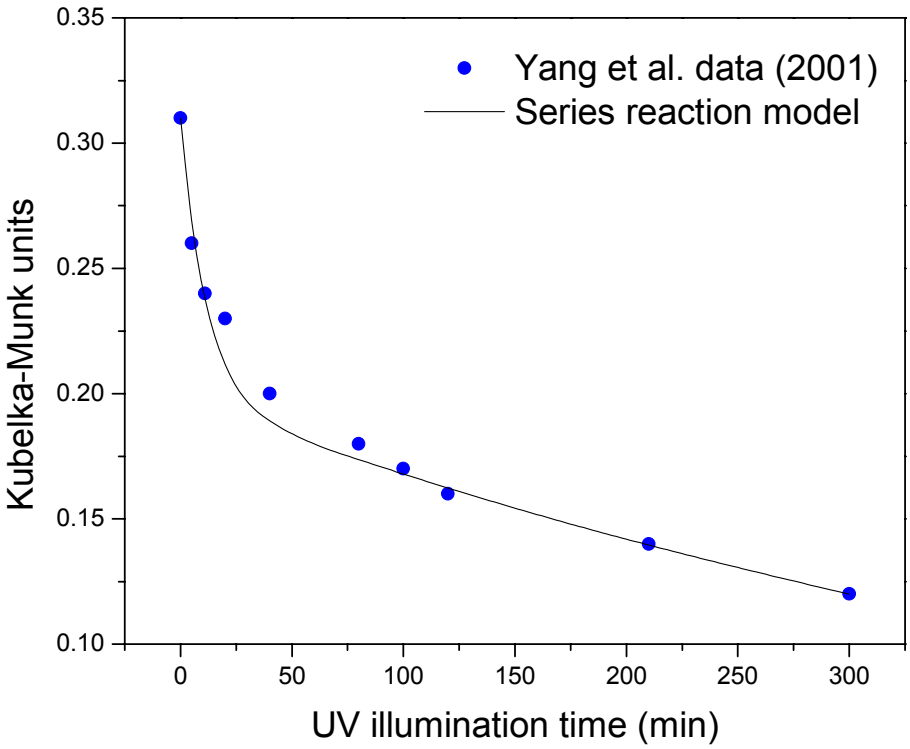

Figure 5.18 Series Reaction model fit to Yang and coworkers' [4] DRIFTS data

5.7 Discussion of Results

A series of reactions, of colored dye converting to colored intermediate by a first order reaction with respect to dye concentration and then to colorless product by a first order reaction with respect to intermediate concentration, has been shown to be a plausible mechanism for the photocatalytic degradation of non-volatile organic dyes adsorbed to TiO_2. An intermediate may form that absorbs light in the UV-visible region in a manner similar to the dye, producing a spectra with similar features, or a change in chemical structure may lead to the absorption of light at a different wavelength. The absorbance spectra shown in Chapter 3 and the reflectance spectra shown in Chapter 4 all have features that change, even if the change is slight, as the reaction proceeds with UV illumination. Probably the most apparent change with UV illumination appears in the data obtained by the Direct Analysis method for Acid Blue 9 on TiO_2 shown in Figures 4.1 and 4.2 in the region between 400 nm and 550 nm. The increase in absorbance and therefore increase in concentration occurring between about 450 nm and 500 nm suggests that a new species is formed and then degrades. Other changes in the spectra occurring with UV illumination discussed in Chapter 4 could be caused by chemical structural changes, justifying the proposed mechanism. The UV-visible spectra do not give detailed information about how the molecules might chemically change and in future work a different technique, such as infrared spectroscopy, could be used to examine these transformations more closely.

The method of parameter determination for k_1, k_2 and α_I/α_D involved examining the limiting values of the Abs model given in Equation 5.4 or the *KM* model given in Equation 5.5. Each of the parameters obtained were comparable for all of the dyes, suggesting that the organic molecules are photocatalytically degraded by a similar mechanism. The

parameters determined for each set of experiments show a good fit to the data as seen in Figure 5.2 through Figure 5.17. One way to examine how well these parameters fit the data is to compare the parameters established by the limiting values analysis to parameters obtained by performing a non-linear curve fit to the data. Origin® software was used to perform a non-linear curve fit to ABa data obtained by the Indirect Analysis method. The software required the Abs model, Equation 5.4 with the value Abs_0 inserted, and initial guesses for the parameters as input and the fit was completed based on the Levenberg-Marquardt algorithm. The initial estimates used for the parameters were those obtained previously in the limiting values analysis; 0.0962 min^{-1}, 0.00148 min^{-1} and 0.504 for k_1, k_2 and α_I/α_D respectively. Results of the fit are shown in Figure 5.19 below and the values determined for k_1, k_2 and α_I/α_D were 0.153 min^{-1}, 0.00244 min^{-1} and 0.586 respectively. These values are comparable to the parameters obtained by examining the limiting values for the model equation.

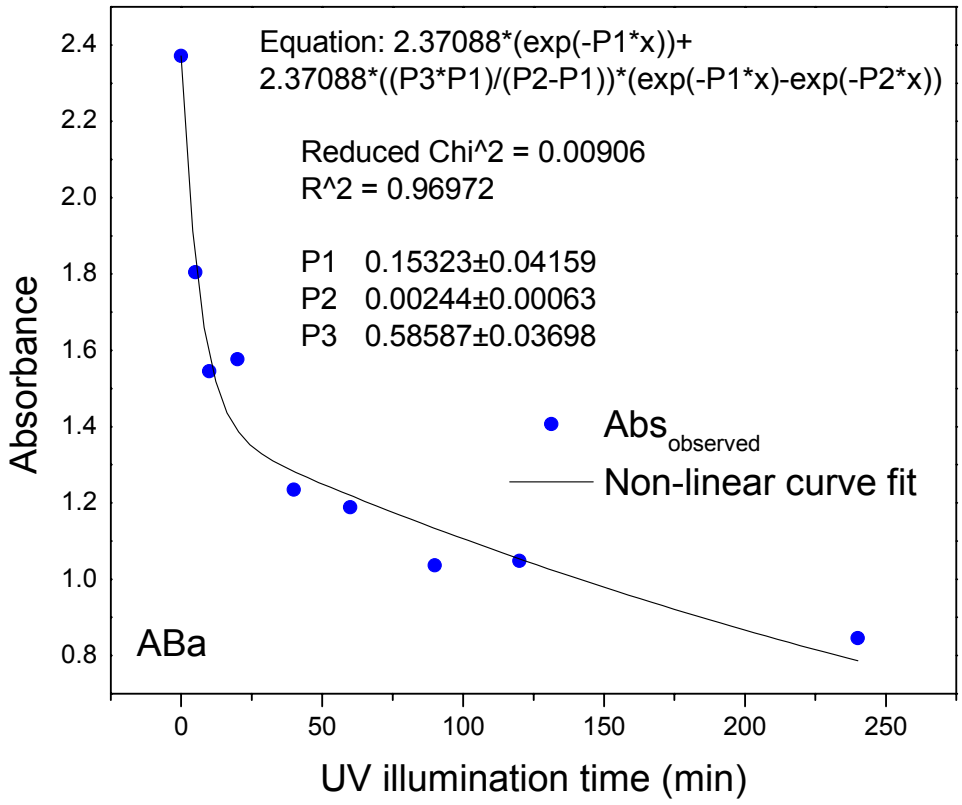

Figure 5.19 Non-linear curve fit to ABa Indirect Analysis data

5.8 References

[1] Lachheb, H., E. Puzenat, A. Houas, M. Ksibi, E. Elaloui, C. Guillard and J.-M. Herrmann, *Photocatalytic degradation of various types of dyes (Alizarin S, Crocein Orange G, Methyl Red, Congo Red, Methylene Blue) in water by UV-irradiated titania*. Applied Catalysis B: Environmental 2002, **39**: p. 75-90.

[2] Tanaka, K., K. Padermpole and T. Hisanaga, *Photocatalytic Degradation of Commercial Azo Dyes*. Water Research 2000, **34**(1): p. 327-333.

[3] Tarasov, V.V., G.S. Barancova, N.K. Zaitsev and Z. Dongxiang, *Photochemical Kinetics of Organic Dye Oxidation in Water*. Process Safety and Environmental

Protection 2003, **81**(B4): p. 243-249.

[4] Yang, T.C.-K., S.-F. Wang, S.H.-Y. Tsai and S.Y. Lin, *Intrinsic photocatalytic oxidation of the dye adsorbed on TiO2 photocatalysts by diffuse reflectance infrared Fourier transform spectroscopy*. Applied Catalysis B: Environmental 2001, **30**: p. 293-301.

6 ALTERNATIVE MODELS FOR PHOTOCATALYZED DYE DEGRADATION: UNEXPOSED PORTION OF SAMPLE MODEL AND LIGHT INTENSITY INFLUENCED RATE CONSTANT MODEL

We have assumed a mechanism involving colored dye converting to colored intermediate by a first order reaction with respect to dye concentration, and then to colorless product by a first order reaction with respect to intermediate concentration. We have shown this to be a plausible mechanism for the photocatalytic decolorization of non-volatile organic dyes adsorbed to TiO_2. Although this mechanism is applicable to the concentration changes measured with UV illumination of the dye-coated samples, other models were explored to determine if alternative descriptions of the photocatalytic degradation might be appropriate. Two alternative models are discussed here. The Unexposed Portion of Sample (UPOS) model accounts for the possibility that the total concentration of dye measured may include dye that was not involved in the photocatalytic reaction, because the TiO_2 support to which it was adsorbed was not exposed to UV illumination. The Light Intensity Influenced Rate Constant (LIIRC) model assumes that the UV intensity varies with distance and absorption by TiO_2, affecting the photocatalytic rate. Models were developed and tested for these two latter possibilities, as described in the following sections, to determine if they were suitable descriptions for the color removal of organic dyes by TiO_2 photocatalysis.

6.1 Unexposed Portion of Sample (UPOS) Model

The photocatalytic process is reported to occur via semiconductor absorption of a photon of energy equal to or than the semiconductor bandgap, which then leads to the promotion of an electron from the valence band to the conduction band creating a hole [1]-

[4]. The holes and electrons then migrate to the surface and are available for oxidation and reduction reactions, respectively, or they recombine to create a photo-inefficient process. The assumption of the UPOS model is that only TiO_2 exposed to UV will allow for the absorption of photons, and that only dye in immediate contact with UV illuminated TiO_2 can be photocatalytically degraded. This model therefore also assumes that the diffusion of electrons and holes from one primary particle to another is minimal.

The total concentration of species absorbing or reflecting light at the same wavelength measured in the Indirect or Direct Analysis methods, respectively, included (1) dye and (2) reaction products exposed to UV illumination and (3) dye not involved in the photocatalytic reaction because it was not exposed. For (3), the TiO_2 to which it was adsorbed was not exposed to UV light. Figure 6.1 below is a schematic of dye-coated TiO_2 particles illuminated with UV light, with dashed red lines indicating dye contacted with UV light and solid red lines representing dye unexposed to light.

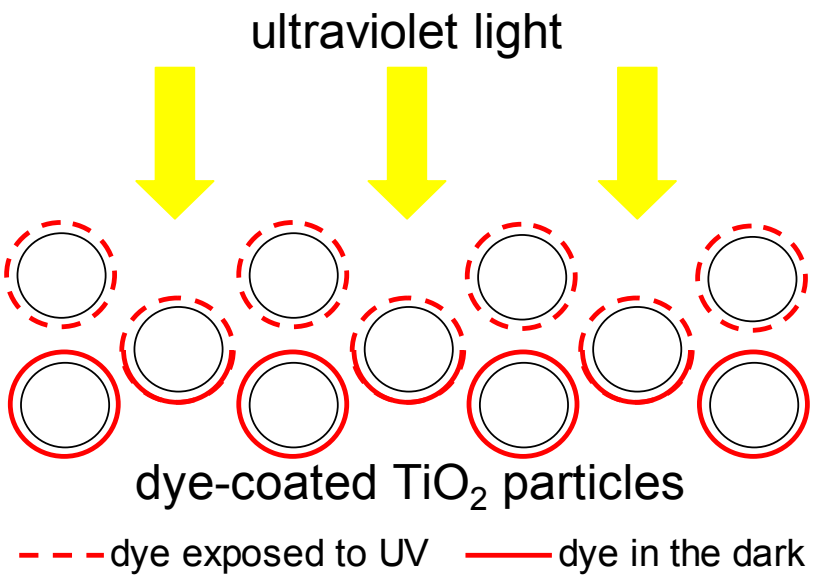

Figure 6.1 Unexposed Portion of Sample schematic.

During the Indirect Analysis experiments, the dye-coated TiO_2 particles were placed in Petri dishes and shaken during UV illumination in attempt to achieve uniform UV exposure throughout the sample. Uniform UV illumination was not achieved for all illumination times examined, because the particles would clump and stick to the Petri dish. As a mound of particles formed, the top layers of particles were accessible to UV light and may have rotated with shaking, achieving exposure to the entire surface, but the bottom layers or internal region of agglomerates were covered and may have been static in reference to the oscillating Petri dish. All of the particles were removed from the dish and a random portion of the sample was used to prepare a solution for transmission UV-visible spectroscopy. The UPOS model assumes the aqueous solution contained concentration contributions from dye-coated particles not involved in the photocatalytic degradation reaction.

During the Direct Analysis experiments, the dye-coated TiO_2 powder was pressed into a sample holder to 0.001 m thickness and illuminated with UV light through a quartz window. The sample was then analyzed by diffuse reflectance spectroscopy with light of longer wavelength than the UV light used for photocatalyst activation, to avoid propagation of the reaction during measurement. The penetration depth of light into a media increases with increasing wavelength, therefore the visible light used for analysis penetrated farther into the sample than the UV light which initiated the photocatalytic reaction, and contributions of dye not involved in the reaction were measured as well as dye/products involved in the reaction. The total concentration contributions from dye-coated TiO_2 exposed to UV and dye-coated TiO_2 kept in the dark in this UPOS model can be used to describe the kinetics of the photocatalytic reaction.

The total concentration of dye measured by UV-visible spectroscopy, $C_D(total)$, is the sum of the dye illuminated with UV, C_D, and dye unexposed to UV, $C_D(dark)$, as shown in Equation 6.1 below.

$$C_D(total) = C_D + C_D(dark)$$

Equation 6.1

The photocatalytic degradation of organic dyes reported in this study can be modeled with a batch reactor model as a first order reaction with respect to dye concentration, C_D, as described in Equation 6.2 below.

$$\frac{dC_D}{dt} = -kC_D$$

Equation 6.2

Initially at $t = 0$, before UV illumination, the total dye concentration, $C_D(total)$, can be described as $C_{D(0)}$. Solving the differential equation, Equation 6.2, then gives:

$$\ln\left(\frac{C_D(total) - C_D(dark)}{C_{D(0)} - C_D(dark)}\right) = -kt$$

Equation 6.3

All of the dye forms have the same molar absorptivity and the spectroscopic data obtained can be fit to Equation 6.3 using the Beer-Lambert law for absorbance (Abs) and the definition of Kubelka-Munk (*KM*) units for reflectance described previously, with the results given in Equation 6.4 and Equation 6.5 respectively.

$$\ln\left(\frac{Abs(total) - Abs(dark)}{Abs_0 - Abs(dark)}\right) = -kt$$

Equation 6.4

$$\ln\left(\frac{KM(total) - KM(dark)}{KM_0 - KM(dark)}\right) = -kt$$

Equation 6.5

Abs(total) is the measured absorbance and *KM*(total) is the transformed measured reflectance, with Abs_0 and KM_0 indicating the initial values for both respectively. The wavelengths used for the analysis were the peak wavelengths previously indicated, namely 629 nm for Acid Blue 9 data, 485 nm for Acid Orange 7, 617 nm for Reactive Black 5 and 596 nm for Reactive Blue 19 data. The concentration of the unexposed dye will appear as a residual dye concentration measured for all reaction times, therefore the Abs(dark) value used was the Abs measured for the longest exposure time; the Abs after 240 min of UV illumination. To be consistent, the *KM*(dark) value used was the value obtained after 240 min of UV illumination, although reflectance measurements were taken for up to 480 min of exposure. Graphs of the left hand side of Equation 6.4 and Equation 6.5 were prepared vs. *t* and a straight line fit to the spectroscopic data to obtain the rate constant, k.

6.1.1 Results: Data Fit to UPOS Model

The rate constants obtained for the UPOS model by the procedure described in the previous section are given in Table 6.1 below. Reported in the table are the rate constants (*k*), the absolute value of the correlation coefficient for each fit (|*R*|) and the averages for each experimental method along with the standard deviation (SD) and percentage the SD is of the average.

Table 6.2 below reports the results by dye and the average for all experiments.

Table 6.1 Unexposed Portion of Sample Model:
First order rate constants

	Indirect Analysis			Direct Analysis		
sample	**k**	**|R|**	**$C_D(dark)/C_{D(0)}$**	**k**	**|R|**	**$C_D(dark)/C_{D(0)}$**
ABa	0.0212	0.937	0.357	0.0324	0.894	0.113
ABb	0.0158	0.906	0.321			
ABc				0.0345	0.914	0.131
AOa	0.0139	0.960	0.338	0.0357	0.881	0.096
AOb	0.0196	0.963	0.399			
AOc				0.0353	0.896	0.089
RBka	0.0181	0.922	0.360			
RBkb	0.0168	0.940	0.352	0.0295	0.925	0.236
RBkc				0.0297	0.946	0.222
RBa	0.0219	0.971	0.370	0.0300	0.958	0.157
RBb	0.0190	0.953	0.309			
RBc				0.0318	0.945	0.151
average:	0.0183	0.944	0.351	0.0324	0.920	0.149
SD:	0.00253	0.0206	0.0265	0.00239	0.0262	0.0512
SD/average:	13.8%	2.2%	7.6%	7.4%	2.9%	34.3%

Table 6.2 Unexposed Portion of Sample Model:
Average first order rate constants for each dye and for all experiments

for all experiments:

dye	average k	SD	SD/average
Acid Blue 9	0.0260	0.00776	29.9%
Acid Orange 7	0.0261	0.00956	36.6%
Reactive Black 5	0.0235	0.00609	25.9%
Reactive Blue 19	0.0256	0.00536	20.9%
for all dyes:	0.0253	0.00745	29.4%

Graphs depicting the fit of the UPOS model to the data are given on the following pages with the results for the Indirect Analysis experiments in subsection 6.1.1.1 and the results for the Direct Analysis experiments in subsection 6.1.1.2.

6.1.1.1 Indirect Analysis

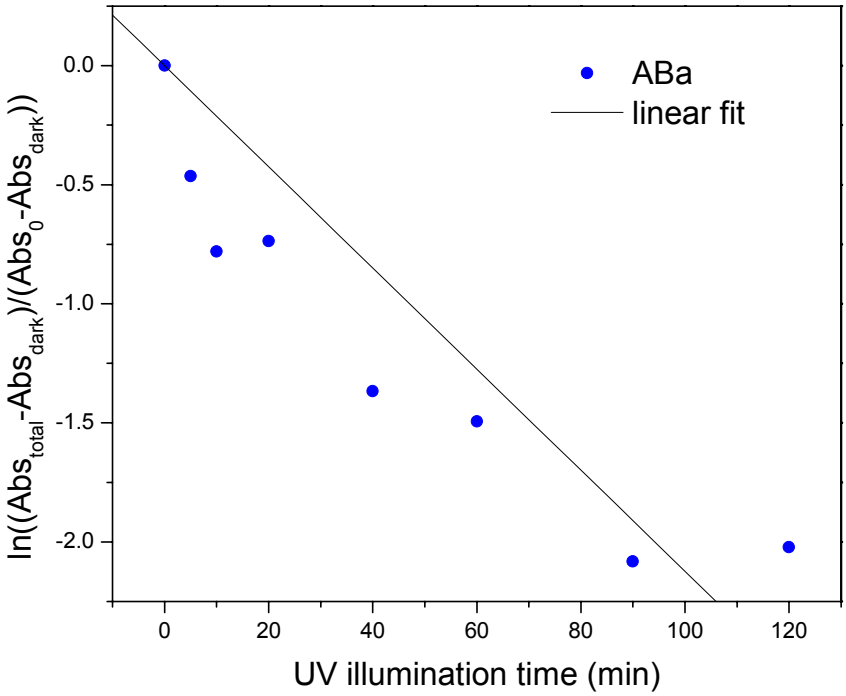

Figure 6.2 UPOS: Indirect Analysis of Acid Blue 9 on TiO_2 (ABa)

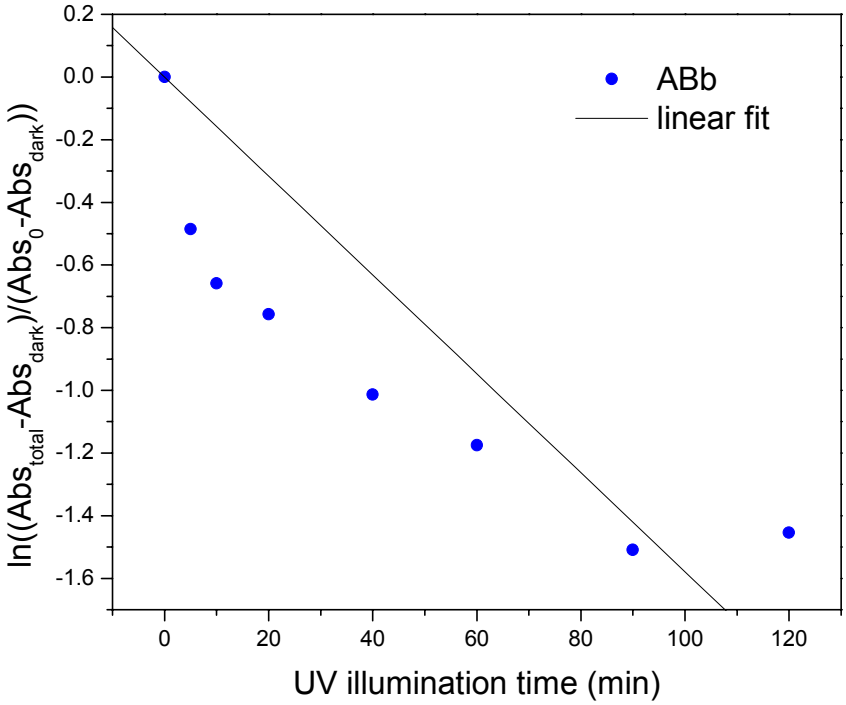

Figure 6.3 UPOS: Indirect Analysis of Acid Blue 9 on TiO_2 (ABb)

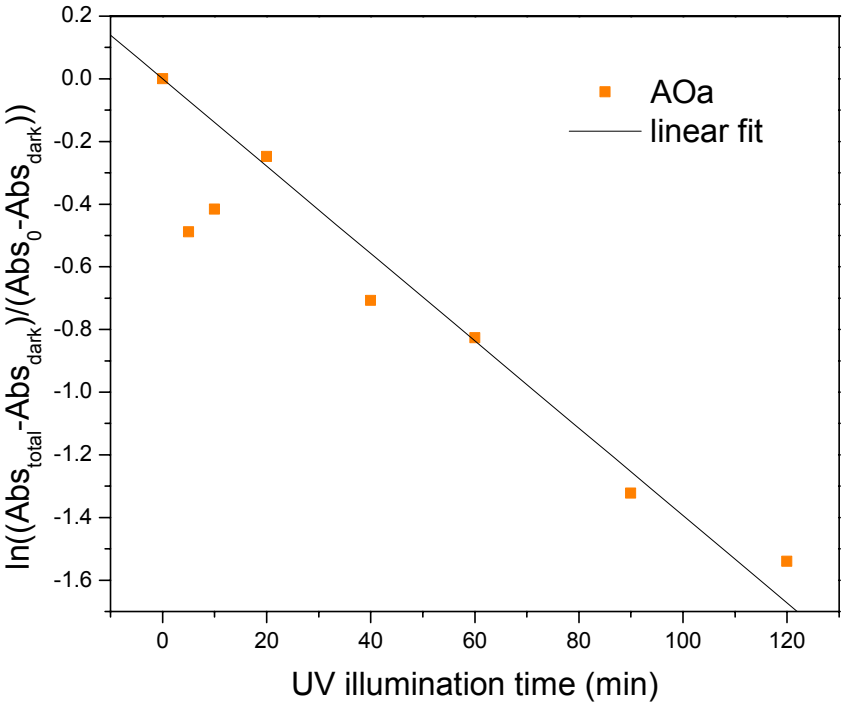

Figure 6.4 UPOS: Indirect Analysis of Acid Orange 7 on TiO_2 (AOa)

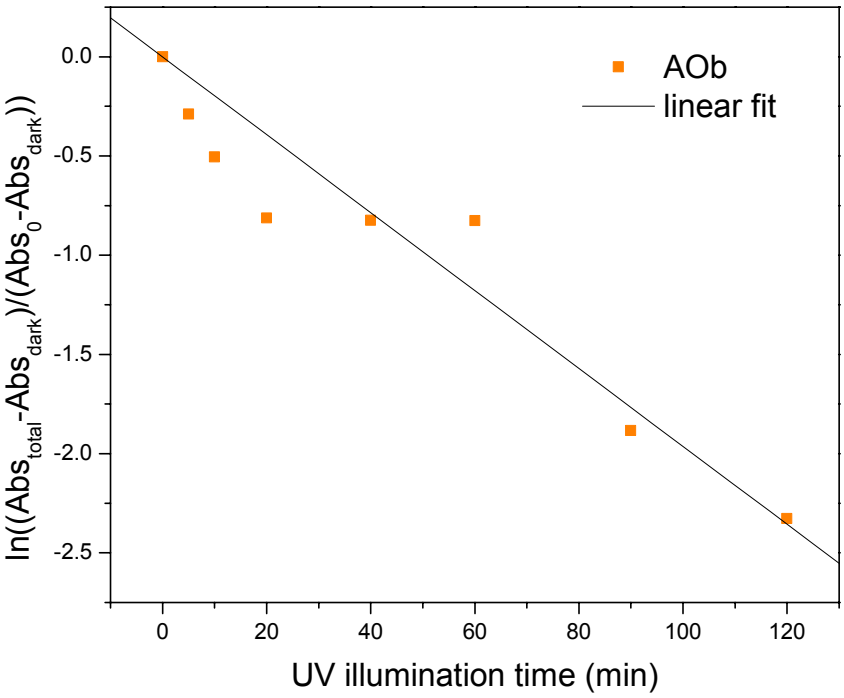

Figure 6.5 UPOS: Indirect Analysis of Acid Orange 7 on TiO_2 (AOb)

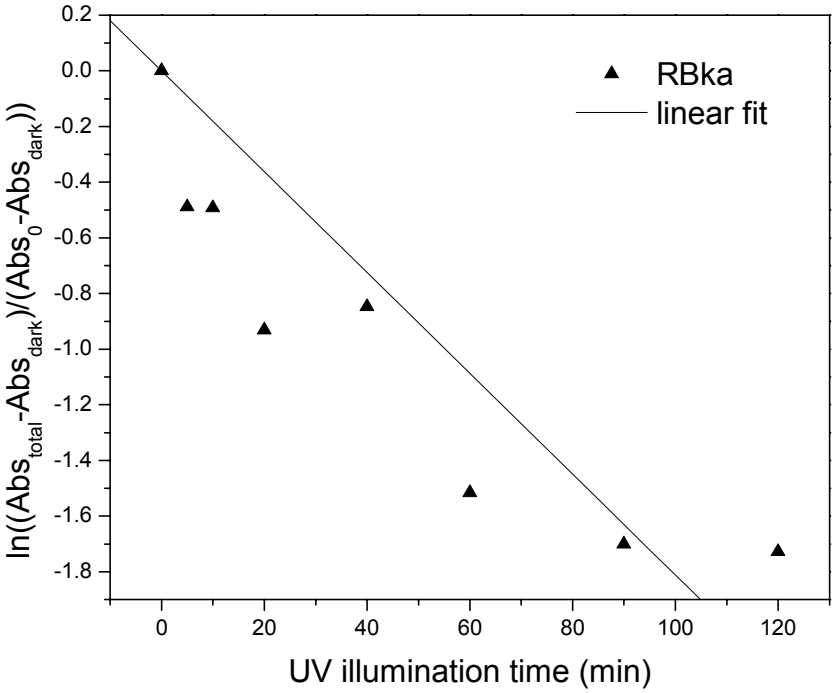

Figure 6.6 UPOS: Indirect Analysis of Reactive Black 5 on TiO_2 (RBka)

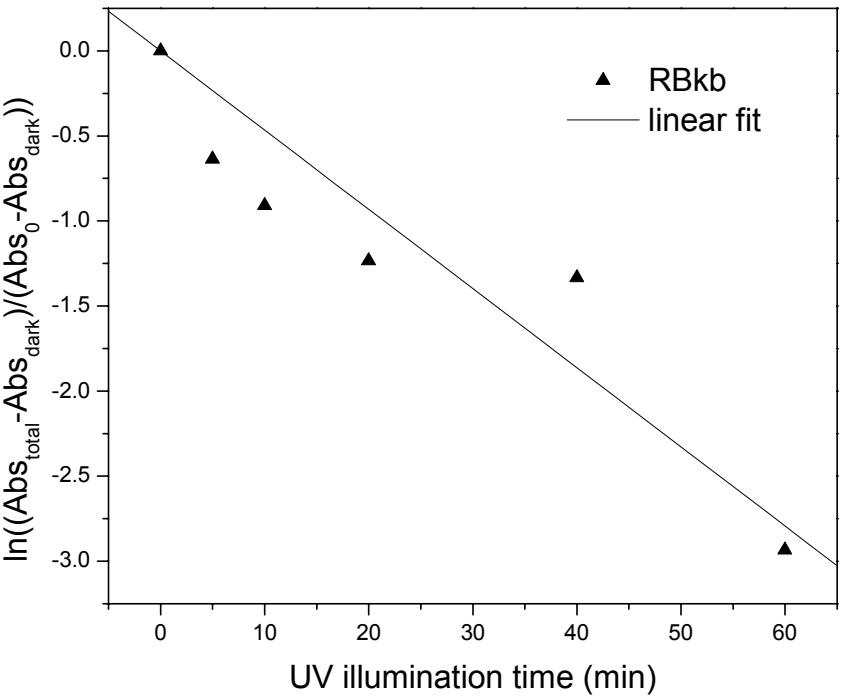

Figure 6.7 UPOS: Indirect Analysis of Reactive Black 5 on TiO_2 (RBkb)

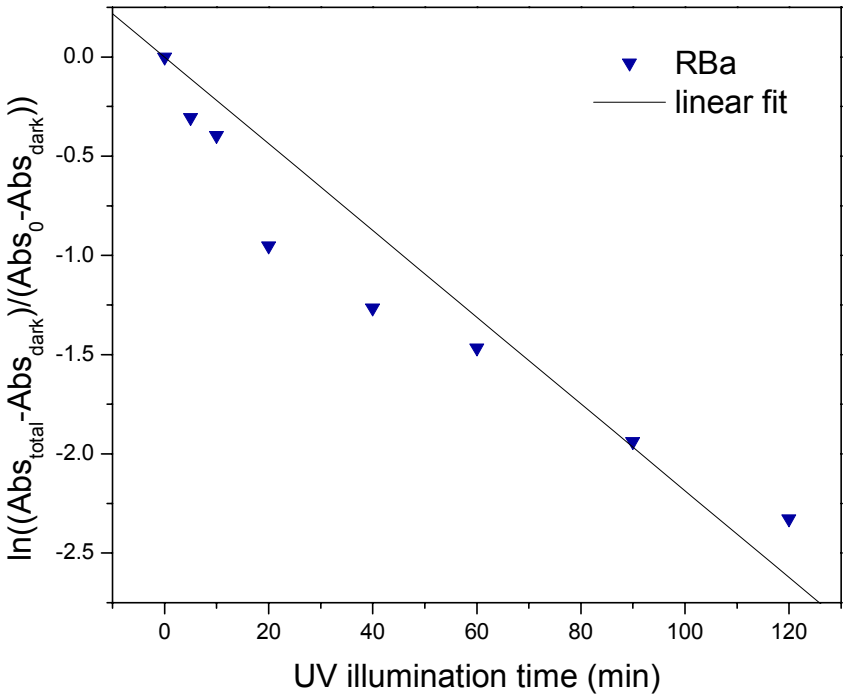

Figure 6.8 UPOS: Indirect Analysis of Reactive Blue 19 on TiO_2 (RBa)

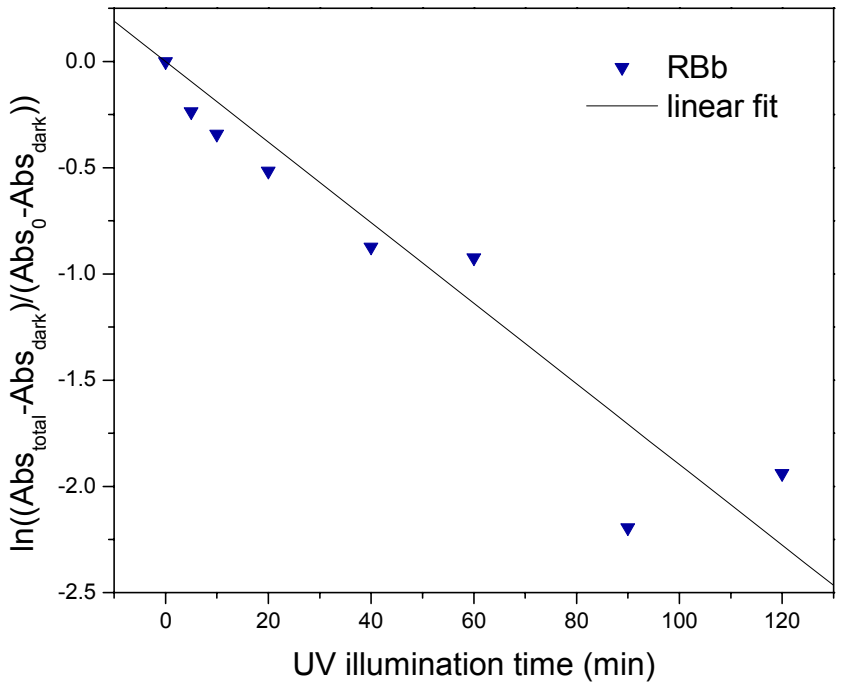

Figure 6.9 UPOS: Indirect Analysis of Reactive Blue 19 on TiO_2 (RBb)

6.1.1.2 Direct Analysis

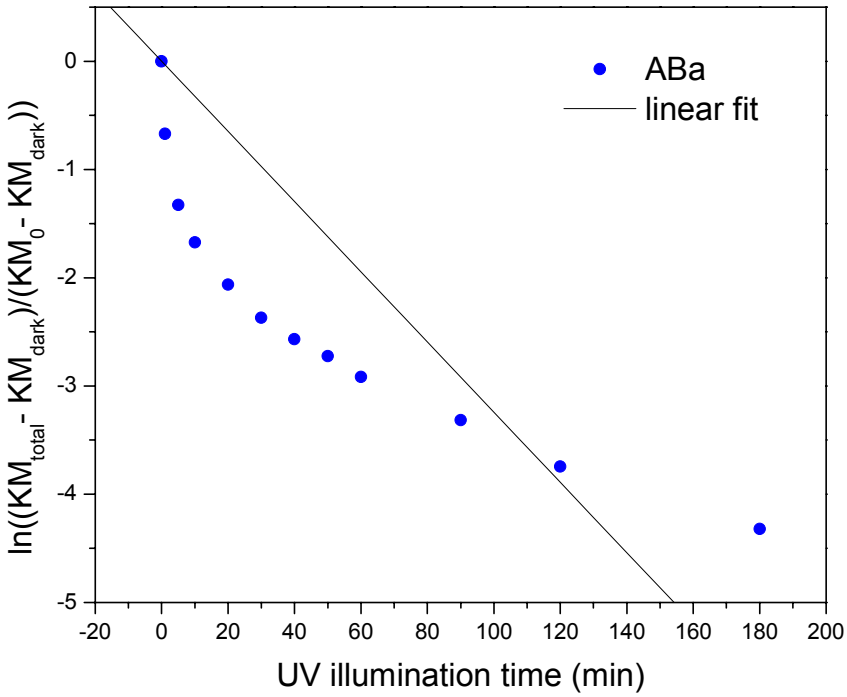

Figure 6.10 UPOS: Direct Analysis of Acid Blue 9 on TiO_2 (ABa)

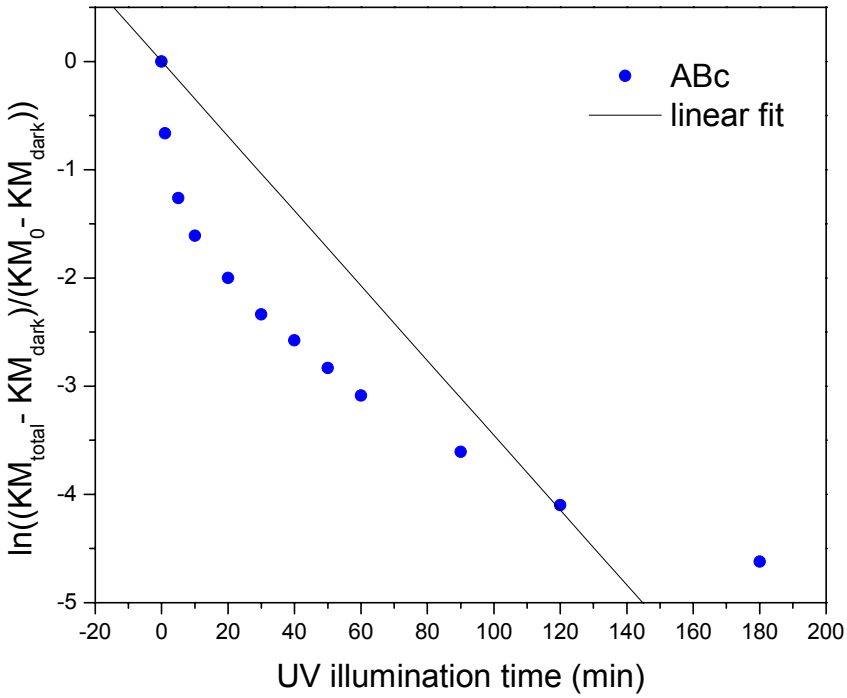

Figure 6.11 UPOS: Direct Analysis of Acid Blue 9 on TiO_2 (ABc)

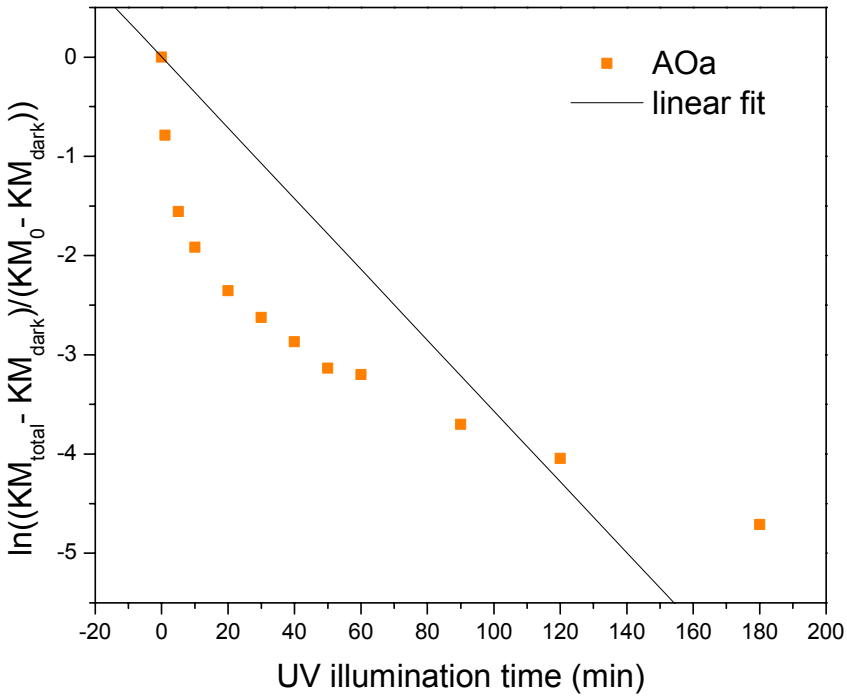

Figure 6.12 UPOS: Direct Analysis of Acid Orange 7 on TiO_2 (AOa)

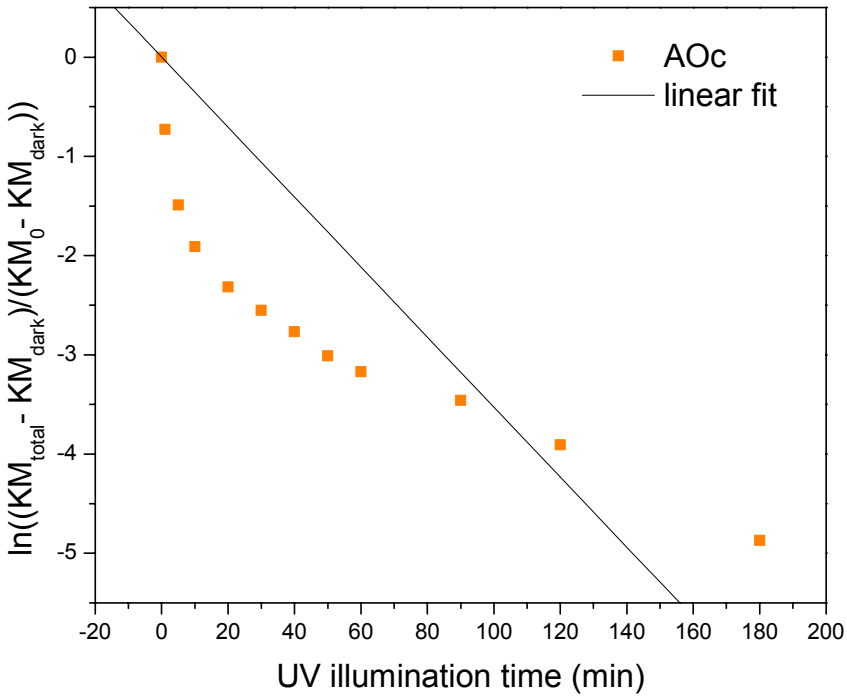

Figure 6.13 UPOS: Direct Analysis of Acid Orange 7 on TiO_2 (AOc)

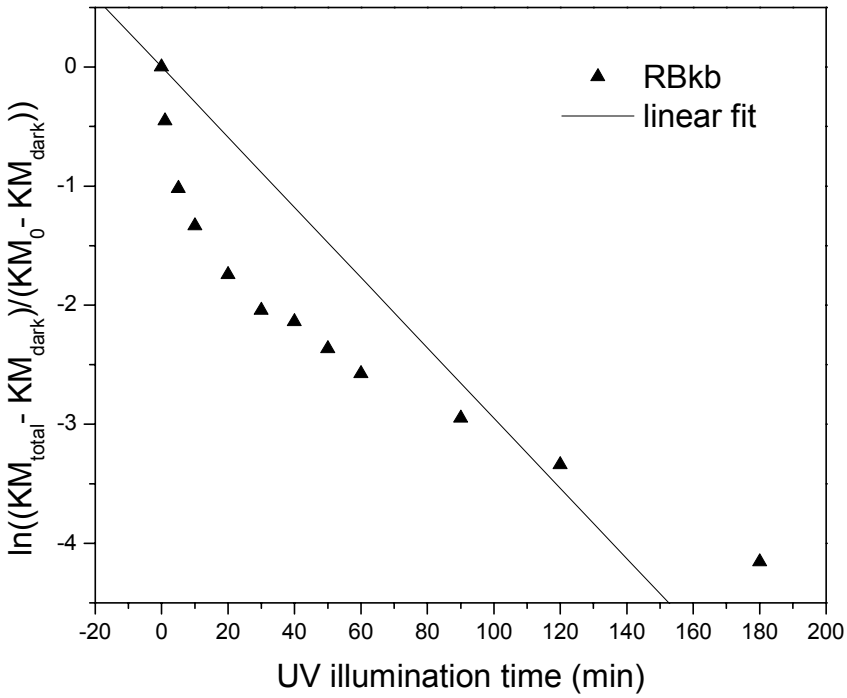

Figure 6.14 UPOS: Direct Analysis of Reactive Black 5 on TiO_2 (RBkb)

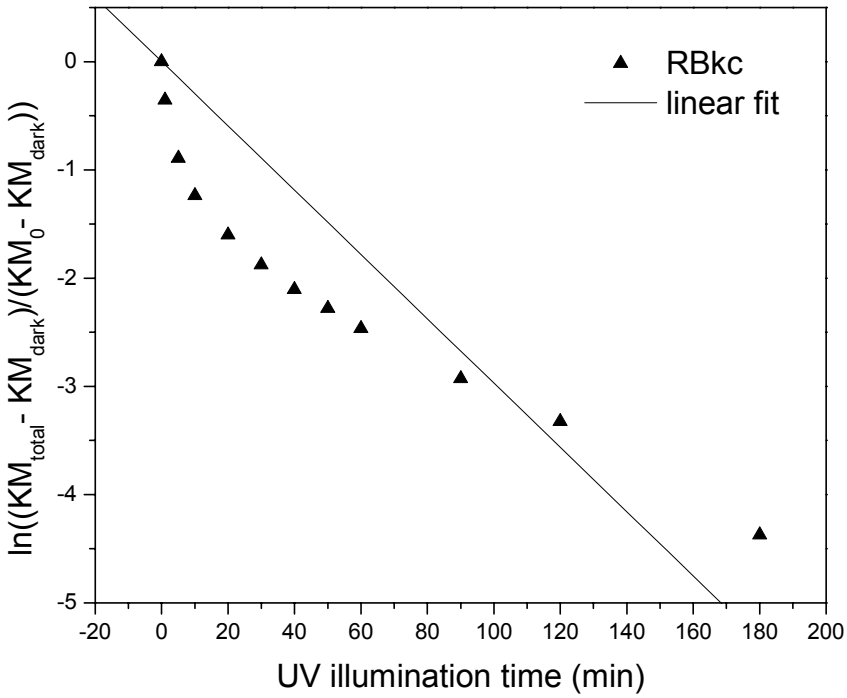

Figure 6.15 UPOS: Direct Analysis of Reactive Black 5 on TiO_2 (RBkc)

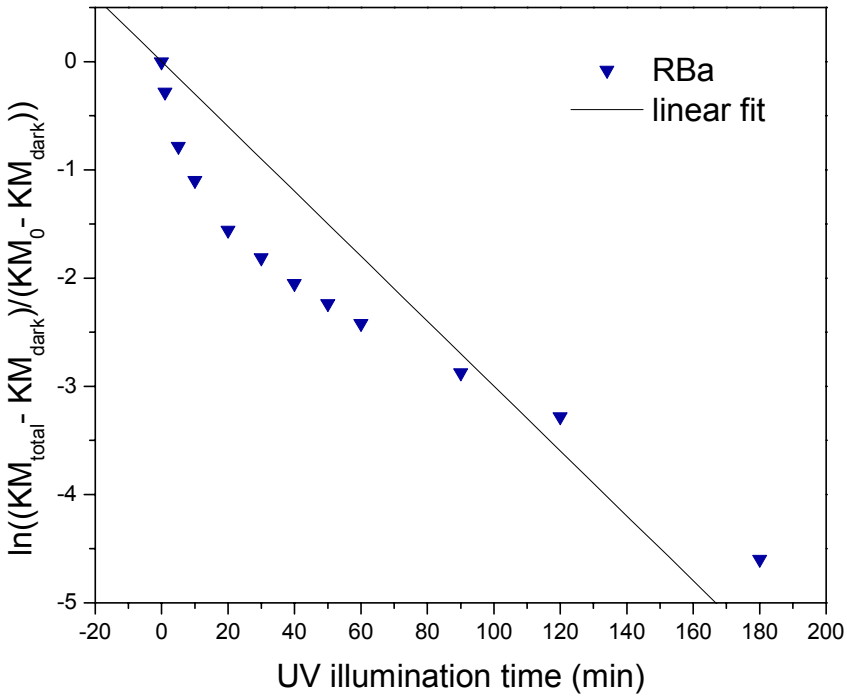

Figure 6.16 UPOS: Direct Analysis of Reactive Blue 19 on TiO_2 (RBa)

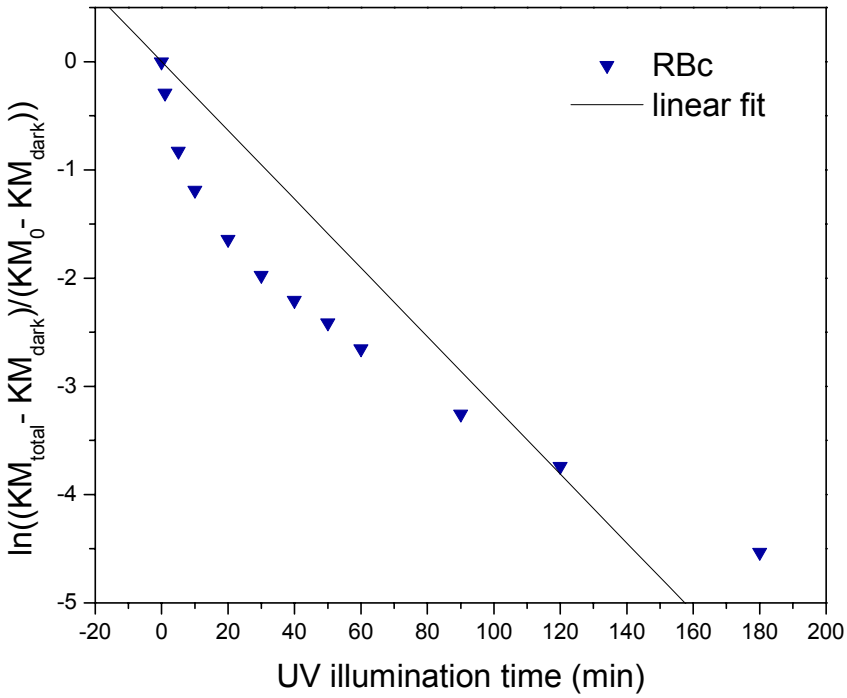

Figure 6.17 UPOS: Direct Analysis of Reactive Blue 19 on TiO_2 (RBc)

6.1.2 UPOS Model Fit to Data of Other Researchers

Previously, Yang et al. [5] reported the photocatalytic oxidation of Acid Blue 9 adsorbed on TiO_2 examined by diffuse reflectance infrared Fourier transform spectroscopy (DRIFTS). An aqueous solution of 10 ppm dye of pH 2.3 was prepared in which a concentration of 1.5 g L^{-1} of TiO_2 was added and stirred overnight for the adsorption to occur. The Acid Blue 9 coated TiO_2 particles were then collected by filteration and dried. The powder was then placed in a sample holder for in situ analysis by DRIFTS during exposure to 15 mW cm^{-2} of UV. The UPOS model was successfully applied to results reported by Yang et al. [5] by analysis of their Fig. 8 data, as shown in Figure 6.18 below, producing a k of 0.0184 min^{-1} with an absolute value of the correlation coefficient ($|R|$) of 0.985 by the fit described in section 6.1. This value of k determined for the Yang et al. [5] DRIFTS data for the photocatalytic degradation of Acid Blue 9 by TiO_2 is comparable to our average result of 0.0260 min^{-1} for the dye.

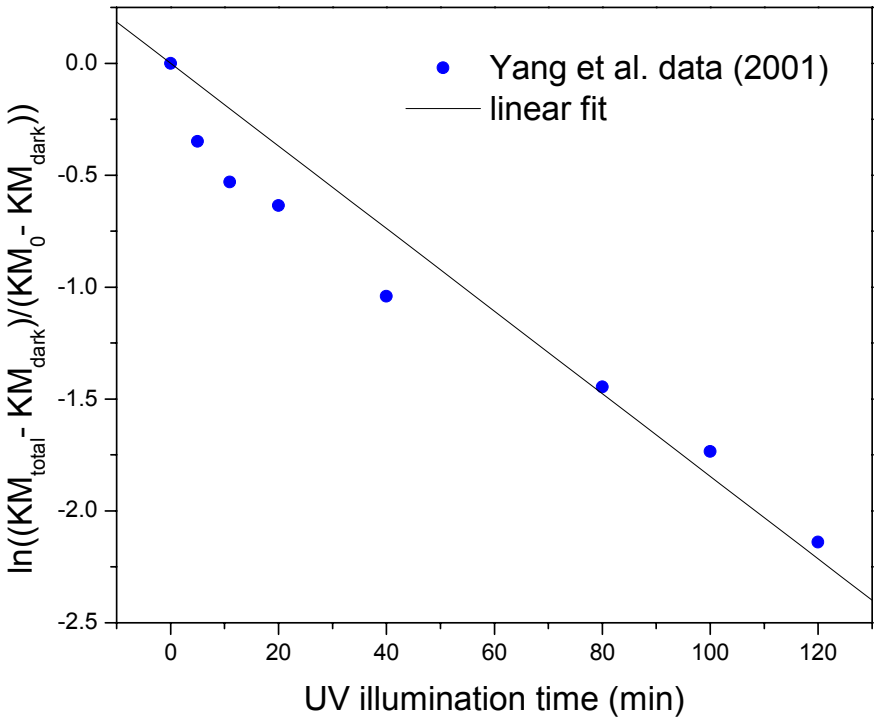

Figure 6.18 UPOS model fit to Yang and coworkers' [5] DRIFTS data

6.1.3 Discussion of Results

The UPOS model accounts for dye adding to the total concentration of dye measured, but not involved in the photocatalytic degradation because it and the underlying TiO_2 was not illuminated with UV. This model assumes that the photocatalytic reaction only occurs on surfaces illuminated with UV light and that the photocatalytic mechanism relies on the absorption of photons by TiO_2. The experimental system involved the illumination of dye-coated TiO_2 particles, with the dye in intimate contact with the semiconductor. A number of researchers [6-9] report the remote oxidation of contaminants not directly adsorbed to the photocatalyst surface, presumably due to migrating oxidizing species, such as OH radicals. The experimental system used in this study involved contaminants directly adsorbed to the TiO_2 surface, although the migrating oxidizing species could possibly have reached dye not

exposed to UV light. This possibility was not explicitly considered in the UPOS model. Although not previously described, the model did account for this phenomenon if it is assumed that the concentration, C_D(dark), was a concentration of dye not reached by the migrating oxidizing species.

The UPOS model appeared to fit the photocatalytic degradation data obtained by the Indirect Analysis method better, as indicated by the higher average correlation coefficient, than the data obtained by the Direct Analysis method. Graphs depicting the application of the UPOS model to the Direct Analysis *KM* data (subsection 6.1.1.2) show a systematic deviation from the linear fit, suggesting that the model does not thoroughly describe the reaction system. Perhaps combination of the UPOS model with the Series Reaction model would more accurately describe the photocatalytic degradation of organic dyes by TiO_2.

6.2 Light Intensity Influenced Rate Constant (LIIRC) Model

One widely reported mechanism for the photocatalytic process begins with the absorption of a photon of light by a semiconductor (e.g. [1-4]). The rate of the photocatalytic degradation of organic dyes by TiO_2 would then be dependent on the quantity and rate at which photons are supplied to the semiconductor surface. Egerton and King [10] reported that the rate of the photo-oxidation of liquid isopropanol by TiO_2 was proportional to light intensity to the half power for intensities above $5x10^{15}$ photons sec^{-1}. For lower intensities the rate was proportional to light intensity. Peral and Ollis [11] modeled the photocatalytic rate constant as Equation 6.6, dependent on an intensity-independent rate constant (k_0), an effective absorption coefficient of TiO_2 (α_T), a constant (a), and the axial coordinate through the TiO_2 layer (y).

$$k(I) = k_0 \exp(-\alpha_T a y)$$

Equation 6.6

This rate constant equation can be derived by assuming that the rate is a function of light transmission through the TiO_2 layer. Transmission through the TiO_2 layer is given by the following;

$$T = \frac{I}{I_0} = \exp(-\kappa C l)$$

Equation 6.7

where κ is the Napierian molar absorption coefficient (κ=2.303α) of TiO_2, C is the molar concentration of the absorbing species (TiO_2) and *l* is the thickness of the layer through which light passes [12]. The equation for transmission can then be used, as shown in Equation 6.8 below, to obtain an equation for the light intensity influenced rate constant. The rate constant, Equation 6.6, is reached if the Napierian molar absorption coefficient (κ) can be assumed to be the effective absorption coefficient for TiO_2 (α_T), the thickness of the layer (*l*) is described by the axial coordinate (*y*) and the product of the power (*p*) and the concentration (*C*) is the constant (*a*).

$$k(I) = k_0 T^p = k_0 \left(\frac{I}{I_0}\right)^p = k_0 \left(\exp(-\kappa C l)\right)^p = k_0 \exp(-\kappa p C l) = k_0 \exp(-\alpha_T a y)$$

Equation 6.8

The light intensity influenced rate constant, *k(I)*, was used to model the photocatalytic degradation of organic dyes by TiO_2. A schematic of the Light Intensity Influenced Rate Constant (LIIRC) model is shown in Figure 6.19.

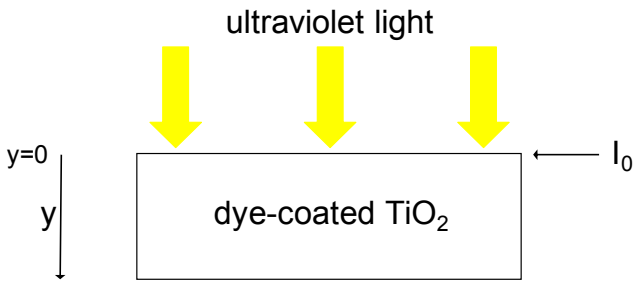

Figure 6.19 LIIRC model schematic

The local destruction of adsorbed organic dyes in UV-TiO_2-air systems can be modeled as a first order reaction with respect to dye concentration using a batch reactor model and the LIIRC as shown in Equation 6.9. The initial concentration of dye is given by $C_{D(0)}$. This model considers that the photocatalytic reaction, by TiO_2 absorption of UV, only varies in one direction (y) and that dye concentration (C_D) is a function of y and time (t). It is assumed that the absorption of near-UV light by the dye is negligible.

$$\frac{dC_D}{dt} = -k_0 \exp(-\alpha_T a y) C_D(y,t) \quad \Rightarrow \quad C_D(y,t) = C_{D(0)} \exp(-k_0 t \exp(-\alpha_T a y))$$

Equation 6.9

To determine the average total concentration ($\overline{C}_D(t)$) of the dye in the TiO_2 layer, C_D is integrated over the entire thickness of the layer (L), as shown in Equation 6.10 below.

$$\overline{C}_D(t) = \frac{1}{L}\int_0^L C_{D(0)} \exp(-k_0 t \exp(-\alpha_T a y))dy$$

Equation 6.10

Solutions to Equation 6.10 can be obtained in multiple forms. One solution can be found using the solution form below [13]:

$$\int \frac{\exp(ax)}{x} = \ln x + \frac{ax}{1 \cdot 1!} + \frac{(ax)^2}{2 \cdot 2!} + \frac{(ax)^3}{3 \cdot 3!} + \ldots$$

Equation 6.11

The average total concentration of dye is then given by Equation 6.12 with $\gamma = \alpha_T a L$.

$$\overline{C}_D(t) = C_0\left(1 + (e^{-\gamma} - 1)\frac{k_0 t}{\gamma} - (e^{-2\gamma} - 1)\frac{{k_0}^2 t^2}{4\gamma} + (e^{-3\gamma} - 1)\frac{{k_0}^3 t^3}{18\gamma} + \ldots\right)$$

Equation 6.12

Another form of the solution can be found by integrating Equation 6.10 by parts, as given in Equation 6.13 below.

$$\overline{C}_D(t) = \frac{C_0 \exp(-k_0 t)}{\gamma}\left(\frac{-1}{k_0 t} + \frac{1}{(k_0 t)^2} + \frac{-2}{(k_0 t)^3} + \ldots\right) +$$
$$\frac{C_0 \exp(-k_0 t \exp(-\gamma))}{\gamma}\left(\frac{1}{(k_0 t \exp(-\gamma))} + \frac{-1}{(k_0 t \exp(-\gamma))^2} + \frac{2}{(k_0 t \exp(-\gamma))^3} + \ldots\right)$$

Equation 6.13

These solutions are not practical because to achieve valid values for the average concentration for all measured times an infinite number of terms need to be taken into account. The nature of these solutions, alternating additive and subtractive quantities, does not allow the series to be truncated after only a few terms in this case. Therefore an alternate method to approximating the average concentration was sought.

To determine the average concentration of dye within the entire TiO_2 layer the right endpoint approximation (R_n) method was used to evaluate Equation 6.10. For each UV illumination time experimentally evaluated, the average concentration of dye was determined by R_n, as shown in Equation 6.14.

$$\overline{C}_D(t) = \frac{1}{L}\int_0^L C_{D(0)} \exp(-k_0 t \exp(-\alpha_T a y))dy \approx R_n = \frac{C_{D(0)}}{L}\sum_i^n \exp(-k_0 t \exp(-\alpha_T a y_i))\Delta y$$

Equation 6.14

Peral and Ollis [11] referenced work reported by Courbon and coworkers [14]; "As reported by Courbon et al., 99% of light absorption (optical density 2) occurs within a TiO_2 anatase layer of 4.5 μm, and so an α_T value of 10211 cm^{-1} was estimated." Therefore, for

this model, 4.5×10^{-4} cm was used for the value of L and 10211 cm^{-1} was used as the value of α_T. For the Direct Analysis experiments, this layer thickness accounts for approximately 0.5% of the total sample thickness. Only the outermost layer of the entire sample was exposed, which was seen when the sample holder was opened to reveal dye-coated TiO_2 powder behind that top layer that was in the same color as the original unexposed sample. Egerton and King [10] report that "at very low intensities the photo-oxidation rate should be directly proportional to I" and at "high" intensities (greater than approximately 1 mW cm^{-2}) the photocatalytic activity was proportional to $I^{0.5}$. The value of *a* used in this model varied from 0.5 to 1.

6.2.1 Results: Data Fit to LIIRC Model

The influence of light intensity on the photocatalytic degradation of adsorbed organic dyes was examined using R_n to determine the average concentration of dye throughout the entire TiO_2 layer at each exposure time. The absorbance (*Abs*) and transformed reflectance (*KM*) data obtained for both the Indirect and Direct Analysis procedures respectively was proportional the total concentration of dye in the TiO_2 layer. Assuming that the *Abs* and *KM* units obtained were only due to contributions from the dye, the data could then be used as shown in the following equation.

$$\overline{Abs\ or\ KM} \approx R_n = \frac{(Abs_0\ or\ KM_0)}{L} \sum_i^n \exp(-k_0 t \exp(-\alpha_T a y_i))\Delta y$$

Equation 6.15

The average *Abs* is the measured absorbance and the average *KM* is the transformed measured reflectance, with Abs_0 and KM_0 indicating the initial values for both respectively. The wavelengths used for the analysis were the peak wavelengths previously indicated,

namely 629 nm for Acid Blue 9 data, 485 nm for Acid Orange 7, 617 nm for Reactive Black 5 and 596 nm for Reactive Blue 19 data.

An Excel spreadsheet was used to perform the calculations for each exposure time with the values of each parameter given in Table 6.3 below. All of the parameters were essentially fixed values expect the value of the intensity-independent rate constant (k_0). This rate constant was varied to determine the best fit of the LIIRC model to the data for all UV illumination times by visually comparing the graph of the calculated *Abs* or *KM* units versus time to the measured values. The parameter "*a*" was varied for one set of comparisons, the Acid Blue 9 sample ABa data, otherwise the value was set at 0.5. The average intensity for all experiments was 1.3 mW cm^{-1}, which was considered a "high" intensity by Egerton and King [10] corresponding to 0.5 for "*a*". The LIIRC model was applied to the Indirect Analysis experimental data for samples ABa, AOa, RBkb and RBa and the Direct Analysis experimental data for the same samples.

Table 6.3 Parameters used for LIIRC

Abs_0 or KM_0:	experimentally determined
L(cm):	0.00045
k_0 (min^{-1}):	variable
t (min):	UV illumination time
α_T(cm^{-1}):	10211
a:	0.5, 0.75 or 1
Δy:	0.0000045
n:	100

The rate constants, k_0, determined as the best fit for each of the Indirect Analysis experiments examined are given in Table 6.4 with the constant "*a*" used for the model indicated. The rate constants, k_0, determined as the best fit for each of the Direct Analysis experiments examined are given in

Table 6.5 again with the constant "*a*" used for the model indicated. Graphical depictions of the visually determined best fits are shown in subsection 6.2.1.1 for the Indirect Analysis experiments and in 6.2.1.2 for the Direct Analysis experiments. The calculated *Abs* and *KM* values are represented as lines and the observed data as symbols. The graphs include the calculated *Abs* or *KM* values for the rate constant determined to best fit the data as well as this k_0 value tripled, doubled, halved and divided by 3. The purpose of showing the five calculated *Abs* or *KM* values for the illumination times examined was to show how varying the intensity-independent rate constant affected the fit of the LIIRC model to the data. The rate constant determined to best fit the data for all of the graphs is shown as the line in the middle of the other four calculated values.

Table 6.4 Parameters for LIIRC model fit to Indirect Analysis experiments

sample	Abs_0	a	k_0 (min^{-1})
ABa	2.37088	0.5	0.03
ABa	2.37088	0.75	0.05
ABa	2.37088	1	0.1
AOa	1.08407	0.5	0.02
RBkb	0.79936	0.5	0.03
RBa	0.30495	0.5	0.03

Table 6.5 Parameters for LIIRC model fit to Direct Analysis experiments

sample	KM_0	a	k_0 (min^{-1})
ABa	2.43241	0.5	0.1
ABa	2.43241	0.75	0.25
ABa	2.43241	1	0.5
AOa	1.49106	0.5	0.16
RBkb	0.99561	0.5	0.06
RBa	0.888	0.5	0.07

6.2.1.1 Indirect Analysis

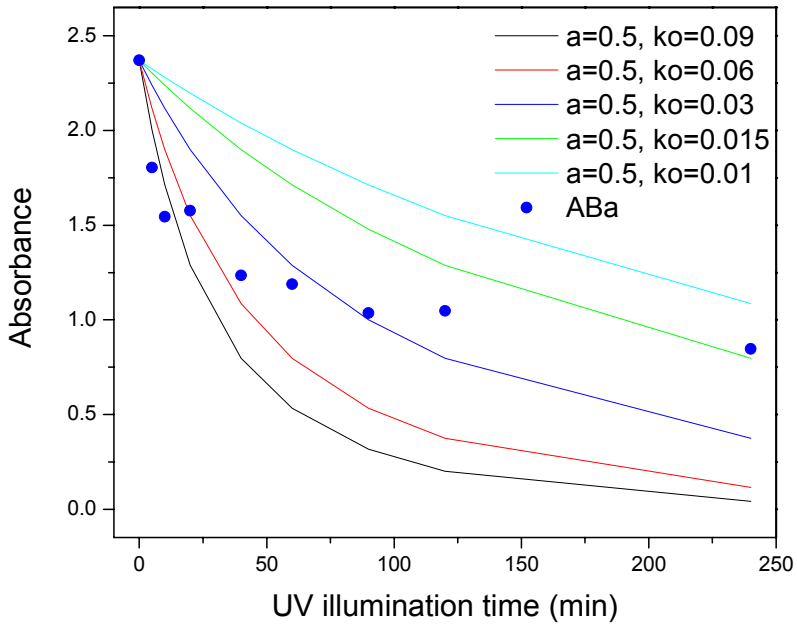

Figure 6.20 LIIRC: Indirect Analysis of Acid Blue 9 on TiO_2 (ABa), a=0.5

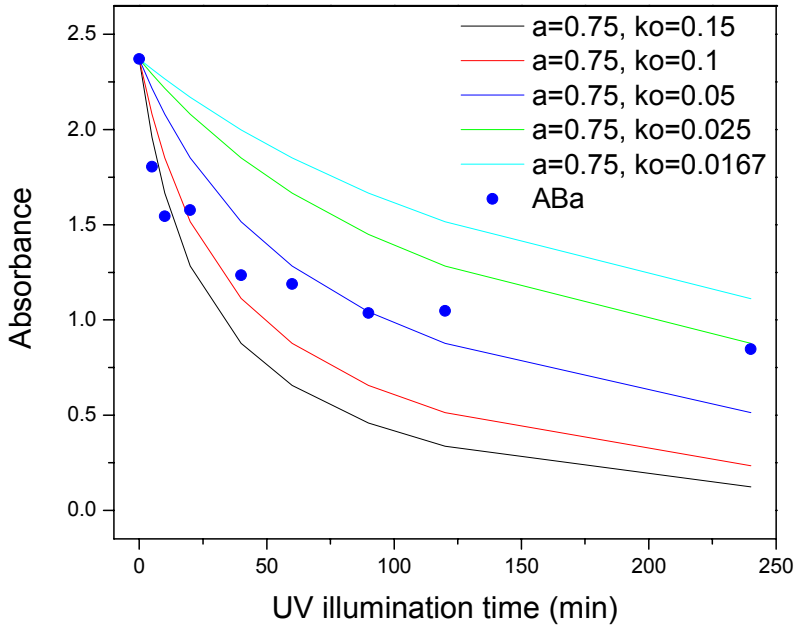

Figure 6.21 LIIRC: Indirect Analysis of Acid Blue 9 on TiO_2 (ABa), a=0.75

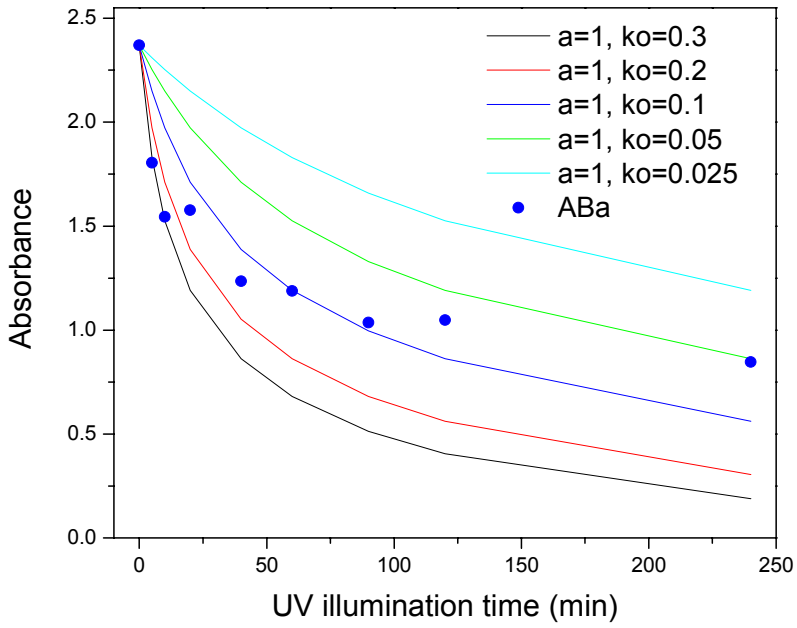

Figure 6.22 LIIRC: Indirect Analysis of Acid Blue 9 on TiO_2 (ABa), a=1

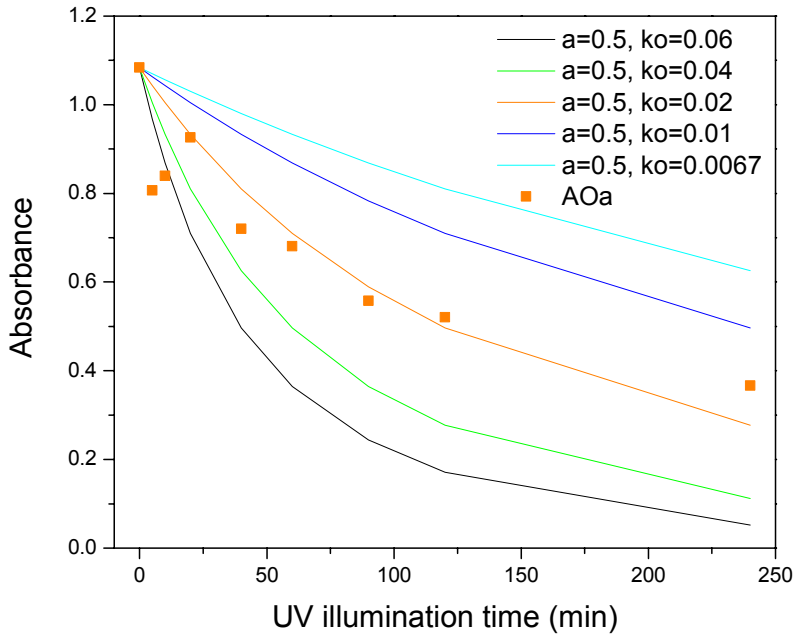

Figure 6.23 LIIRC: Indirect Analysis of Acid Orange 7 on TiO_2 (AOa), a=0.5

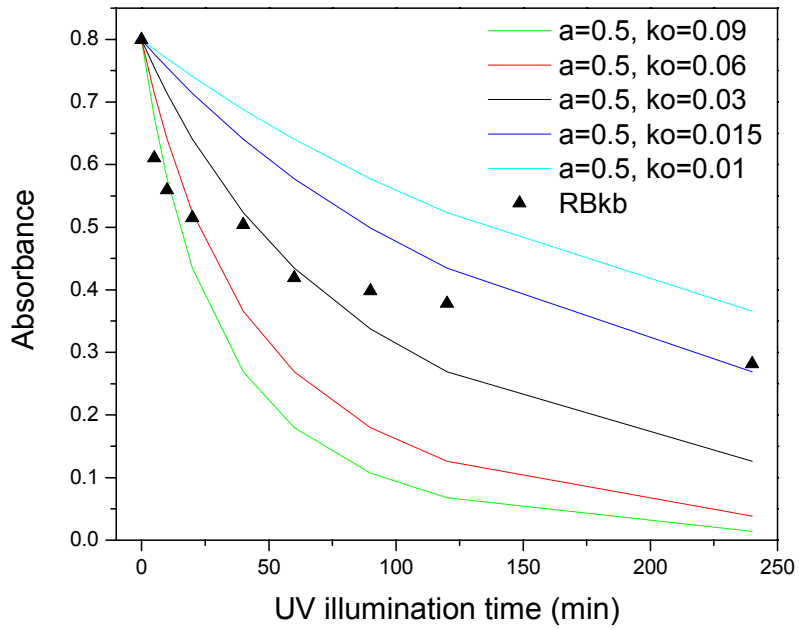

Figure 6.24 LIIRC: Indirect Analysis of Reactive Black 5 on TiO_2 (RBkb), a=0.5

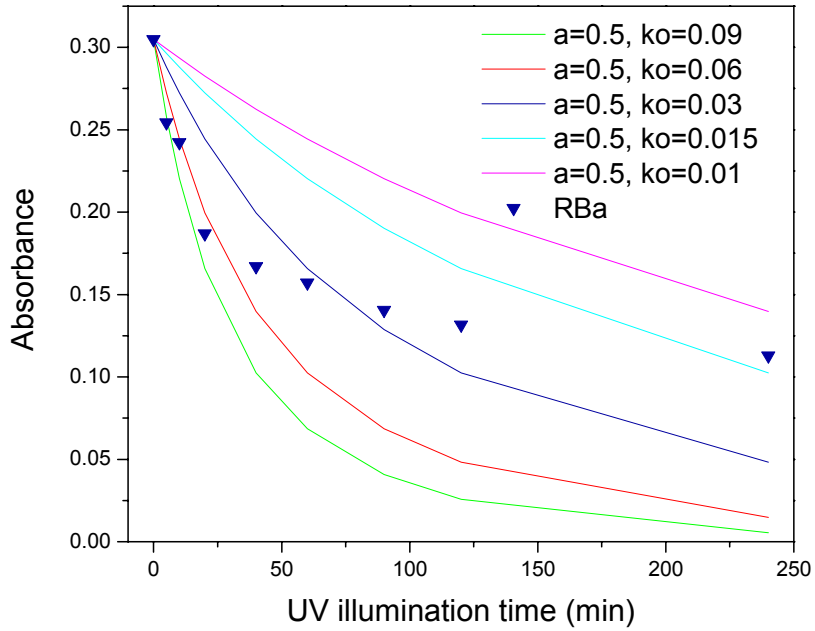

Figure 6.25 LIIRC: Indirect Analysis of Reactive Blue 19 on TiO_2 (RBa), a=0.5

6.2.1.2 Direct Analysis

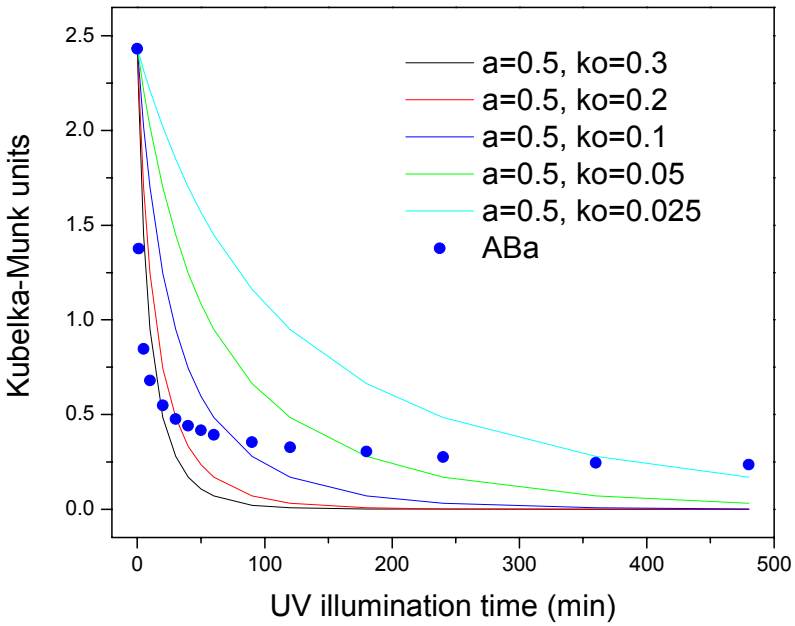

Figure 6.26 LIIRC: Direct Analysis of Acid Blue 9 on TiO_2 (ABa), a=0.5

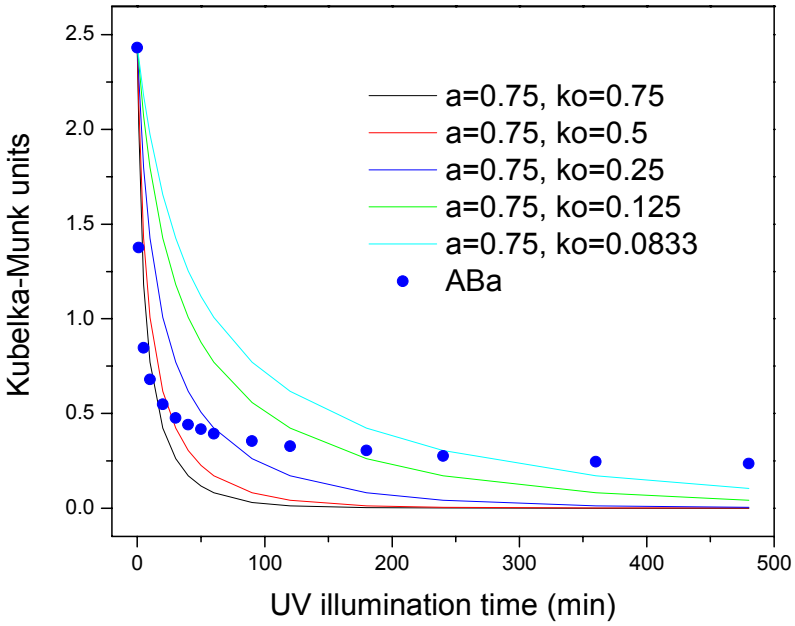

Figure 6.27 LIIRC: Direct Analysis of Acid Blue 9 on TiO_2 (ABa), a=0.75

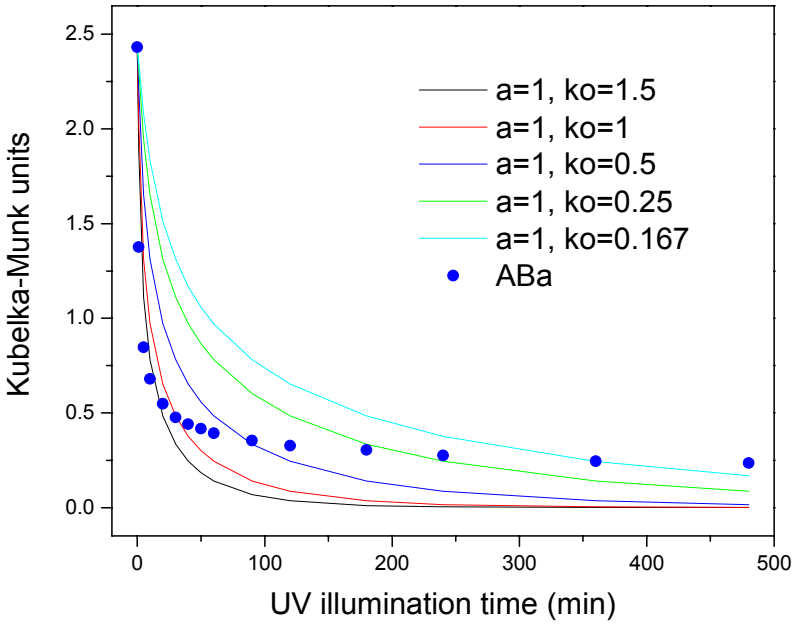

Figure 6.28 LIIRC: Direct Analysis of Acid Blue 9 on TiO_2 (ABa), a=1

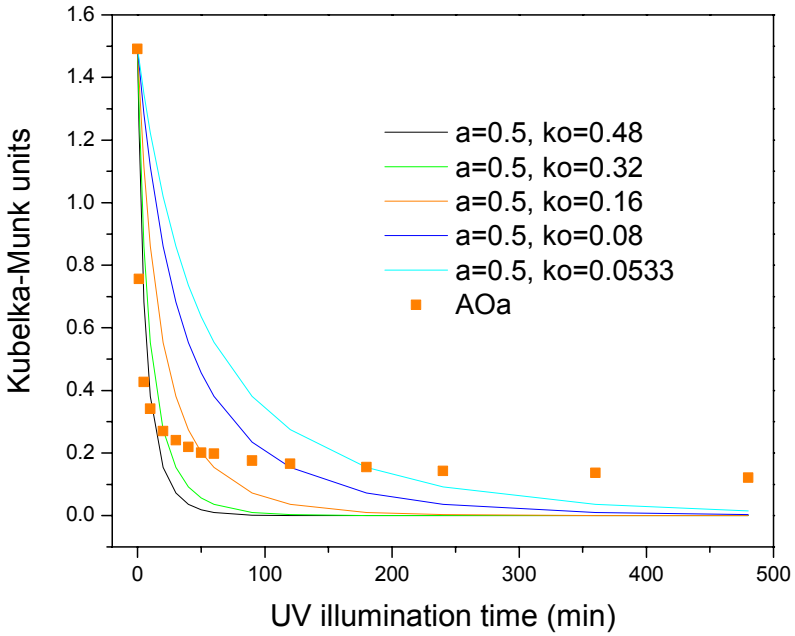

Figure 6.29 LIIRC: Direct Analysis of Acid Orange 7 on TiO_2 (AOa), a=0.5

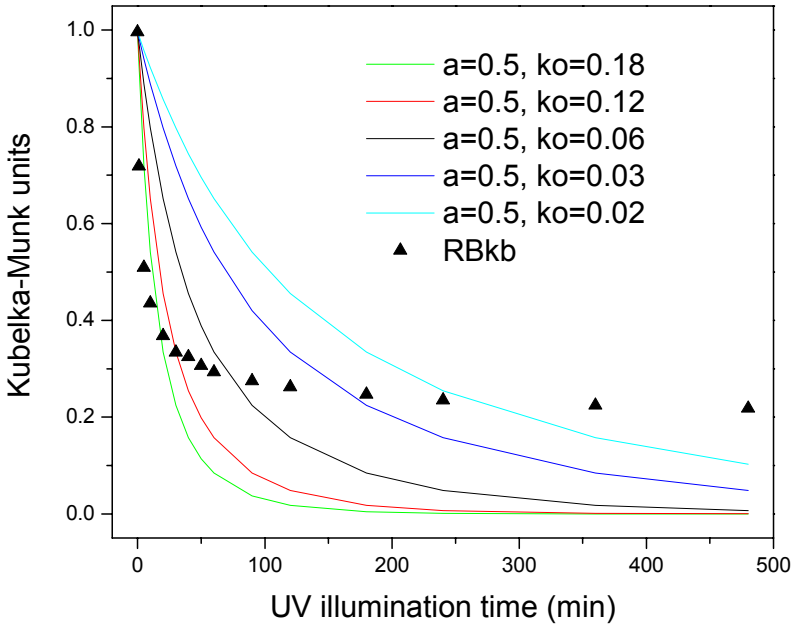

Figure 6.30 LIIRC: Direct Analysis of Reactive Black 5 on TiO_2 (RBkb), a=0.5

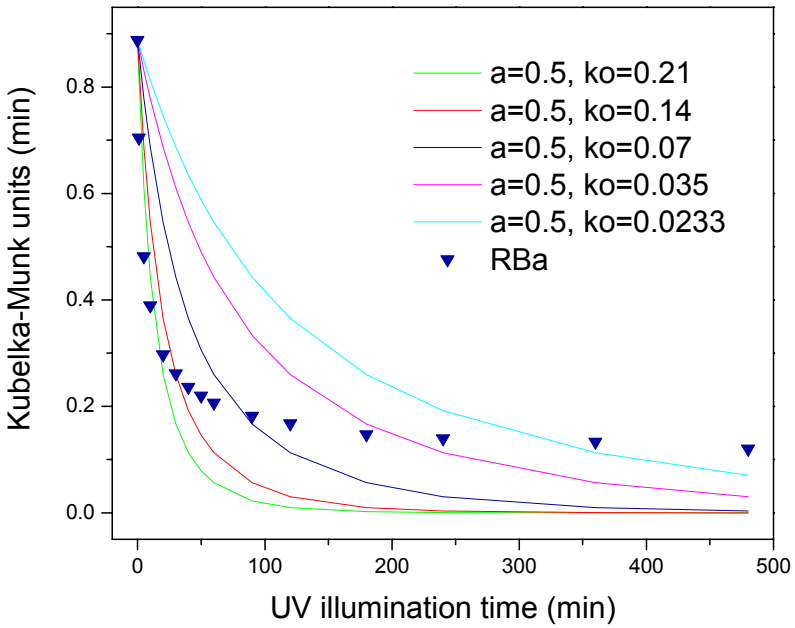

Figure 6.31 LIIRC: Direct Analysis of Reactive Blue 19 on TiO_2 (RBa), a=0.5

6.2.2 Discussion of Results

The rate constants, k_0, determined to best fit the *Abs* data obtained by the Indirect Analysis method for each dye were given in Table 6.4 and the rate constants determined to best fit the *KM* data obtained by the Direct Analysis method for each dye were given in Table 6.5. The Acid Blue 9 data was fit to the LIIRC model using varying values of the constant "*a*" and determining the appropriate k_0 value. The intensity-independent rate constant value varied significantly as "*a*" changed from 0.5 to 0.75 to 1. This was expected because only one "*a*" value should be used to describe the system. The constant "*a*" is proportional to the influence of intensity on the photocatalytic reaction and there is an optimum value for the experimental system. The rate of the reaction measured was determined, therefore varying the constant "*a*" changed the intensity-independent rate constant, k_0, because the light intensity influenced rate constant, *k(I)* in Equation 6.6, was constant.

The rate constants determined using $a = 0.5$ were the same order of magnitude for the experiments performed using the same procedure. The average k_0 determined for the photocatalytic degradation of all dyes analyzed by the Indirect Analysis method was approximately 0.03 min^{-1} and the average value determined for the reaction monitored by the Direct Analysis method was 0.1 min^{-1}. The higher value obtained for the Direct Analysis experiments may be closer to the true value because the experimental system more closely resembled the LIIRC model, as shown in Figure 6.19.

The LIIRC model discussed here does not appropriately describe the photocatalytic degradation of organic dyes by TiO_2. This can be seen in the figures shown in subsections 6.2.1.1 and 6.2.1.2. Although a "best" fit k_0 value was reported, the calculated *Abs* and *KM*

values did not correspond well with the observed values for the entire period the reaction was monitored. The LIIRC model may be applicable to the photocatalytic system, but perhaps the model needs to be combined with the Series Reaction or UPOS model to completely describe the system.

6.3 References

[1] Childs, L.P. and D.F. Ollis, *Is Photocatalysis Catalytic?* Journal of Catalysis, 1980. **66**: p. 383-390.

[2] Tang, W.Z., Z. Zhang, H. An, M.O. Quintana and D.F. Torres, *TiO_2/UV Photodegradation of Azo Dyes in Aqueous* Solutions. Environmental Technology 1997, **18**: p. 1-12.

[3] Sauer, T., G.C. Neto, H.J. Jose and R.F.P.M. Moreira, *Kinetics of photocatalytic degradation of reactive dyes in a TiO_2 slurry reactor*. Journal of Photochemistry and Photobiology A: Chemistry 2002, **149**: p. 147-154.

[4] Serpone, N. and E. Pelizzetti, *Photocatalysis: Fundamentals and Applications* 1989, New York, NY: John Wiley & Sons, Inc. 3-7. Photocatalysis already defined by J. Plotnikov in his book Allgemeine Photochemie, 2nd ed., Walter de Gruyter, West Berlin, 1936, pp. 362-375.

[5] Yang, T.C.-K., S.-F. Wang, S.H.-Y. Tsai and S.Y. Lin, *Intrinsic photocatalytic oxidation of the dye adsorbed on TiO_2 photocatalysts by diffuse reflectance infrared Fourier transform spectroscopy*. Applied Catalysis B: Environmental 2001. **30**: p. 293-301.

[6] Lee, M.C. and W. Choi, *Solid Phase Photocatalytic Reaction on the Soot/TiO_2*

Interface: The Role of Migrating OH Radicals. Journal of Physical Chemistry B 2002. **106**(45): p. 11818-11822.

[7] Lee, S.-K., S. McIntyre and A. Mills, *Visible illustration of the direct, lateral and remote photocatalytic destruction of soot by titania*. Journal of Photochemistry and Photobiology A: Chemistry 2004. **162**: p. 203-206.

[8] Tatsuma, T., S. Tachibana, T. Miwa, D.A. Tryk and A. Fujishima, *Remote Bleaching of Methylene Blue by UV-Irradiated TiO_2 in the Gas Phase*. Journal of Physical Chemistry B 1999. **103**(38): p. 8033-8035.

[9] Tatsuma, T., S. Tachibana and A. Fujishima, *Remote Oxidation of Organic Compounds by UV-Irradiated TiO_2 via the Gas Phase*. Journal of Physical Chemistry B 2001. **105**(29): p. 6987-6992.

[10] Egerton, T.A. and C.J. King, *The influence of light intensity on photoactivity in TiO_2 pigmented systems*. Journal of the Oil & Colour Chemists Association 1979. **62**(10): p. 386-391.

[11] Peral, J. and D.F. Ollis, *Heterogeneous Photocatalytic Oxidation of Gas-Phase Organics for Air Purification: Acetone, 1-Butanol, Butyraldehyde, Formaldehyde, and m-Xylene Oxidation.* Journal of Catalysis 1992. **136**: p. 554-565.

[12] Braun, A.M., M.-T. Maurette and E. Oliveros (Translation by D.F. Ollis and N. Serpone), *Photochemical Technology*. 1991, New York, NY: John Wiley & Sons, Ltd. p. 4.

[13] Spiegel, M.R and J. Liu, *Schaum's Outlines: Mathematical Handbook of Formulas and Tables*. 2nd Edition 1999, New York, NY: McGraw-Hill. p. 96.

[14] Courbon, H., M. Formenti, F. Juillet, A.A. Lisachenko, J. Martin and S.J. Teichner,

Photoactivity of nonporous titanium dioxide (anatase), Kinetics and Catalysis 1973, **14**: p. 84.

7 DYE DEGRADATION: PHOTOCATALYSIS OR HOMOGENEOUS PHOTODEGRADATION?

The previous chapters reported destruction of sub-monolayer organic dyes deposited on TiO_2 with near-UV illumination. It is believed that the degradation of adsorbed organics was predominately due to a photocatalytic phenomenon, as reported in the literature by, for example, Romeas and coworkers [1]. Control experiments by Romeas et al. revealed that without UV irradiation or TiO_2 the degradation of palmitic acid did not occur. We also examined, by experiment, the importance of TiO_2 and will show results validating the theory that dye degradation was due to photocatalysis.

The mechanism of self-sensitized photodegradation via absorption of light by the dye was not examined, although other researchers report the importance of the photocatalyst in this mechanism. Figure 7.1 below is a diagram by Vinodgopal et al. [2] depicting the self-sensitization mechanism. Vinodgopal and coworkers [2] observed no photo-induced bleaching of Acid Orange 7 adsorbed on Al_2O_3 when illuminated with light of wavelength greater than 380 nm. Porada and Gade [3] probed the influence of TiO_2 on the self-sensitzed photodegradation of AR44 by monitoring the reflectance of samples with exposure to 546 nm light of dye-coated MgO, a photo-inert support. They reported that the dye did not degrade, and concluded that the photodegradation only takes place in the presence of a photocatalyst. They did not examine photodegradation with illumination of near-UV light, the region of absorption by TiO_2.

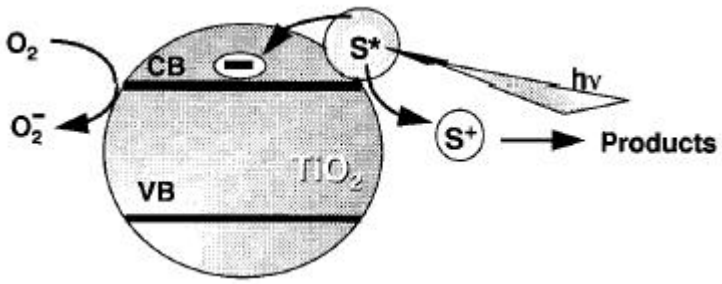

Figure 7.1 Illustration of photosensitized degradation of colored pollutant. Reprinted with permission from [2]. Copyright 1996 American Chemical Society.

7.1 Experiments and Results

To determine whether the degradation of adsorbed dyes on TiO_2 occurred due solely to photocatalysis or also to homogeneous photodegradation contributions, control experiments were performed using dye coated on a photo-inactive support, Al_2O_3. Dye-coated Al_2O_3 particles were prepared by the method described in Chapter 2. The dye-coated Al_2O_3 samples prepared were labeled as follows; Acid Blue 9: AAB, Acid Orange 7: AAO, Reactive Black 5: ARBk and Reactive Blue 19: ARB. Dye-coated powders were exposed to near-UV light using the Direct Analysis method described in Chapter 4. Briefly, the powders were placed in a closed sample holder with a UV transmissive quartz window, and illuminated with near-UV light; meanwhile the reaction was monitored by diffuse reflectance UV-visible spectroscopy, at intervals up to 8 hrs of exposure.

7.1.1 Spectroscopic Results

Figure 7.2 to Figure 7.5 show the transformed reflectance spectra in Kubelka-Munk (*KM*) units, proportional to concentration as described in section 4.1.1, of dye-coated Al_2O_3 with UV exposure. The spectra were shifted incrementally for the viewer to discern the

spectra for each exposure time. For all figures (Figure 7.2-Figure 7.5) the spectra of highest *KM* units received 0 min of near-UV illumination and the spectra were shifted incrementally downward from the top for 1, 5, 10, 20, 30, 40, 50, 60, 90, 120, 180, 240 and 360 min to the spectra of lowest *KM* units for 480 min of UV exposure. The reflectance profiles of the dye spectra show negligible change with near-UV illumination time; therefore the dye is not converting to another species. If not incrementally shifted, all of the spectra within an experiment virtually overlap; therefore the concentration of dye adsorbed to Al_2O_3 is not changing with UV exposure. These results prove that TiO_2 is necessary for the photodegradation of adsorbed organic dyes and that indeed a photocatalytic process is occurring.

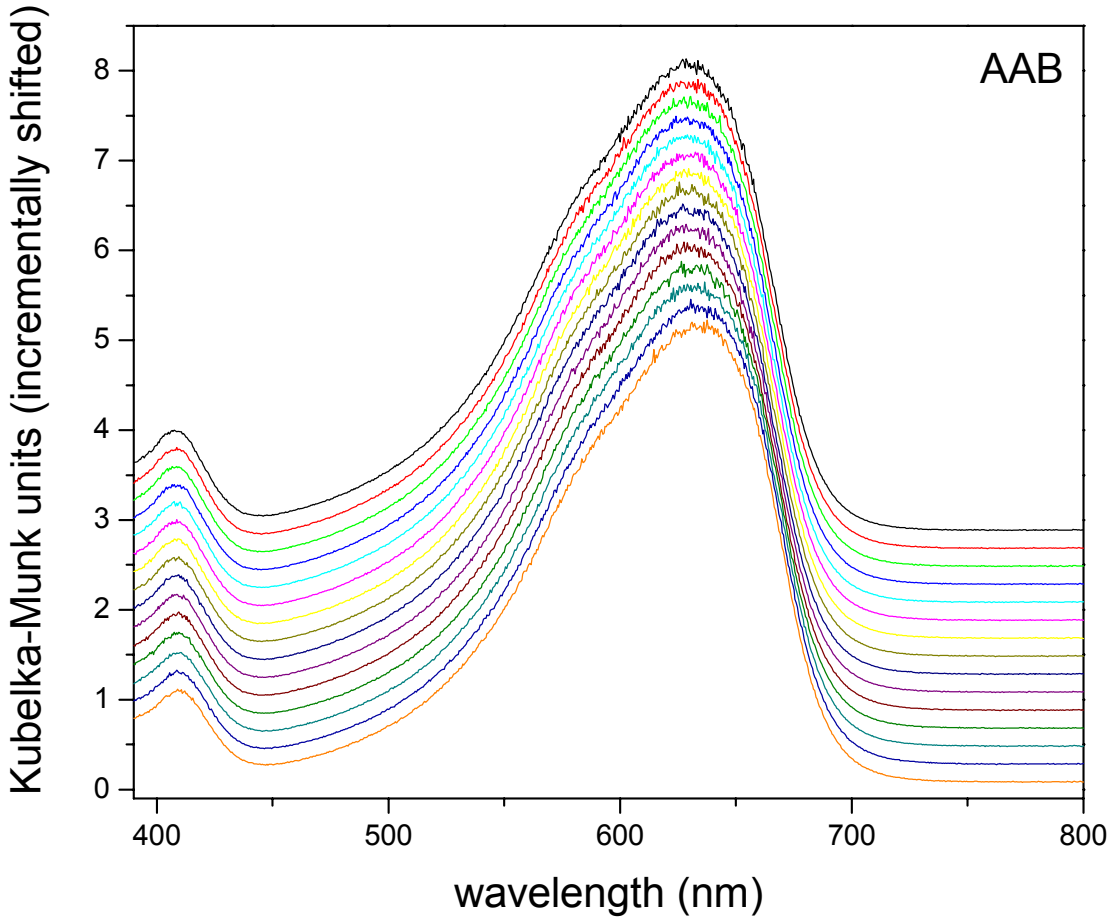

Figure 7.2 Direct Analysis: UV illumination from 0 to 480 min (top to bottom) of Acid Blue 9 on Al_2O_3 (AAB)

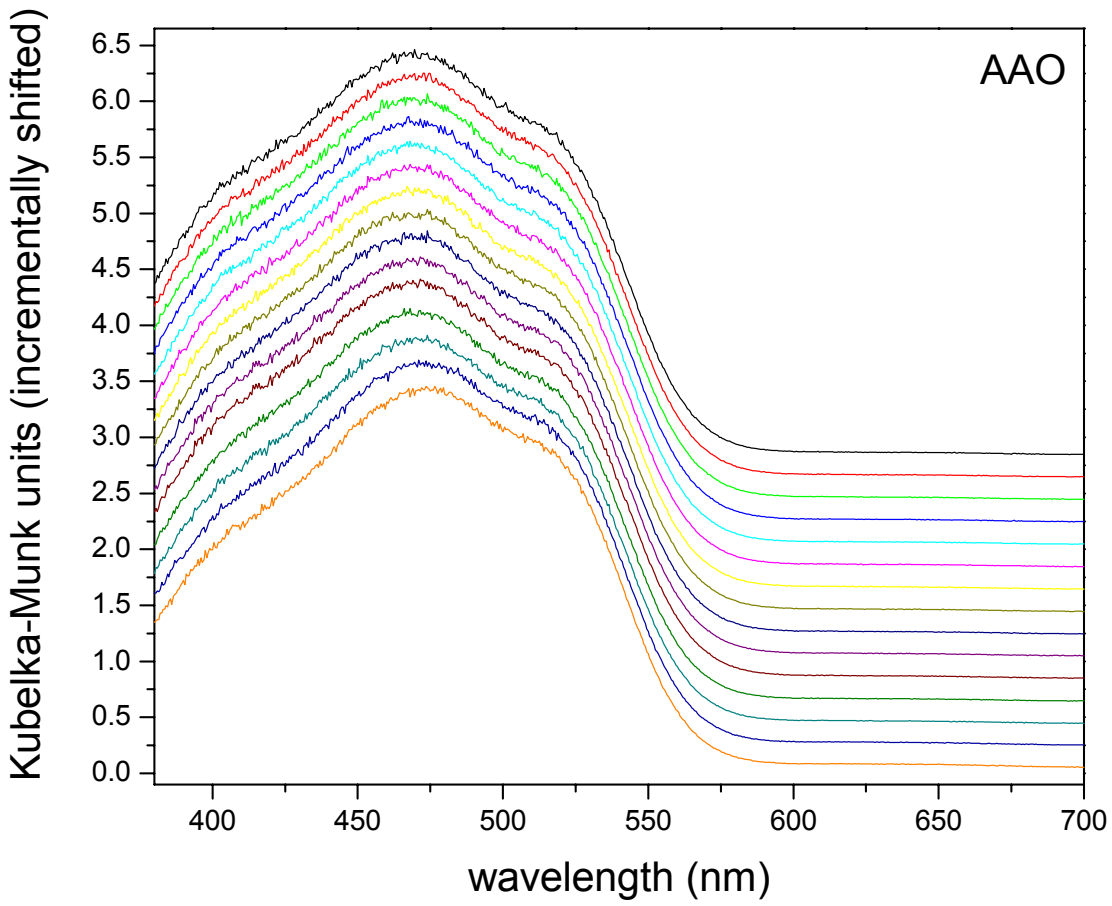

Figure 7.3 Direct Analysis: UV illumination from 0 to 480 min (top to bottom) of Acid Orange 7 on Al_2O_3 (AAO)

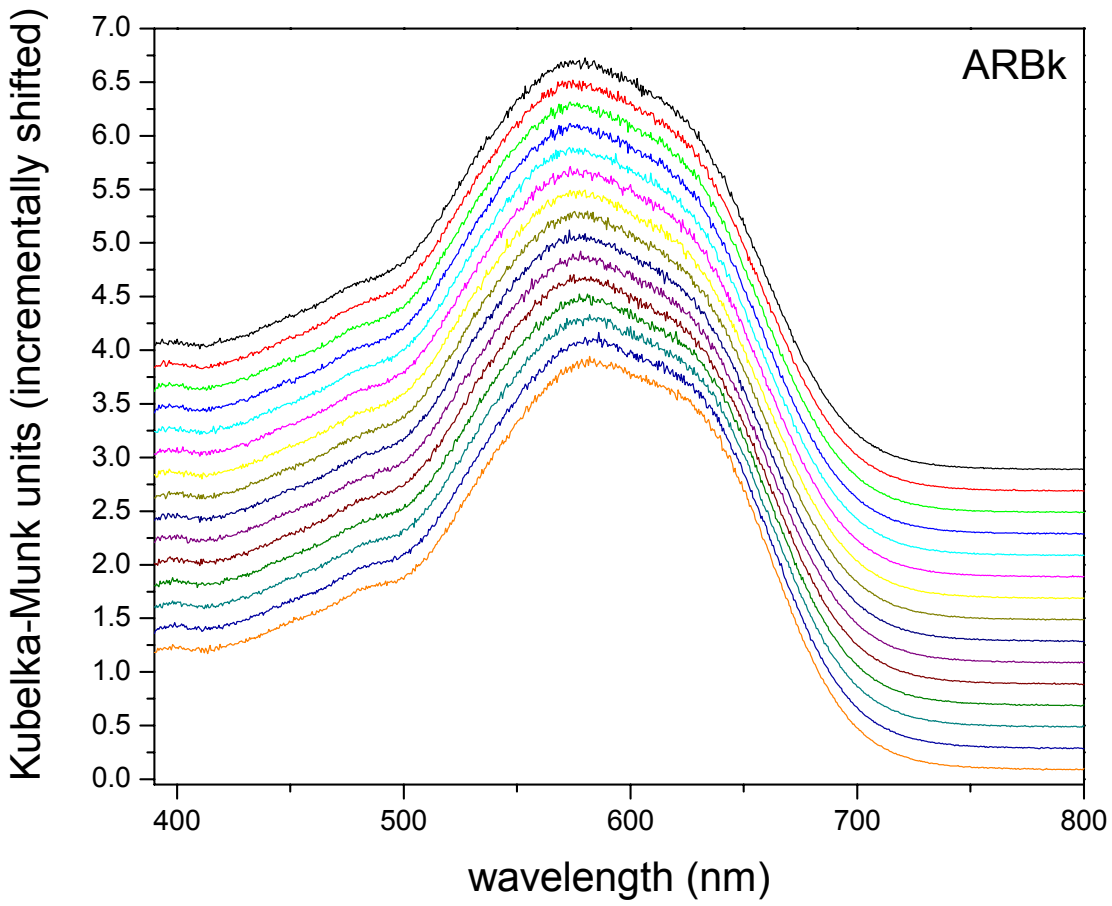

Figure 7.4 Direct Analysis: UV illumination from 0 to 480 min (top to bottom) of Reactive Black 5 on Al_2O_3 (ARBk)

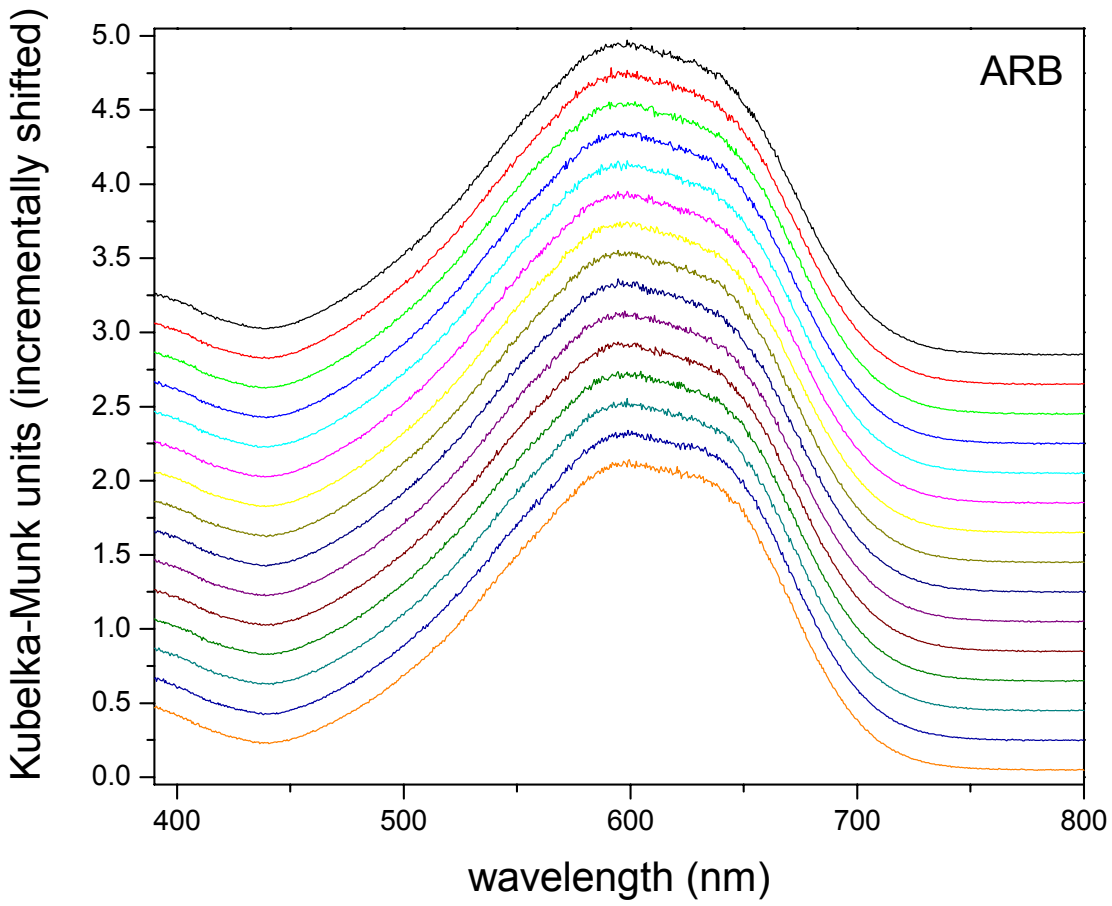

Figure 7.5 Direct Analysis: UV illumination from 0 to 480 min (top to bottom) of Reactive Blue 19 on Al_2O_3 (ARB)

7.1.2 Visual Results

Visual evidence of negligible color removal with UV illumination of dye-coated Al_2O_3 powders is shown in Figure 7.6. The photographs, taken with a Kodak EasyShare CX6330 3.1 mega-pixel camera, show each of the four samples (AAB, AAO, ARBk and ARB) before UV illumination and after 8 hr of exposure. No change in color is detectable, therefore confirming that the dyes do not photodegrade in the absence of the photocatalyst.

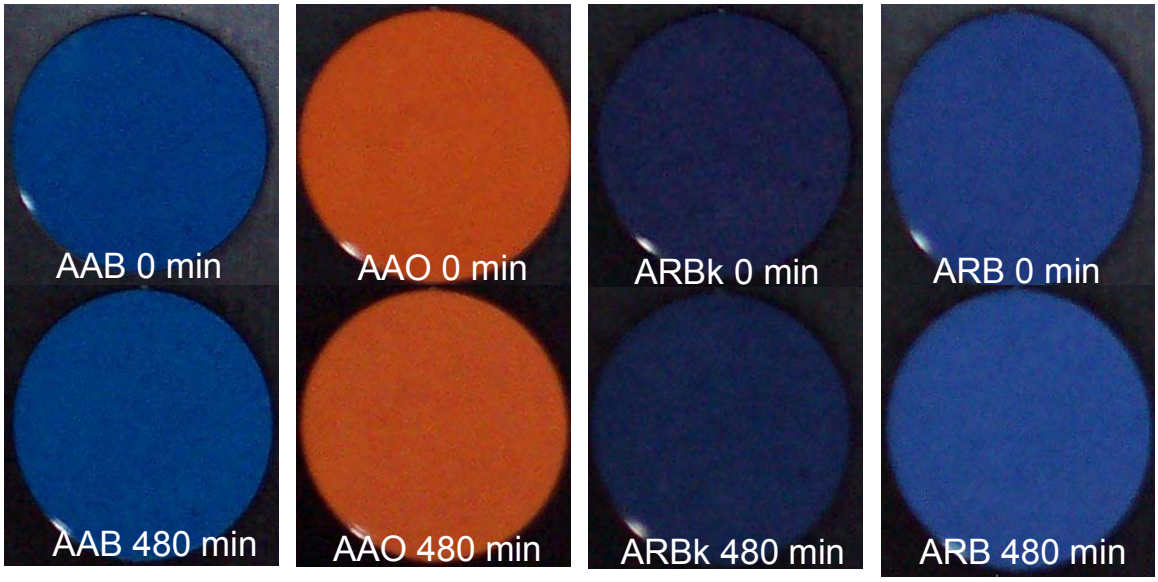

Figure 7.6 Visual result of negligible color removal

7.1.3 First-order Rate Constants for Single Reaction Model

Although the photodegradation of organic dyes on TiO_2 is predominantly a photocatalytic process, there may be some contribution to the degradation due to the homogeneous photodegradation of the dyes. In order to quantify this contribution, the UV-visible diffuse reflectance data was used. As described in Chapter 4 the reflectance data, R'_{∞}, can be transformed to Kubelka-Munk (*KM*) units by:

$$KM = \frac{(1 - R'_{\infty})^2}{2R'_{\infty}} = \alpha b' C$$

Equation 7.1

where *KM* is proportional to concentration, *C*. Using the *KM* units obtained for a chosen wavelength, the degradation of dye on Al_2O_3 can then be modeled as a first order reaction with respect to dye concentration, C_D, using a batch reactor model as described by Equation

7.2. The wavelengths chosen for the kinetic analysis were those used for the modeling of data obtained for the TiO_2 systems; 629 nm for Acid Blue 9 data, 485 nm for Acid Orange 7, 617 nm for Reactive Black 5 and 596 nm for Reactive Blue 19 data.

$$\frac{dC_D}{dt} = -k'C_D$$

Equation 7.2

The solution to this differential equation, assuming an initial concentration $C_{D(0)}$ described by KM_0, reveals that the rate constant, *k'*, can be found by plotting $ln(KM/KM_0)$ vs. *t* (time) and fitting a straight line to the data. The negative of the slope of this line is then *k'*.

The results for the fit of this first order reaction model to the photodegradation of dyes on Al_2O_3 are shown in the following figures. The fit of Acid Blue 9 data, Figure 7.7, to the reaction model gives a rate constant of 7.66×10^{-5} min^{-1}. Acid Orange 7, Figure 7.8, exhibits homogeneous photodegradation at a rate constant of 1.09×10^{-4} min^{-1}. The Reactive Black 5 data, Figure 7.9, shows curious behavior; *k'* has a value of -7.41×10^{-5} min^{-1}. The negative rate constant value is very small and the data is likely inaccurate, or an intermediate is formed that absorbs light at the same wavelength as the dye. The first order degradation rate constant for Reactive Blue 19, Figure 7.10, has a value of 3.14×10^{-5} min^{-1}. The average value of the rate constants, excluding the Reactive Black 5 value, is 7.23×10^{-5} min^{-1}. This rate constant is approximately 2000 times smaller than the average rate constant, k_1, for the first step in the series reaction described in Chapter 5 and 350 times smaller than the average rate constant, *k*, for the Unexposed Portion of Sample Model described in Chapter 6. Therefore, any contribution to the photodestruction of organic dyes by homogeneous self-photodegradation is very small compared to the rate of conversion due to photocatalysis.

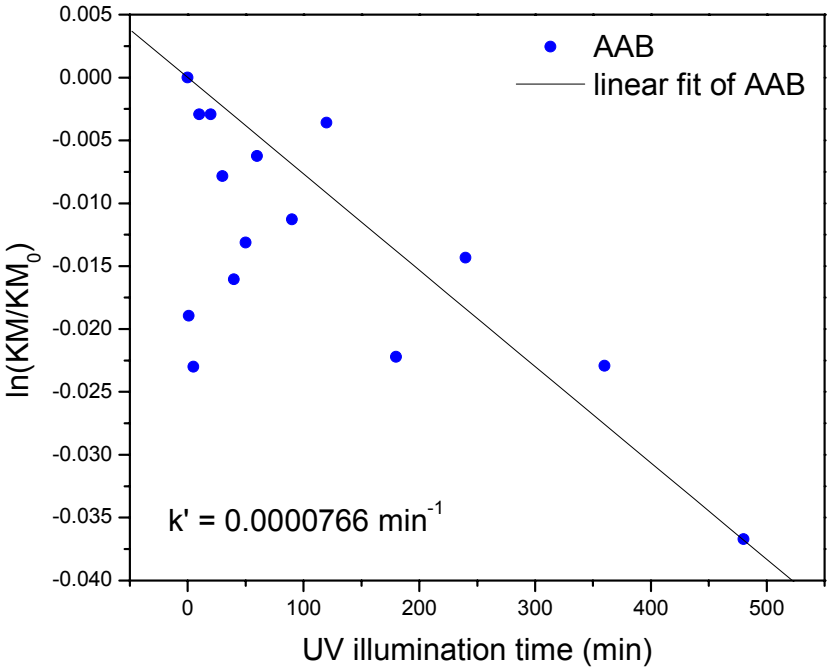

Figure 7.7 First order decay reaction model: Acid Blue 9 on Al_2O_3 (AAB)

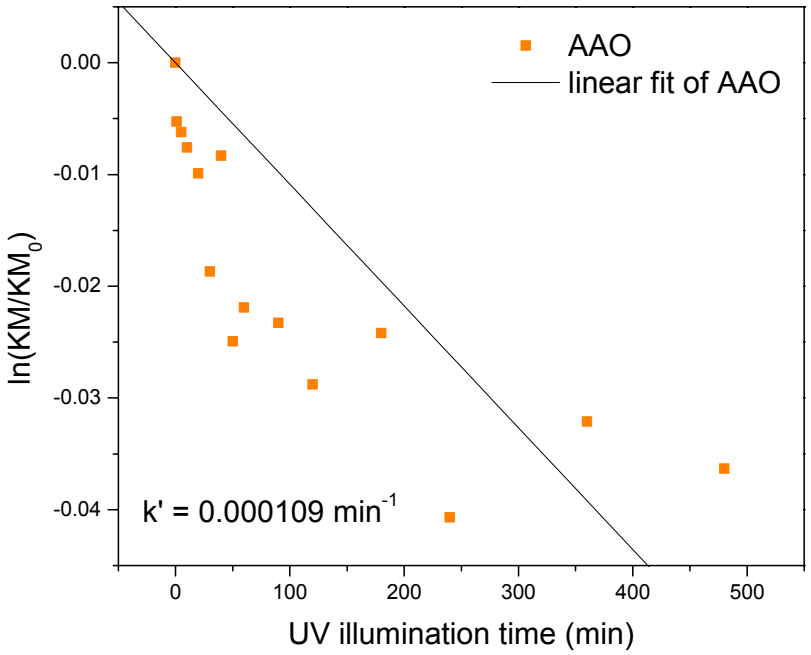

Figure 7.8 First order decay reaction model: Acid Orange 7 on Al_2O_3 (AAO)

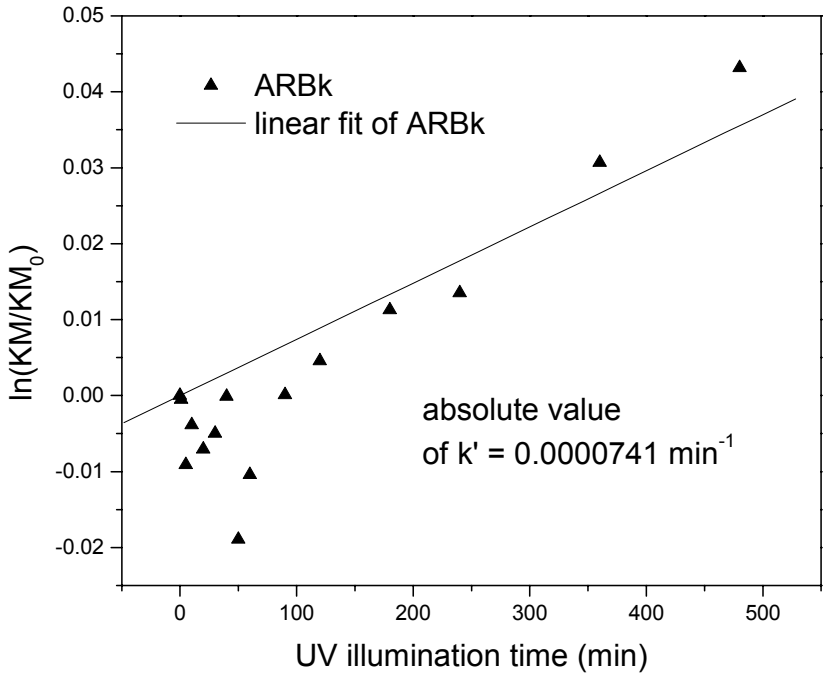

Figure 7.9 First order decay reaction model: Reactive Black 5 on Al_2O_3 (ARBk)

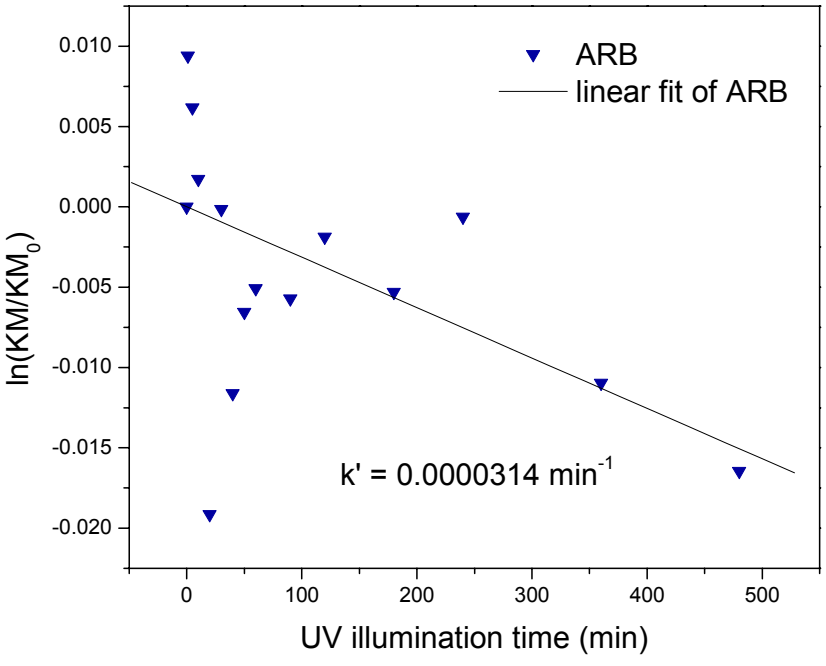

Figure 7.10 First order decay reaction model: Reactive Blue 19 on Al_2O_3 (ARB)

7.2 References

[1] Romeas, V., P. Pichat, C. Guillard, T. Chopin and C. Lehaut, *Degradation of palmitic (hexadecanoic) acid deposited on TiO_2-coated self-cleaning glass: kinetics of disappearance, intermediate products and degradation pathways*. New Journal of Chemistry 1999, **23**: p. 365-373.

[2] Vinodgopal, K, D.E. Wynkoop and P.V. Kamat, *Environmental Photochemistry on Semiconductor Surfaces: Photosensitized Degradation of a Textile Azo Dye, Acid Orange 7, on TiO_2 Particles Using Visible Light*. Environmental Science and Technology 1996, **30**(5): p. 1660-1666.

[3] Porada, T. and R. Gade, *Determination of the Quantum Yield for the Self-sensitized Photodegradation of Acid Red 44 Adsorbed on TiO_2*. Zeitschrift fur Physikalische Chemie – International Journal of Research in Physical Chemistry & Chemical Physics 1999, **210**(1): p. 113-126.

8 CONCLUSIONS

8.1 Conclusions

UV-visible spectroscopy was used to monitor changes in unreacted dye concentration with near-UV illumination compared to unexposed controls. The technique was useful to examine the disappearance of a species with reaction, as well as to determine if new species were formed that absorb within the UV-visible region. Absorbance (*Abs*) spectra were obtained by the Indirect Analysis method. The concentration of dye could be determined using the Beer-Lambert law, which states that concentration is proportional to *Abs*. The spectra obtained show that the general trend with near-UV exposure is a decrease in the original dye concentration. Some of the decays in *Abs* were out of sequence with exposure time, but this was likely an artifact of error occurring in the exposure and analysis method. The inconsistencies in sequence of *Abs* decay with UV illumination time were not consistent in duplicate experiments, supporting the theory that experimental error led to the non-ideal results. Reflectance spectra were obtained during the Direct Analysis method. The reflectance spectra were converted to Kubelka-Munk (*KM*) units for all of the dye-coated TiO_2 and Al_2O_3 samples studied. The concentration of dye is proportional to *KM* units. All of the samples show, with a sequential decrease in *KM* units, a decrease in dye concentration in succession with UV illumination time.

The data obtained by UV-visible spectroscopy was used to model the kinetics of the photocatalytic degradation. A number of kinetic models were developed and applied to the reaction data. The most plausible mechanism developed for the photocatalytic degradation of organic dyes adsorbed to TiO_2 assumed a series of reactions, of colored dye converting to

colored intermediate by a first order reaction with respect to dye concentration and then to colorless product by a first order reaction with respect to intermediate concentration, as shown below.

$$\text{dye} \xrightarrow{k_1} \text{intermediate} \xrightarrow{k_2} \text{colorless products} \qquad \text{(Reaction 5.1)}$$

An intermediate may form that absorbs light in the UV-visible region in a manner similar to the dye, producing a spectra with similar features, or a change in chemical structural may lead to the absorption of light at a different wavelength. The absorbance spectra shown in Chapter 3 and the reflectance spectra shown in Chapter 4 all have features that change, even if the change is slight, as the reaction proceeds with UV illumination. The most apparent change with UV illumination appears in the data obtained by the Direct Analysis method for Acid Blue 9 on TiO_2 shown in Figures 4.1 and 4.2 in the region between 400 nm and 550 nm. The increase in *Abs* and therefore increase in concentration occurring between about 450 nm and 500 nm suggests that a new species is formed and then degrades. Other changes in the spectra occurring with UV illumination, discussed in Chapter 4, could be caused by chemical structural changes, justifying the proposed mechanism.

The rate of the series reaction mechanism was described by the rate constant k_1 for the first step of dye converting to intermediate and by the rate constant k_2 for the second step of intermediate converting to colorless product. These rate constants were determined by examining the limiting values, as discussed in Chapter 5, of the model equations for the Indirect and Direct Analysis data shown below in Equation 5.4 and Equation 5.5

respectively. The average rate constant k_1 determined for all experiments was approximately 0.13 min^{-1} and the average k_2 value was 0.0014 min^{-1}.

$$\left(\mathrm{Abs}_{\mathrm{model}}(t)\right) = \mathrm{Abs}_0\left(\left(\frac{\alpha_I}{\alpha_D}\frac{k_1}{k_2 - k_1}\right)\left(\exp(-k_1 t) - \exp(-k_2 t)\right) + \exp(-k_1 t)\right) \quad \text{(Equation 5.4)}$$

$$\left(KM_{\mathrm{model}}(t)\right) = KM_0\left(\left(\frac{\alpha_I}{\alpha_D}\frac{k_1}{k_2 - k_1}\right)\left(\exp(-k_1 t) - \exp(-k_2 t)\right) + \exp(-k_1 t)\right) \quad \text{(Equation 5.5)}$$

The Unexposed Portion of Sample (UPOS) model accounted for dye that added to the total concentration of dye measured, but was not involved in the photocatalytic degradation because it and the underlying TiO_2 was not illuminated with UV. This model assumes that the photocatalytic reaction only occurs on surfaces illuminated with near-UV light and that the photocatalytic mechanism relies on the absorption of photons by TiO_2. The experimental system involved the illumination of dye-coated TiO_2 particles, with the dye in intimate contact with the semiconductor. A number of researchers [1-4] report the remote oxidation of contaminates not directly adsorbed to the photocatalyst surface by migrating oxidizing species, such as OH radicals. The experimental system used in this study involved contaminates directly adsorbed to the TiO_2 surface, although the migrating oxidizing species could possibly have reached dye not exposed to near-UV light, but this was not explicitly considered in the UPOS model. Although not previously described, the model did account for this phenomenon if the concentration of unexposed dye was assumed a concentration of dye not reached by the migrating oxidizing species.

The UPOS model was used to fit the photocatalytic degradation data to a single step first order reaction using a batch reactor model. The reaction rate was described by the rate constant *k*. The UPOS model was better fit to the data obtained by the Indirect Analysis method than the data obtained by the Direct Analysis method. The average rate constant, *k*, obtained for all dyes for the Indirect Analysis experiments was 0.02 min^{-1}. The application of the UPOS model to the Direct Analysis *KM* data showed systematic deviation from the linear fit, suggesting that the model does not thoroughly describe the reaction system.

The Light Intensity Influenced Rate Constant (LIIRC) model was applied to the experimental data to account for the reduced intensity of near-UV light as it traveled through the TiO_2 layer and was absorbed by the photocatalyst. The intensity influenced rate constant is described by the equation below.

$$k(I) = k_0 \exp(-\alpha_T a y) \quad \text{(Equation 6.6)}$$

The LIIRC model was used to fit the photocatalytic degradation data to a single step first order reaction using a batch reactor model. The data obtained by the UV-visible spectroscopic analysis was proportional to the average concentration of dye throughout the entire layer and could be described by the LIIRC model using:

$$\overline{C}_D(t) = \frac{1}{L}\int_0^L C_{D(0)} \exp(-k_0 t \exp(-\alpha_T a y))dy \quad \text{(Equation 6.10)}$$

To determine the average concentration of dye within the entire TiO_2 layer the right endpoint approximation (R_n) method was used to evaluate Equation 6.10. For each UV

illumination time experimentally evaluated, the average concentration of dye was determined by R_n, as shown in Equation 6.14.

$$\overline{C}_D(t) = \frac{1}{L}\int_0^L C_{D(0)} \exp(-k_0 t \exp(-\alpha_T a y))dy \approx R_n = \frac{C_{D(0)}}{L}\sum_i^n \exp(-k_0 t \exp(-\alpha_T a y_i))\Delta y$$

(Equation 6.14)

The rate constants, k_0, determined to best fit the *Abs* data obtained by the Indirect Analysis method for each dye were given in Table 6.4 and the rate constants determined to best fit the *KM* data obtained by the Direct Analysis method for each dye were given in Table 6.5. The rate constants determined using $a = 0.5$ (where a is proportional to the influence of intensity on the reaction) were the same order of magnitude for the experiments performed using the same procedure. The average k_0 determined for the photocatalytic degradation of all dyes analyzed by the Indirect Analysis method was approximately 0.03 min^{-1} and the average value determined for the reaction monitored by the Direct Analysis method was 0.1 min^{-1}. The higher value obtained for the Direct Analysis experiments may be closer to the true value because the experimental system more closely resembled the LIIRC model, as shown in Figure 6.19.

The LIIRC model reported does not appropriately describe the photocatalytic degradation of organic dyes by TiO_2. Although a "best" fit k_0 value was reported, the calculated *Abs* and *KM* values did not correspond well with the observed values for the entire period the reaction was monitored. The LIIRC model may be applicable to the photocatalytic system, but perhaps the model needs to be combined with the series reaction mechanism or the UPOS model to completely describe the system.

To determine whether the degradation of non-volatile dyes adsorbed to TiO_2 occurred solely due to photocatalysis or also due to homogeneous photodegradation contributions, control experiments were performed using dye coated on a photo-inactive support, Al_2O_3. The powders were illuminated with near-UV light and analyzed using the Direct Analysis method. The reflectance profiles of the dyes did not change with near-UV illumination; therefore there was no significant conversion of dye to another species detected. The results reported in Chapter 7 prove that TiO_2 is necessary for the photodegradation of adsorbed organic dyes and that indeed a photocatalytic process is occurring.

8.2 Recommendations for Future Work

The motivation for this work was the application of color removal for self-cleaning surfaces. The rate of color removal by the photocatalytic degradation of adsorbed organic dyes on TiO_2 surfaces could be used to monitor the activity of a photocatalyst in the field. A method would need to be developed to easily monitor the reaction rate of the photodegradation occurring on a fixed surface. The experimental procedures reported here were useful to study the system in the laboratory, but not practical for examining, for example, the photocatalytic activity of self-cleaning window glass on a building.

The Series Reaction mechanism was the model developed that was most applicable to the data obtained for the photocatalytic degradation of non-volatile organic dyes. Although some evidence of intermediates was found in the UV-visible spectroscopic data, more investigation needs to be done to determine the chemical identity of these intermediates. For the Series Reaction mechanism to be valid, chemicals with structures

different from the original dye need to be detected. The reaction pathway may be determined by using another spectroscopy technique, such as FTIR, to track chemical changes occurring with the photoreaction.

The Series Reaction mechanism, the Unexposed Portion of Sample, and the Light Intensity Influenced Rate Constant models were all applied separately to describe the photocatalytic degradation of organic dyes adsorbed to TiO_2. Although the series reaction mechanism adequately described the system, there were valid physical interpretations included in the other two models. The reaction system may be thoroughly described by combining the UPOS and LIIRC models with the Series Reaction mechanism. A complex model could be developed to include all of these contributions, but the simplicity of the Series Reaction mechanism model is appealing.

8.3 References

[1] Lee, M.C. and W. Choi, *Solid Phase Photocatalytic Reaction on the Soot/TiO_2 Interface: The Role of Migrating OH Radicals*. Journal of Physical Chemistry B 2002. **106**(45): p. 11818-11822.

[2] Lee, S.-K., S. McIntyre and A. Mills, *Visible illustration of the direct, lateral and remote photocatalytic destruction of soot by titania*. Journal of Photochemistry and Photobiology A: Chemistry 2004. **162**: p. 203-206.

[3] Tatsuma, T., S. Tachibana, T. Miwa, D.A. Tryk and A. Fujishima, *Remote Bleaching of Methylene Blue by UV-Irradiated TiO_2 in the Gas Phase*. Journal of Physical Chemistry B 1999. **103**(38): p. 8033-8035.

[4] Tatsuma, T., S. Tachibana and A. Fujishima, *Remote Oxidation of Organic*

Compounds by UV-Irradiated TiO_2 via the Gas Phase. Journal of Physical Chemistry B 2001. **105**(29): p. 6987-6992.

APPENDICES

APPENDIX A: DATA USED FOR KINETIC MODELING

Table A.1 Absorbance data for Indirect Analysis dye coated TiO_2 experiments

UV illumination time (min)	Absorbance of sample at indicated wavelength:			
	ABa (629 nm)	ABb (629 nm)	AOa (485 nm)	AOb (485 nm)
0	2.37088	1.85643	1.08407	0.97701
5	1.80448	1.37128	0.80675	0.82968
10	1.54457	1.24822	0.83964	0.74423
20	1.57623	1.18701	0.92638	0.65026
40	1.23429	1.05308	0.72022	0.64704
60	1.18808	0.98464	0.68049	0.6468
90	1.03571	0.87441	0.5577	0.47891
120	1.04763	0.89002	0.52033	0.44688
240	0.84568	0.59551	0.36652	0.38959

UV illumination time (min)	Absorbance of sample at indicated wavelength:			
	RBka (617 nm)	RBkb (617 nm)	RBa (596 nm)	RBb (596 nm)
0	0.89917	0.79936	0.30495	0.30524
5	0.67675	0.61013	0.25443	0.26092
10	0.67533	0.55943	0.24235	0.24415
20	0.55042	0.51476	0.18706	0.22023
40	0.57023	0.50354	0.16715	0.18232
60	0.45011	0.41915	0.15728	0.17803
90	0.42881	0.39783	0.14057	0.11776
120	0.4259	0.37809	0.13166	0.12459
240	0.3237	0.28142	0.11293	0.09422

Table A.2 Reflectance data for Direct Analysis dye coated TiO_2 experiments

UV illumination time (min)	Kubelka-Munk units of sample at indicated wavelength:			
	ABa (629 nm)	ABc (629 nm)	AOa (485 nm)	AOc (485 nm)
0	2.43241	2.00418	1.49106	1.47131
1	1.37655	1.157	0.7568	0.77881
5	0.84647	0.75523	0.42709	0.43298
10	0.67933	0.61017	0.34105	0.32973
20	0.54864	0.4978	0.27063	0.2637
30	0.47652	0.43039	0.2405	0.23602
40	0.44037	0.39475	0.21935	0.21572
50	0.4164	0.36487	0.20147	0.19764
60	0.39177	0.34181	0.19767	0.18789
90	0.35323	0.30962	0.17612	0.17379
120	0.32588	0.29121	0.16643	0.15854
180	0.30357	0.27945	0.155	0.1419
240	0.27489	0.26231	0.14285	0.13162
360	0.24542	0.25303	0.13681	0.12383
480	0.23451	0.23795	0.12075	0.11757

UV illumination time (min)	Kubelka-Munk units of sample at indicated wavelength:			
	RBkb (617 nm)	RBkc (617 nm)	RBa (596 nm)	RBc (596 nm)
0	0.99561	0.99074	0.888	0.81319
1	0.71852	0.75935	0.70453	0.63986
5	0.50936	0.53515	0.48165	0.42434
10	0.43544	0.44323	0.38961	0.33366
20	0.36821	0.37524	0.29747	0.25672
30	0.33368	0.33769	0.26193	0.21872
40	0.32461	0.31379	0.23626	0.19899
50	0.30636	0.29865	0.21992	0.1847
60	0.29292	0.28528	0.20655	0.17147
90	0.27485	0.26112	0.182	0.14942
120	0.26199	0.24767	0.16795	0.1392
180	0.24693	0.22967	0.14736	0.13021
240	0.23502	0.21992	0.13982	0.12277
360	0.22396	0.19683	0.13327	0.1218
480	0.21795	0.19534	0.12039	0.11616

Table A.3 Reflectance data for Direct Analysis dye coated Al_2O_3 experiments

UV illumination time (min)	Kubelka-Munk units of sample at indicated wavelength:			
	AAB (629 nm)	AAO (485 nm)	ARBk (617 nm)	ARB (596 nm)
0	5.30287	3.46487	3.49182	2.13174
1	5.20339	3.44665	3.49003	2.15186
5	5.18225	3.44338	3.46016	2.14496
10	5.28735	3.43868	3.47838	2.13542
20	5.28735	3.43073	3.46718	2.09133
30	5.26143	3.40071	3.47452	2.13141
40	5.21849	3.43618	3.49143	2.10713
50	5.23366	3.37952	3.42625	2.11781
60	5.26981	3.38975	3.45565	2.12095
90	5.24335	3.38516	3.49217	2.11963
120	5.28383	3.36655	3.50781	2.12774
180	5.18633	3.38199	3.53133	2.12045
240	5.22745	3.32675	3.5393	2.1304
360	5.18263	3.35534	3.60066	2.1085
480	5.11174	3.34128	3.6459	2.09699

APPENDIX B: PAPER SUBMITTED TO NINTH INTERNATIONAL CONFERENCE ON TITANIUM DIOXIDE PHOTOCATALYSIS: FUNDAMENTALS AND APPLICATIONS

PHOTOCATALYTIC DEGRADATION OF ORGANIC DYES BY TITANIUM DIOXIDE IN AN AIR-CATALYST SYSTEM

Alison J. Julson and David F. Ollis*

North Carolina State University
Department of Chemical and Biomolecular Engineering
Box 7905, Raleigh, NC 27695-7905, ollis@eos.ncsu.edu

1. Abstract

With the goal of color removal, we report photocatalytic degradation of adsorbed organic dyes in air for potential catalyst characterization and application in self-cleaning surfaces.

A laboratory photoreactor was the source for near-UV exposure of 1.2 mW cm^{-2} of dye-coated Degussa P25 TiO_2 particles. Dyes examined include Acid Orange 7, Reactive Blue 19, Reactive Black 5 and Acid Blue 9. The photo-oxidation kinetics of these dye-solid systems was investigated with UV-visible spectroscopy. For powder catalyst particles of sub-monolayer initial dye coverage, the photocatalytic batch degradation of the dyes can be fit to a two step, first order kinetics model: dye to intermediate to colorless product. The average apparent rate constant for the first step for all dyes was 0.1 min^{-1} and for the second step was 0.002 min^{-1}. The homogeneous photodegradation contribution to color removal was found to be less than 1% of the photocatalytic degradation.

2. Introduction

Photocatalytic degradation of organic substances by titanium dioxide (TiO_2) and other photocatalysts has been extensively investigated in liquid-catalyst [1-5] and air-catalyst systems [6-10], but relatively little work has been reported on photocatalytic oxidations of solid contaminants in air. The information gained from the examination of photocatalytic degradation of solid contaminants in air-catalyst systems could be applied to self-cleaning surfaces and also used for catalyst characterization. Self-cleaning surfaces have potential environmental, financial, aesthetic, and time-saving benefits. For example, diminished or eliminated need for harsh chemical cleaning agents reduces consequent water and air pollution, as well as maintenance costs. Light-mediated stain removal has both aesthetic and time-saving benefits. Companies, such as Pilkington and PPG, are currently marketing photocatalytic self-cleaning window glass. A standard method is needed to test the effectiveness of photocatalysts and photocatalytic coated surfaces in degrading contaminants for successful application of products. This study reports the photocatalytic degradation of adsorbed organic dyes, with the goal of color removal, on TiO_2 in air. A non-photocatalytic control, Al_2O_3, was tested to demonstrate that degradation on TiO_2 was predominately occurring due to a photocatalytic mechanism. Reaction kinetics of the photocatalytic batch degradation of the dyes was examined using UV-visible spectroscopy.

3. Experimental

The photocatalyst, Degussa P25 titanium dioxide, was a gift from the Degussa Corporation and used as received. The company's specifications on the product include a primary particle size of 21 nm and a BET surface area of 50 +/- 15 m^2 g^{-1}. The inert powder support, alumina (basic, 60-325 mesh), was purchased from Fisher Scientific and used as received. The vendor reports typical BET surface area of 150 +/- 15 m^2 g^{-1} for the Al_2O_3 product. Acid Blue 9, Acid Orange 7, Reactive Black 5 and Reactive Blue 19 were purchased from Fisher Scientific and used as received. Figure 1 depicts the dye chemical structures.

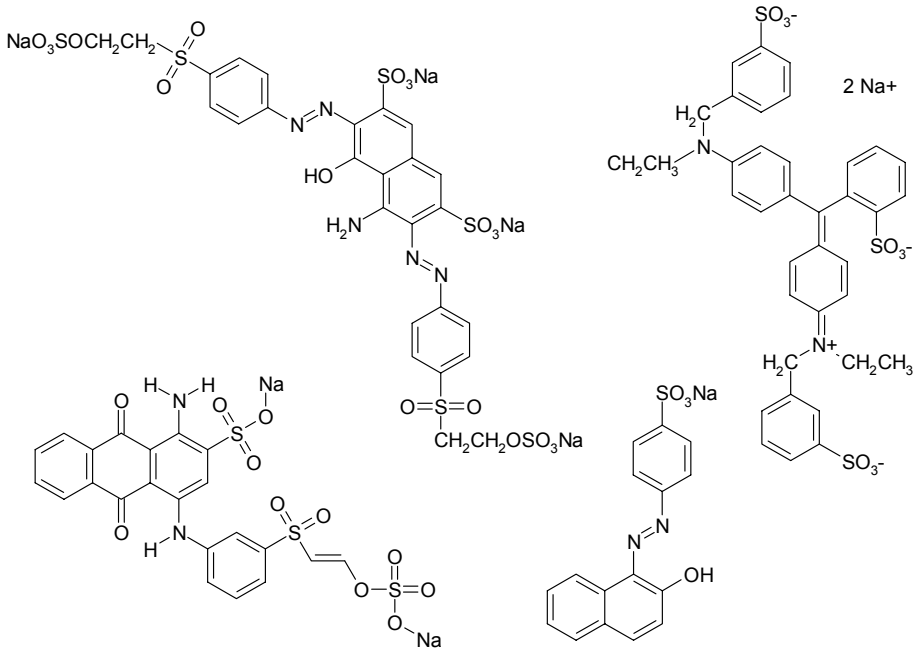

Figure 1 Clockwise from top left: Reactive Black 5, Acid Blue 9, Acid Orange 7 and Reactive Blue 19.

In this study, a laboratory photoreactor equipped with 8 GE Blacklight Blue 20W lamps with peak emission at 365 nm was the source for near-UV exposure of dye-coated Degussa P25 TiO_2 particles as well as dye-coated photo-inert aluminum oxide (Al_2O_3) particles. Dyes were deposited onto catalyst particles and inert supports in aqueous solution, the coated particles were captured by centrifugation, dried, and hand ground to powder before UV exposure. The average UVA intensity of exposure measured with a Traceable® UV Light Meter was 1.2 mW cm^{-2}. During UV exposure, samples were subject to ambient humidity, and nearly ambient temperature was maintained by fans located near the lamps within the photoreactor. Powder samples were shaken in uncovered Petri dishes during the photoreaction to achieve uniform UV exposure of particles. Sub-monolayer initial dye coverage of support particles was used, as reported in [11].

Because visible stain removal was the goal of this research, we chose to examine, by UV-visible spectroscopy, the disappearance of the original colored dye and changes in colored intermediate concentrations with near-UV illumination by comparison with unexposed controls. The photo-oxidation kinetics of these dye-solid systems was investigated with a Jasco V-550 UV-visible spectrophotometer. Results were obtained by

desorbing the dye from the support particle into basic solution, removing TiO_2 or Al_2O_3 particles by centrifugation, and using the resulting solution for spectral analysis for each illumination time. Data analysis, based on the Beer-Lambert law, was performed by first determining a wavelength of maximum absorbance (Abs) for each dye to be used for analysis of the calibration data as well as the sample data. Baseline corrected Abs was obtained by subtracting the baseline drawn by connecting the endpoints of the peak of interest from sample Abs at the chosen wavelength. The molar absorptivity (α_D), units of L mol^{-1} cm^{-1}, of each dye was determined by fitting a straight line through zero to data of baseline corrected Abs at the chosen wavelength versus molar concentration (C) of calibration solutions.

A kinetic analysis, assuming a constant volume batch reactor model, was performed to determine a reaction model to describe each photoreaction as well as rate constants for the reactions. Literature reports that photocatalytic dye oxidation reactions can be described by first order reaction models [2, 12-14] with respect to dye concentration, which is consistent with the results found in this study, although we report a two step reaction mechanism to explain our photocatalytic oxidation data.

4. Results and Discussion

Digital images, presented elsewhere [11], of dye-coated TiO_2 sample particles exposed for 0, 5, 10, 20, 40, 60, 90, 120 and 240 min clearly show the progression of color removal within this period, consistent with data obtained by UV-visible analysis. Single step zero order and first order reaction models with respect to dye concentration were tested, but did not fit data obtained from near-UV illumination of dye-coated TiO_2 powders. Instead, the semilog plot of Abs (Acid Blue 9 on TiO_2) vs. time shows two regions, suggesting a two step reaction model.

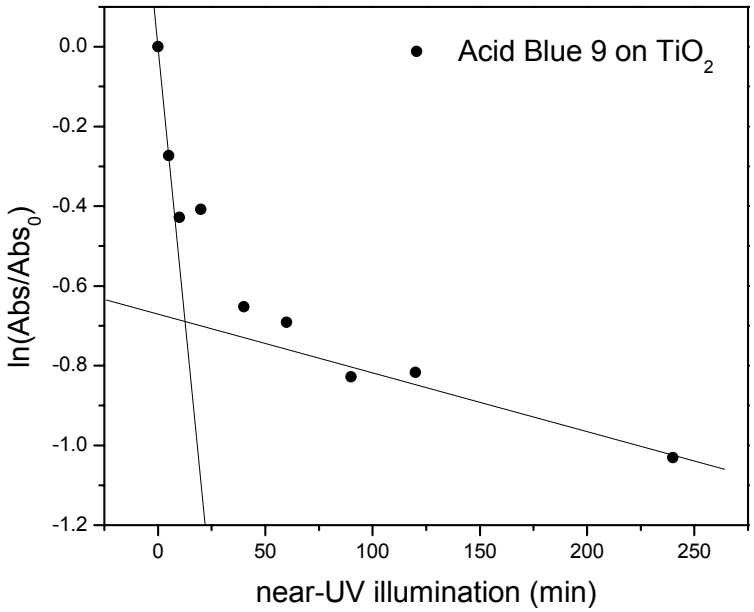

Figure 2 Semilog plot of Abs(t)/Abs(0) vs. illumination time for Acid Blue 9 on TiO_2

The photocatalytic reaction data was fit to the series reaction model below, (1). The differential equations describing the change in concentration of dye and intermediate with near-UV illumination were solved to obtain equations describing the concentrations dependent on time, rate constants and initial dye concentration. Absorbance measured was the sum of dye and intermediate absorbances, therefore the Beer-Lambert law was used with the concentration equations to obtain a model for absorbance, (2), where α_D and α_I are the molar absorptivity of dye and intermediate, respectively, k_1 and k_2 are first order rate constants, t is the near-UV illumination time, and Abs_0 is the initial absorbance of the unexposed sample.

$$\text{dye} \xrightarrow{k_1} \text{intermediate} \xrightarrow{k_2} \text{colorless products} \qquad (1)$$

$$\left(\text{Abs}_{\text{model}}(t)\right) = \text{Abs}_0\left(\left(\frac{\alpha_I}{\alpha_D}\frac{k_1}{k_2 - k_1}\right)\left(\exp(-k_1 t) - \exp(-k_2 t)\right) + \exp(-k_1 t)\right) \qquad (2)$$

The parameters k_1, k_2, and α_I/α_D were determined by examining the limiting values of Abs_{model} with respect to time, given in (3) for near-UV illumination time approaching zero and (4) for time approaching infinity, assuming k_1 is greater than k_2. Data obtained for 0 and 5 min of exposure was fit to (3) and data obtained for 90, 120 and 240 min of near-UV exposure was fit to (4), with results analyzed simultaneously to obtain k_1, k_2, and α_I/α_D. For our model, the values of α_D and α_I were not needed explicitly, only the ratio of α_I to α_D was needed, which was obtained by the limiting values analysis. Therefore, the calibration analysis was unnecessary for determination of rate constants. Parameters obtained by the analysis described above for duplicate experiments are given in Table 4.1.

$$\left(\frac{\mathrm{Abs}_{\mathrm{model}}}{\mathrm{Abs}_0}-1\right)=\left(\frac{\alpha_I}{\alpha_D}-1\right)k_1 t \qquad (3)$$

$$\ln\left(\frac{\mathrm{Abs}_{\mathrm{model}}}{\mathrm{Abs}_0}\right)=-k_2 t+\ln\left(\frac{-\alpha_I k_1}{\alpha_D(k_2-k_1)}\right) \qquad (4)$$

Table 4.1 Summary of Duplicate Results

	Acid Blue 9 on TiO_2		Acid Orange 7 on TiO_2	
samples:	**ABa_{629nm}**	**ABb_{629nm}**	**AOa_{485nm}**	**AOb_{485nm}**
Abs_0	2.37088	1.85643	1.08407	0.97701
D_0 (mol L^{-1})	6.264E-05	4.904E-05	1.299E-04	1.171E-04
α_D (L mol^{-1} cm^{-1})	37852	37852	8346	8346
α_I (L mol^{-1} cm^{-1})	19059	23479	5473	4450
k_1 (min^{-1})	9.62E-02	1.38E-01	1.49E-01	6.46E-02
k_2 (min^{-1})	1.48E-03	2.79E-03	2.83E-03	1.31E-03

	Reactive Black 5 on TiO_2		Reactive Blue 19 on TiO_2	
samples:	**$RBka_{617nm}$**	**$RBkb_{617nm}$**	**RBa_{596nm}**	**RBb_{596nm}**
Abs_0	0.89917	0.79936	0.30495	0.30524
D_0 (mol L^{-1})	3.729E-05	3.315E-05	6.604E-05	6.610E-05
α_D (L mol^{-1} cm^{-1})	24116	24116	4618	4618
α_I (L mol^{-1} cm^{-1})	13846	14671	2341	2113
k_1 (min^{-1})	1.16E-01	1.21E-01	6.72E-02	5.35E-02
k_2 (min^{-1})	1.99E-03	2.35E-03	1.41E-03	1.73E-03

The apparent first order rate constants for the first step of the proposed mechanism, k_1, for all dyes were very similar, and averaged 0.101 min^{-1} from the eight experiments. The average apparent first order rate constant for the second step, k_2, was 0.00199 min^{-1}. This value of k_1 is approximately 50 times greater than k_2, therefore validating our assumption, $k_1>k_2$, used in the analysis of the limiting values. Abs_{model} data calculated with these parameters describes well the observed Abs data, $Abs_{observed}$, with examples for Acid Blue 9, Acid Orange 7, Reactive Black 5 and Reactive Blue 19 given in Figure 3, Figure 4, Figure 5 and Figure 6 respectively.

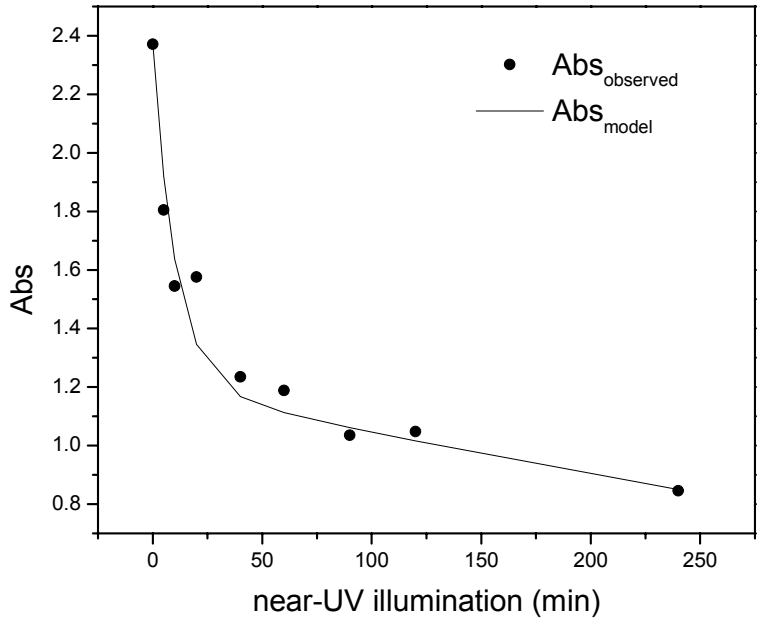

Figure 3 Acid Blue 9 on TiO_2, ABa

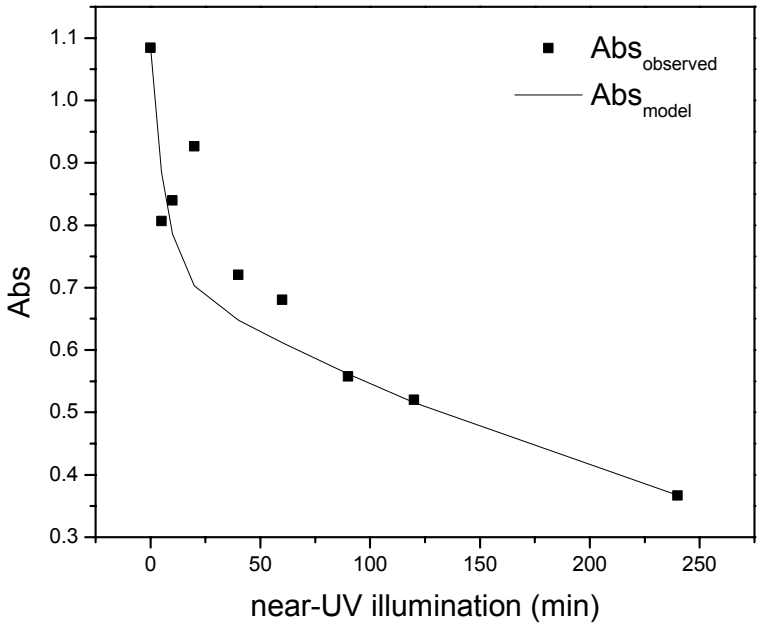

Figure 4 Acid Orange 7 on TiO_2, AOa

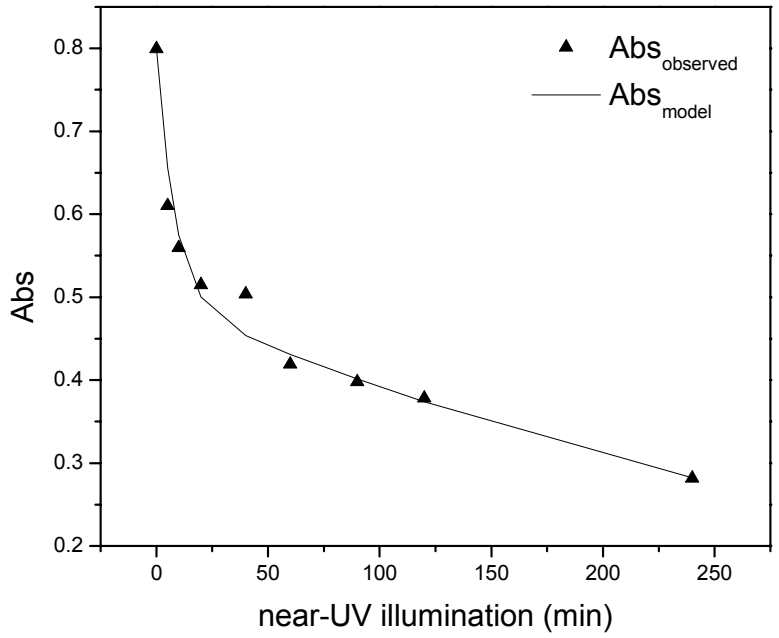

Figure 5 Reactive Black 5 on TiO_2, RBkb

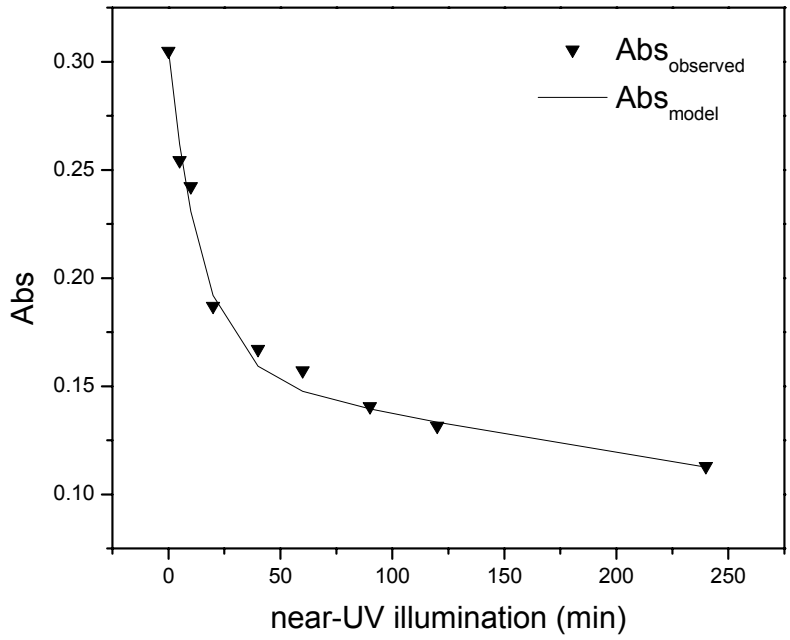

Figure 6 Reactive Blue 19 on TiO_2, RBa

Previously, Yang et al. [12] reported the photocatalytic oxidation of Acid Blue 9 adsorbed on TiO_2 from an aqueous solution of 10 ppm dye of pH 2.3 under 15 mW cm^{-2} of UV exposure. We were able to successfully apply our model to results reported by Yang et al. by analysis of their Fig. 8 data [12], as shown in Figure 7 below, producing a k_1 of 0.0868 min^{-1} and k_2 of 0.00168 min^{-1}, comparable to our results.

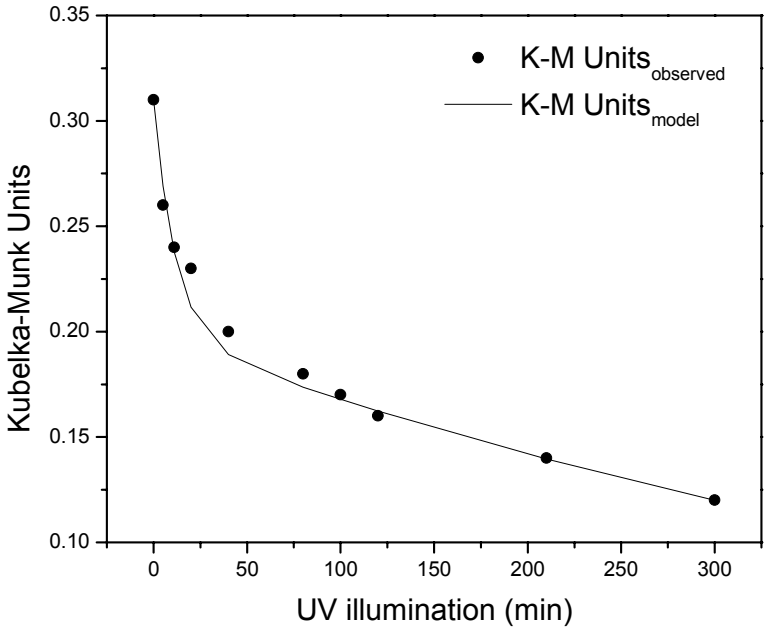

Figure 7 Our model fit to data of Yang et al.[2001]

With near-UV illumination, the photodegradation of organic dyes occurs on TiO_2 in an air-photocatalyst system as shown by the UV-visible spectroscopic results reported. To determine the relative contributions of homogeneous vs. heterogeneous photochemistry to the observed dye conversions, we compared the rate of homogeneous destruction of dyes on a photo-inactive support, Al_2O_3, to the rate reported for the heterogeneous photocatalytic destruction on TiO_2. Reaction data obtained by UV-visible spectroscopy [11] indicates that dyes supported on an assumed photo-inactive support, Al_2O_3, degrade very slowly with near-UV illumination; but the rate of photobleaching is slow compared to that of the photocatalytic reaction, with an average apparent first order homogeneous rate constant for all dyes of 0.000244 min^{-1}. The average photobleaching rate for all dyes, assuming first order reaction kinetics with respect to dye concentration, compared to the first step of the proposed model for photocatalytic degradation is approximately 0.24%. Thus while photodegradation of these organic dyes does occur without the presence of a photocatalyst, the catalyst increases the rate of reaction by nearly two orders of magnitude, and thereby speeds the color removal process.

5. Conclusion

With the goal of color removal, we report the photocatalytic degradation of organic dyes adsorbed to TiO_2 in air. The photo-oxidation kinetics of these dye-solid systems was investigated with UV-visible spectroscopy, revealing a two step first order photocatalytic reaction mechanism; dye to intermediate to colorless product. The average apparent rate constant for the first step of the proven photocatalytic degradation mechanism for all dyes was 0.1 min^{-1} and for the second step was 0.002 min^{-1}. We found that our model could be fit to data obtained by another lab, i.e. Yang et al. [12].

6. Acknowledgements

The authors thank the State of North Carolina for research support and Dr. Orlin D. Velev for use of the UV-visible spectrophotometer. The NSF REU center for Green Processing at NCSU provided summer support for undergraduate Jack H. Garrison who performed the experiments with alumina supports.

7. References

1. Tang, W. Z.; Zhang, Z.; An, H.; Quintana, M. O.; Torres, D. F. *Environ. Technol.* **1997**, *18*, 1-12.
2. Lachheb, H.; Puzenat, E.; Houas, A.; Ksibi, M.; Elaloui, E.; Guillard, C.; Herrmann, J.-M. *Appl. Catal. B* **2002**, *39*, 75-90.
3. Lizama, C.; Freer, J.; Baeza, J.; Mansilla, H. D. *Catal. Today* **2002**, *76*, 235-246.
4. Sauer, T.; Neto, G. C.; Jose, H. J.; Moreira, R. F. P. M. *J. Photochem. Photobiol. A* **2002**, *149*, 147-154.
5. Zielinska, B.; Grzechulska, J.; Kalenczuk, R. J.; Morawski, A. W. *Appl. Catal. B* **2003**, *45*, 293-300.
6. Gratzel, M.; Thampi, K. R.; Kiwi, J. *J. Phys. Chem.* **1989**, *93*, 4128-4132.
7. Dibble, L. A.; Raupp G. B. *Environ. Sci. Technol.* **1992**, *26*, 492-495.
8. Luo, Y.; Ollis, D. F. *J. Catal.* **1996**, *163*, 1-11.
9. Lim, T. H.; Jeong, S. M.; Kim, S. D.; Gyenis, J. *J. Photochem. Photobiol. A* **2000**, *134*, 3, 209-217.
10. Gonzalez-Garcia, N.; Ayllon, J. A.; Domenech, X; Peral, *J. Appl. Catal. B* **2004**, *52*, 69-77.
11. Paper submitted to Applied Catalysis B: Environmental.
12. Yang, T. C. K.; Wang, S.-F.; Tsai, S. H.-Y.; Lin, S. Y. *Appl. Catal. B*. **2001**, 293-301.
13. Tanaka, K.; Padermpole, K.; Hisanaga, T. Wat. Res. **2000**, *34*, 1, 327-333.
14. Tarasov, V. V.; Barancova, G. S., Zaitsev, N. K.; Dongxiang, Z. *Trans IChemE Part B*, **2003**, *81*, 243-249.